

AD-774 436

DETERMINATION OF THE EFFECTS OF MASS
AND STIFFNESS ON THE VIBRATION RESPONSE
OF RIBBED PANELS SUBJECTED TO RANDOM
ACOUSTIC NOISE

Clarence M. Bose

Air Force Institute of Technology
Wright-Patterson Air Force Base, Ohio

December 1973

DISTRIBUTED BY:

NTIS

National Technical Information Service
U. S. DEPARTMENT OF COMMERCE
5285 Port Royal Road, Springfield Va. 22151

UNCLASSIFIED

Security Classification

AD-774436

DOCUMENT CONTROL DATA - R & D

(Security classification of title, body of abstract and indexing annotations must be entered when the overall report is classified)

1. ORIGINATING ACTIVITY (Corporate author)

Air Force Institute of Technology (AU)
Wright-Patterson AF Base, Ohio

2a. REPORT SECURITY CLASSIFICATION

UNCLASSIFIED

2b. GROUP

3. REPORT TITLE

Determination of the Effects of Mass and Stiffness of the Vibration
Response of Ribbed Panels Subjected to Random Acoustic Noise

4. DESCRIPTIVE NOTES (Type of report and inclusive dates)

Thesis

5. AUTHOR(S) (First name, middle initial, last name)

Clarence M. Bose, Captain, USAF

6. REPORT DATE

December 1973

7a. TOTAL NO. OF PAGES

96

7b. NO. OF REFS

18

8a. CONTRACT OR GRANT NO.

b. PROJECT NO

c.

d.

9a. ORIGINATOR'S REPORT NUMBER(S)

GA/MC/73A-1

9b. OTHER REPORT NO(S) (Any other numbers that may be assigned
this report)

10. DISTRIBUTION STATEMENT

Approved for public release; distribution unlimited.

11. SUPPLEMENTARY NOTES

Approved for public release; IAW AFR 190-
JERRY C. FAX, Captain, USAF
Director of Information

12. SPONSORING MILITARY ACTIVITY

WFDDL-FYS
AF Flight Dynamics Laboratory
Wright-Patterson AFB, Ohio

13. ABSTRACT

The purpose of this report is to experimentally determine the effects of localized mass and stiffness parameters on the vibration response of stiffened panel structures excited by acoustic noise. Eleven panels were constructed, similar in weight and configuration with typical aircraft panel structures. A baseline panel was used to determine reference mass and stiffness properties; five panels were varied in mass with stiffness kept constant, and five panels with constant mass were varied in stiffness. The panels were excited in an acoustic reverberation test facility using a broad-band siren and horn assembly. Excitation and response measurements were taken using microphone and accelerometer transducers attached to the panels. The data were then reduced and correlated to construct vibration prediction curves as a function of excitation/response levels, frequency, and mass and stiffness parameters. In addition, an empirical mathematical model was derived to predict response levels knowing the excitations and the mass and stiffness parameters of a panel structure. A frequency dependent variable based on measured data was determined to relate these parameters to the panel responses. It was concluded that the vibration prediction curves and the empirical prediction model were sufficient to adequately predict responses to acoustic excitation provided certain limitations and assumptions were recognized. Further testing of many different types of panel structures was recommended to determine if these prediction techniques could be applied to all classes of panels.

Reproduced by
NATIONAL TECHNICAL
INFORMATION SERVICE
U S Department of Commerce
Springfield VA 22151

DD FORM 1473
1 NOV 68

UNCLASSIFIED

Security Classification

UNCLASSIFIED

Security Classification

14. KEY WORDS	LINK A		LINK B		LINK C	
	ROLE	WT	ROLE	WT	ROLE	WT
Acoustic Vibration Random Vibration Vibration Prediction Ribbed Panels Panel Vibration Vibration Response Mass and Stiffness Effects on Panel Vibration						

UNCLASSIFIED

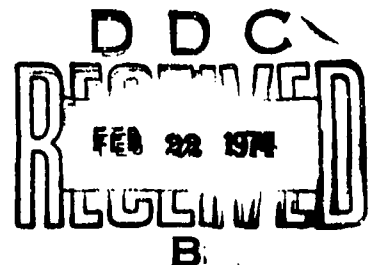
Security Classification

DETERMINATION OF THE EFFECTS OF MASS
AND STIFFNESS ON THE VIBRATION RESPONSE
OF RIBBED PANELS SUBJECTED
TO RANDOM ACOUSTIC NOISE

THESIS

GA/MC/73A-1

Clarence M. Bose
Captain USAF



Approved for public release, unlimited distribution.

DETERMINATION OF THE EFFECTS OF MASS AND STIFFNESS
ON THE VIBRATION RESPONSE OF RIBBED PANELS
SUBJECTED TO RANDOM ACOUSTIC NOISE

THESIS

Presented to the Faculty of the School of Engineering
of the Air Force Institute of Technology

Air University

In Partial Fulfillment of the
Requirements for the Degree of
Master of Science

by

Clarence M. Bose, B. S.
Captain USAF

Graduate Astronautical Engineering

December 1973

Approved for public release; distribution unlimited.

Preface

This report is the result of my attempt to develop empirical techniques which will better enhance the accuracy of vibration prediction methods as applied to complex aerospace structures. The work represented here has been interesting and challenging primarily due to difficulties inherent with the problem and the general lack of knowledge which has frustrated anyone working in this field. A large measure of credit for my understanding of this complex area of study is due to the assistance given to me by others.

I would like to publicly acknowledge my indebtedness to my advisor, Dr. P. J. Nemergut, for his insight and guidance throughout this study. I would also like to express my appreciation to Mr. Charles Thomas and the personnel of the Dynamics Technology Applications Branch of the Flight Dynamics Laboratory, whose assistance with experimental apparatus and data analysis made this study a reality. In addition, I would especially like to express my gratitude to Capt James E. Marsh, who worked closely with me, providing valuable assistance and knowledge, enabling me to overcome a myriad of problems encountered in completing this study.

Clarence M. Bose

Contents

	Page
Preface	iii
List of Figures	vi
List of Tables	ix
Symbols and Abbreviations	x
Abstract.	xii
I. Introduction	1
The Problem	2
Background	2
Scope	4
Subproblems	5
Attack of Subproblems	5
II. Theory	7
Determination of Panel Damping	7
The Random Vibration Prediction Model	9
III. Panel Construction	16
Variation in Panel Mass	16
Variation in Panel Stiffness	18
Static Deflection Tests	18
IV. Sinusoidal Sweep Testing	23
Purpose of the Experiment	23
Description of Test Apparatus	23
Other Apparatus	25
Calibration of the Apparatus	28
Experimental Techniques	28
Modal Tests	28
Impedance Measurements	32
Results of Experiment	32
V. Random Vibration Experimentation	35
Purpose of the Experiment	35
Description of the Wide Band Acoustic Facility	35
Experimental Techniques	39
Facility Instrumentation	43
Data Analysis	43

Contents

VI. Data Reduction and Results	47
Effects of Panel Damping	47
Correlation of Static Stiffness Data	47
Determination of Mass and Stiffness Parameters	48
Construction of Vibration Prediction Curves	49
Application of Empirical Prediction Model	51
Summary of Results	56
Discussion of the Prediction Curves	56
Discussion of the Empirical Prediction Model	56
VII. Conclusions and Recommendations	59
Conclusions	59
Recommendations	61
Bibliography	61
Appendix A: Derivation of Angle Section Moment of Inertia and Area Equations	63
Appendix B: Excitation and Response Levels from the Random Vibration Tests	65
Appendix C: Empirical Prediction Curves; Response Versus Variation in Mass	76
Appendix D: Empirical Prediction Curves; Response Versus Variation in Stiffness	86
VITA	96

List of Figures

Figure		Page
1	The Single Mass Oscillator	8
2	The Stiffened Panel Cross-Section	14
3	Test Panel Configuration	17
4	Test Panel with Bonded Lead Weights	19
5	Block Diagram of Test Apparatus	24
6	Experimental Apparatus	26
7	Ling-Tempco-Vought Vibration Console	27
8	Test Panel and Shaker Mounted to Test Bed	29
9	Reference Accelerometer and Force Gage Attachment	30
10	Accelerometer Attachment for Sinusoidal Tests	31
11	Acceleration Response, Panel A, Accelerometer 4	33
12	Acceleration Response, Panel K, Accelerometer 4	33
13	Wide Band Acoustic Facility	36
14	Floor Plan of Test Facility	37
15	Test Fixture	38
16	Accelerometer Positions for Random Tests	40
17	Front View of Mounted Test Panel	41
18	Rear View of Mounted Test Panel	42
19	Data Collection and Monitoring System	44
20	One-Third Octave Band Analysis System	46
21	Overall Response Levels for Variation in Mass	52
22	Overall Response Levels for Variations in Stiffness	53
23	Frequency Dependent Variable, $C(f)$, for Empirical Prediction Model	55

List of Figures

Figure		Page
24	Angle Stiffener Configuration	64
25	Acoustic Sound Pressure Levels, Panel A	66
26	Acceleration Response, Panel A, Accelerometer 1	67
27	Acceleration Response, Panel A, Accelerometer 2	68
28	Acceleration Response, Panel A, Accelerometer 3	69
29	Acceleration Response, Panel A, Accelerometer 4	70
30	Acceleration Response, Panel A, Accelerometer 5	71
31	Acceleration Response, Panel A, Accelerometer 6	72
32	Acceleration Response, Panel A, Accelerometer 7	73
33	Acceleration Response, Panel A, Accelerometer 8	74
34	Acceleration Response, Panel A, Accelerometer 9	75
35	Prediction Curve, Accelerometer 1, Variation in Mass	77
36	Prediction Curve, Accelerometer 2, Variation in Mass	78
37	Prediction Curve, Accelerometer 3, Variation in Mass	79
38	Prediction Curve, Accelerometer 4, Variation in Mass	
39	Prediction Curve, Accelerometer 5, Variation in Mass	
40	Prediction Curve, Accelerometer 6, Variation in Mass	82
41	Prediction Curve, Accelerometer 7, Variation in Mass	83
42	Prediction Curve, Accelerometer 8, Variation in Mass	84
43	Prediction Curve, Accelerometer 9, Variation in Mass	85
44	Prediction Curve, Accelerometer 1, Variation in Stiffness	87
45	Prediction Curve, Accelerometer 2, Variation in Stiffness	88

List of Figures

Figure		Page
46	Prediction Curve, Accelerometer 3, Variation in Stiffness	89
47	Prediction Curve, Accelerometer 4, Variation in Stiffness	90
48	Prediction Curve, Accelerometer 5, Variation in Stiffness	91
49	Prediction Curve, Accelerometer 6, Variation in Stiffness	92
50	Prediction Curve, Accelerometer 7, Variation in Stiffness	93
51	Prediction Curve, Accelerometer 8, Variation in Stiffness	94
52	Prediction Curve, Accelerometer 9, Variation in Stiffness	95

List of Tables

Table		Page
I.	24" by 30" Aluminum Panel Specifications	20
II.	Test Panel Static Stiffnesses	21
III.	Characterized Mass and Stiffness Parameters	50

Symbols and Abbreviations

Symbol

A	total panel surface area
A_a	modal area
a, b	overall panel dimensions
c	coefficient of damping
c_c	coefficient of critical damping
C(f)	frequency dependent variable determined empirically from measured data
d	rib thickness
D	flexural plate rigidity
dB	decibel
E	Young's modulus
F	complex sinusoidal force
F(t)	mean square force per Hz
f	frequency, Hz
"g"	32.2 ft/sec ²
\bar{g}	mean square acceleration with respect to earth's gravity
g_{rms}	root mean square acceleration with respect to earth's gravity
h	panel skin thickness
Hz	hertz, 1/sec
i	$(-1)^{\frac{1}{2}}$
$I_{a,b}$	moment of inertia of panel cross-section of width a or b
I_{xx}	moment of inertia of stiffener cross-section

Symbols and Abbreviations

Symbol	
k	generalized stiffness or single stiffness
l_1, l_2	length of angle stiffener legs
l	height of generalized stiffener
m, n	mode number or effective half-wavelength
m	mass
N_r	number of stringers or frames over the panel cross-section
$P(f)$	mean square pressure per Hz
ρ	density
ζ	damping ratio; c/c_0
SPL	sound pressure level
t	plate thickness
V	complex velocity
ν	Poisson's ratio
ω	frequency
ω_n	natural frequency
W	total panel weight
W_a	modal weight
$x(t)$	displacement, time dependent
\bar{y}	distance of centroidal axis from reference plane
Z	complex mechanical impedance

Abstract

The purpose of this report is to experimentally determine the effects of localized mass and stiffness parameters on the vibration response of stiffened panel structures excited by acoustic noise. Eleven panels were constructed, similar in weight and configuration with typical aircraft panel structures. A baseline panel was used to determine reference mass and stiffness properties; five panels were varied in mass with stiffness kept constant, and five panels with constant mass were varied in stiffness. The panels were excited in an acoustic reverberation test facility using a broad-band siren and horn assembly. Excitation and response measurements were taken using microphone and accelerometer transducers attached to the panels. The data were then reduced and correlated to construct vibration prediction curves as a function of excitation/response levels, frequency, and mass and stiffness parameters. In addition, an empirical mathematical model was derived to predict response levels knowing the excitations and the mass and stiffness parameters of a panel structure. A frequency dependent variable based on measured data was determined to relate these parameters to the panel responses. It was concluded that the vibration prediction curves and the empirical prediction model were sufficient to adequately predict responses to acoustic excitation provided certain limitations and assumptions were recognized. Further testing of many different types of panel structures was recommended to determine if these prediction techniques could be applied to all classes of panels.

DISCRIMINATION OF THE EFFECTS OF MASS AND STIFFNESS
ON THE VIBRATION RESPONSE OF RIBBED PANELS
SUBJECTED TO RANDOM ACOUSTIC NOISE

I. Introduction

Predictions of vibrations are needed early in aircraft development to enable the design engineer to make reasonable estimates of preliminary specifications for components and equipment (Ref 1:1). Analytical techniques involving the solution of equations of motion of a structure provide the necessary vibration tools for the low frequency regime. At middle and higher frequency regimes, however, present methods prove inadequate in predicting response levels of structures, due to the highly coupled and complex nature of the excitations and responses. The use of statistical techniques to relate vibration response levels with the significant parameters which describe the excitation and the structure appears to be the only reasonable approach to this complex problem. The few limited attempts to develop empirical or semi-empirical vibration prediction methods show several orders of magnitude of scatter in measured data even when some scaling or normalization scheme is used to account for variations in local parameters. Major consideration should be given, therefore, to the improvement of existing empirical techniques in which statistical analysis is used to correlate the measured excitations and responses with detailed local structural parameters. Once these relationships are developed and the necessary numerical evaluations made for representative flight vehicle structural components, a practical engineering method should result for vibration prediction during initial design (Ref 2:6).

The Problem

The purpose of this report is to experimentally determine the effects of localized mass and stiffness parameters on the vibration response levels of ribbed panels excited by random acoustic noise. Analysis of response data taken from a group of simplified panel structures is performed. These response data are then correlated in order to develop empirical relations, expressed in engineering terms, which can be incorporated into existing prediction techniques.

Background

The response of many types of structures has been studied in the past both analytically and experimentally. By far the largest class of problems treated has been simple panels, and good results have been obtained for this class of structures. More recent studies have considered the responses of complex rib-stringer systems and integrally stiffened panels using several approximate techniques. Very little experimental work has been introduced, however, and results have been somewhat inconclusive; results for the most part being based on a limited amount of data.

Experimentation has proceeded in three main areas. First, full-scale proof testing of aircraft structures, primarily in the study of sonic fatigue, has been explored. Most of the full-scale measurements have and are being made by aircraft manufacturers, and little of the data has been fully analyzed and published.

Second, effort has been exerted to develop design curves to aid in design of structures subjected to acoustic noise. The curves are primarily semi-empirical in nature and are generally based on a few scattered tests on real or representative structures.

Finally, a number of reasonably well controlled test results are available, mostly for simple panels, although some multi-bay panel data are given in Refs 5-9. For the most part, however, little documented data are available (Ref 10:9-10).

Much of the experimentation on multi-bay panel systems thus far has been concerned primarily with stress and fatigue responses of structural elements. Little effort has been observed concerning the effects on responses of such local parameters as mass, stiffness, curvature, effective thickness, and so on. Roberts (Ref 11:77-91) attempted to relate flight vehicle response with excitation and vehicle operating conditions. In addition to emphasis on local dynamic properties of panel structures, a study of local responses was correlated against circumferential attenuation, local mass and stiffness. Overall acceleration response levels were plotted against variations in stiffness and mass. Roberts determined that overall response levels were insensitive to structural stiffnesses, however, no dependence of these mass and stiffness parameters on frequency was discussed.

White, et al (Ref 2), recognizes the need for a major effort to develop vibration response prediction methods which account for necessary excitation parameters and local structural parameters. The report discusses the general philosophy of the problem, develops general equations for predicting vibration responses of complex, linear structures, and sets forth methods for developing prediction tools from these relations. Experimental methods are not discussed.

A more recent study performed by Bolt, Beranek, and Newman, Inc. (Ref 1:81-97), applies several vibration prediction techniques to responses from aero-acoustic excitations. Experimental data were taken from two radically different locations on an RF-4C fighter aircraft, one

location characterized by a "limp," unstiffened panel-like structure, and the other location characteristic of a massive structure. One particular vibration prediction method, a modified form of the Franken Method, was chosen because of its ability to account for gross structural and configurational differences. Data were plotted as a function of acceleration/pressure ratios versus frequency. Results showed that below 2000 Hz, a single prediction plot was sufficient to cover both structures. Above 2000 Hz, two plots were shown; one applicable to a massive, stiffened structure, and one applicable to the "limp" panel structure. Although the technique demonstrates the applicability of the method, the results were somewhat questionable due to the limited amount of data collected and structures examined.

Scope

Typical aircraft structures vary considerably in configuration, materials and construction. Variations in mass and stiffness in any particular panel structure can be dependent on many variables. In order to achieve a measure of control and accuracy, a highly simplified panel model was used for experimentation. Only a limited number of nine-bay, aluminum panels, identical in overall dimensions and configuration, were tested. Stiffener cross-sectional area was the only variable in construction, while lead weights were added to the panels to vary total mass. The response data from these panels were analyzed and correlated with respect to mass, stiffness and excitation/response levels in an attempt to develop a method for accounting for variations in these parameters which could be used for future testing of more complicated structures.

Subproblems

Many empirical prediction techniques attempt to account for structural parameters by applying some type of normalization scheme, or by use of appropriate mass and stiffness scaling. These parameters are very difficult to account for, however, due to the complex nature of the panel structure. Such variables as damping, mass loading, and construction techniques can have marked results on experimental data. An attempt was made in this study to construct panels which would minimize these variable effects. For example, the addition of lead to the panels is bound to affect both the damping and stiffness of the structures to some degree. The effects of this lead addition were studied.

In order that the response data will have some significance, it is important that the correlation of excitation and response be expressed through statistical analysis into a form which is readily usable. Empirical relationships in the form of prediction curves are explored to compare mass and stiffness of the panels. In addition, a mathematical model is derived based on measured test data and the characterized mass and stiffness parameters for the panels.

Experimental accuracy, of course, will have some effect on the usefulness of the data obtained and the resulting analysis. Causes of error resulting from equipment and test procedures will be pointed out in this study.

Attack of Subproblems. This study is divided into four major parts. The first part involves the fabrication of a number of simplified representative aircraft panel structures. Eleven panels are constructed with one panel representing a baseline panel to determine reference mass and stiffness properties. Five panels are varied in mass while stiffness

is kept constant, and an additional five panels are varied in stiffness with mass remaining constant. Measurements of weight, stiffener cross-sectional area, and stiffener moment of inertia values are tabulated.

The second part of the study involved vibration testing of the panels with the use of a mechanical shaker driven by a sinusoidal force to obtain acceleration frequency plots. The plots are then used to examine the resonant modes of the panels and to determine the relative damping caused by addition of lead to the panel stiffeners. A static deflection test is then performed on each of the panels to determine static stiffnesses. Experimental errors in the apparatus will be examined.

Following the sinusoidal testing, the panels are subjected to random acoustic excitation. A random noise producing siren is used to excite the panels, and excitation and response levels are recorded in digital and graphical form. The last section of the study then combines the sinusoidal and random test data in an attempt to correlate the random excitations and responses of the panels with variations in mass and stiffness. A theoretical single-mass-oscillator model will be applied to the results to derive relations which account for these variations. The theory for application of this model is presented in the next section of this report.

II. Theory

Determination of Panel Damping

The amount of damping present in a complex structure, such as a multi-bay panel, is very difficult to accurately determine and requires rather sophisticated test equipment. Where it is desired only to compare damping between similar structures, a much simpler approach may be used which provides a good approximation. Such a method involves consideration of the mechanical impedance of a single-mass-oscillator subjected to a harmonic force (See Fig.1). At frequencies much higher than the fundamental, panel modes are essentially decoupled, and the single mass model is quite representative of the panel response characteristics (Ref 15:345-346).

Complex mechanical impedance is defined as

$$Z = \frac{F}{V} \quad (1)$$

where . Z is the complex mechanical impedance

 F is the complex harmonic force

 V is the complex velocity

Crandall, et al (Ref 12:Cht 1-27), derives the complex mechanical impedance for the single-mass-oscillator as shown in Fig.1 as

$$Z = \frac{K}{i\omega} + c + i\omega m \quad (2)$$

where K is the spring constant

 c is the coefficient of damping

ω is the steady-state frequency of the system

Or expressed in a more convenient form,

$$Z = \frac{(K - \omega^2 m) + i\omega c}{i\omega} \quad (3)$$

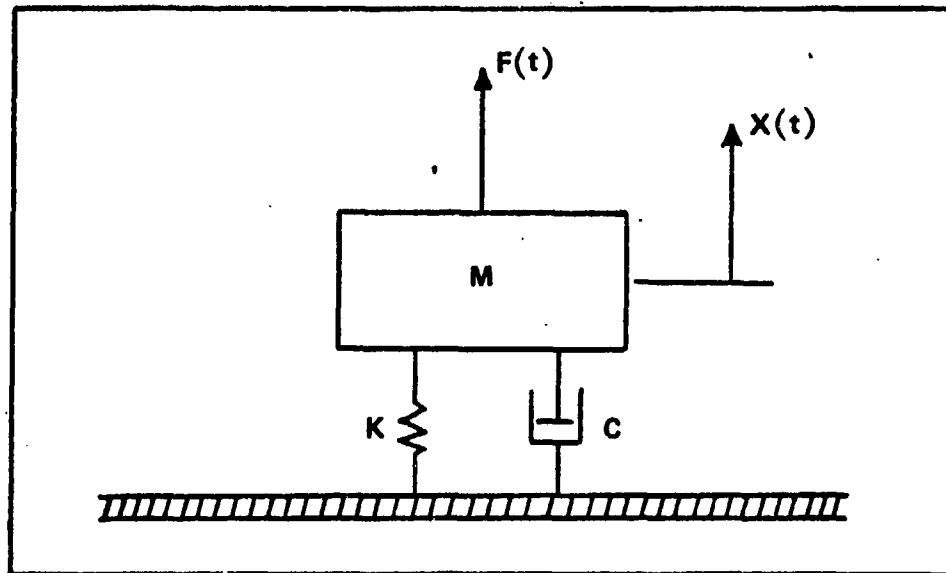


Fig. 1. The Single Mass Oscillator

Resonance of the system shown in Fig. 1 occurs when the steady-state frequency of the forced system is equal to the natural frequency of the system, ω_n , or

$$\omega = \omega_n = \sqrt{k/m} \quad (4)$$

Substituting Eq (4) into Eq (3), the complex mechanical impedance at resonance then becomes

$$Z = c \quad (5)$$

Thus, by modeling a single panel mode with the response of a single-mass-oscillator, the impedance at a resonant frequency is equal to the damping coefficient of the structure. With the coefficient of damping once determined, it is then possible to define the damping ratio of the system as

$$\xi = \frac{c}{c_c} \quad (6)$$

where ξ is the damping ratio; dimensionless

c is the damping coefficient

c_c is the critical damping coefficient, equal to $2m\omega_n$

For a panel vibrating at a resonant frequency, m is now defined as the modal mass which can be determined by plotting impedance versus frequency as a function of mass.

The Random Vibration Prediction Model

It is well known that the natural vibration characteristics of many complex structures can be approximated by consideration of each individual resonance or mode of vibration, assuming it to be essentially unaffected by, or decoupled from, any other modes (Ref 15:345-346). Considering vibrational modes at frequencies far above the first few bending modes of the total structure, responses to acoustic excitations tend to be quite localized, and independent of similar resonant responses for modes which differ by a few wavelengths. Assuming that the responses in these higher modes are independent and somewhat linear, i.e., the modal responses in a given band vary linearly with the sound pressure level, then the vibration response becomes the net of the contributions of many resonant modes. This also implies that the vibration level can be expected to vary linearly with the response of a single excited mode.

Making the above assumptions, the response of a particular panel mode of vibration can be approximated by analysis of the same single mass oscillator discussed previously and shown in Fig 1. The mean square acceleration for this model when subjected to a continuous random forcing function is given in Ref 2:78 as

$$\frac{\bar{a}^2}{g^2} = \frac{\pi f \overline{P(f)}^2}{4 c/c_w^2} \quad (7)$$

where \bar{g}^2 is the mean square acceleration of the mass,
referenced to earth's gravity

f is the natural frequency in Hz

$\overline{P(f)}^2$ is the mean square force in lb^2 per Hz

c/c_c is the damping ratio; dimensionless

W is the weight of the mass in pounds

If this model is now adapted to the case of a single panel mode responding to random fluctuating pressure, Eq (7) becomes (Ref 14),

$$\bar{g}^2 = \frac{f \overline{P(f)}^2 A_a^2}{4 \frac{c}{c_c} W_a^2} \quad (8)$$

where, now \bar{g}^2 is approximately the mean square acceleration of the mode

f is the resonant frequency of the mode in Hz

$\overline{P(f)}^2$ is the mean square pressure in psi squared per Hz

A_a is the model area participating in the response; in²

W_a is the model weight in pounds involved in the responding mode

In considering the manner in which vibratory response might vary with structural mass and stiffness, it is sufficient to lump constant terms into a single parameter. Assuming damping to be constant, the rms response can then be expressed

$$g_{\text{rms}} = B_1 \left[\frac{f \overline{P(f)}^2}{(W/A_a)^2} \right]^{\frac{1}{2}} \quad (9)$$

where B_1 is now some constant of proportionality.

In order to derive an equation which is explicitly a function of structural stiffness, it is recognized that the modal frequency, f , is

a function of stiffness. If the panel structure is modeled by an equivalent isotropic plate having comparable stiffness properties, the equivalent plate frequency for a resonant mode can be expressed as

$$f = \frac{\pi}{2} \left(\frac{m^2}{a^2} + \frac{n^2}{b^2} \right) \left(\frac{D}{\rho t} \right)^{1/2} \quad (10)$$

where the plate flexural rigidity is

$$D = \frac{Et^3}{12(1-\nu^2)} \quad (11)$$

and m, n refer to the mode numbers, or effective half-wavelengths of a mode

a, b are the dimensions of the plate in inches

ρ is the density in pounds per inch cubed

t is the thickness in inches

E is Young's Modulus in pounds per inches squared

ν is Poisson's Ratio; dimensionless

Substituting the value for frequency into Eq (10) and grouping terms

$$g_{rms} = B_1 \left[\frac{m^2}{a^2} + \frac{n^2}{b^2} \right]^{1/2} \left[\frac{D}{\rho t} \right]^{1/4} \left(\frac{P(f)}{W/A} \right)_a \quad (12)$$

Evaluation of Eq (12) would require a knowledge of the half-wavelengths for each mode as well as the modal weight and area. This would necessitate an unwieldy number of computations. It is desirable, therefore, to approximate Eq (12) by considering

$$(W/A)_a = G(f) W/A \quad (13)$$

and

$$\frac{m}{a}^2 + \frac{n}{b}^2 = H(f) \left(\frac{1}{a^2} + \frac{1}{b^2} \right) \quad (14)$$

where now, W/A is the total panel weight per unit area; $G(f)$ and $H(f)$ are some functions of frequency. Performing these substitutions into Eq (12) and defining a new variable, $C(f)$, the rms response becomes

$$e_{\text{rms}} = C(f) \left[\frac{1}{a^2} + \frac{1}{b^2} \right]^{\frac{1}{4}} \left[\frac{D}{\rho t} \right]^{\frac{1}{4}} \frac{P(f)}{W/A} \quad (15)$$

Since $C(f)$ is now the only parameter in Eq (15) which is a function of frequency and mode shape, it can be determined empirically from measured data. Further, recognizing that the function ρt is in units of weight per unit area, the response can finally be expressed as

$$e_{\text{rms}} = C(f) (a^2 + b^2)^{\frac{1}{4}} \left[\frac{D}{(W/A)^5} \right]^{\frac{1}{4}} \frac{P(f)}{A} \quad (16)$$

In terms of common engineering parameters, Eq (16) relates the excitation and response characteristics of a panel structure knowing the dimensions, the weight per unit area, and the characterized stiffness; $C(f)$ being determined by empirical means.

To represent the structural stiffness of a stiffened panel with an equivalent plate of bending rigidity D , it is necessary to evaluate the equivalent plate thickness for the structure. Assuming, in general, an orthotropic panel with stringers and frames in opposing directions, a representative method of quantifying stiffness would be to sum the bending moments of inertia in each direction for the panel. Since the moment of inertia about the neutral axis of the structure is proportional to the moment of inertia about some other reference plane, the edge of the

panel can be conveniently chosen as the datum for ease of calculations (See Fig 2). The moment of inertia of the cross-section can then be expressed as

$$I_{a,b} = \frac{(a+b)h^3}{3} + N_p \left[\frac{dt^3}{12} + d \left(h + \frac{t}{2} \right)^2 \right] \quad (17)$$

where $I_{a,b}$ is the moment of inertia of the panel cross-section of width a or b; in⁴

a, b are the dimensions of the panel in inches

h is the thickness of the panel in inches

d is the height of a stringer or frame in inches

t is the thickness of the stringer or frame in inches

N_p is the number of stringers or frames over the panel cross-section; dimensionless

The sum of the moments of inertia can then be equated to the sum of the bending moments of inertia of an equivalent isotropic plate having the same dimensions. Again, using the edge of the plate as the datum

$$I_a + I_b = \frac{at^3}{3} + \frac{bt^3}{3} = \frac{(a+b)t^3}{3} \quad (18)$$

where the parameter, t, is the equivalent plate thickness. In quantifying stiffness in this manner, torsional rigidities have been ignored since these values are proportional to the bending rigidities for structures of similar configuration. Solving Eq (18) for the equivalent plate thickness and substituting into Eq (11), the flexural rigidity for the equivalent plate becomes

$$D = \frac{3E}{12(a+b)(1-\nu^2)} \left[I_a + I_b \right] \quad (19)$$

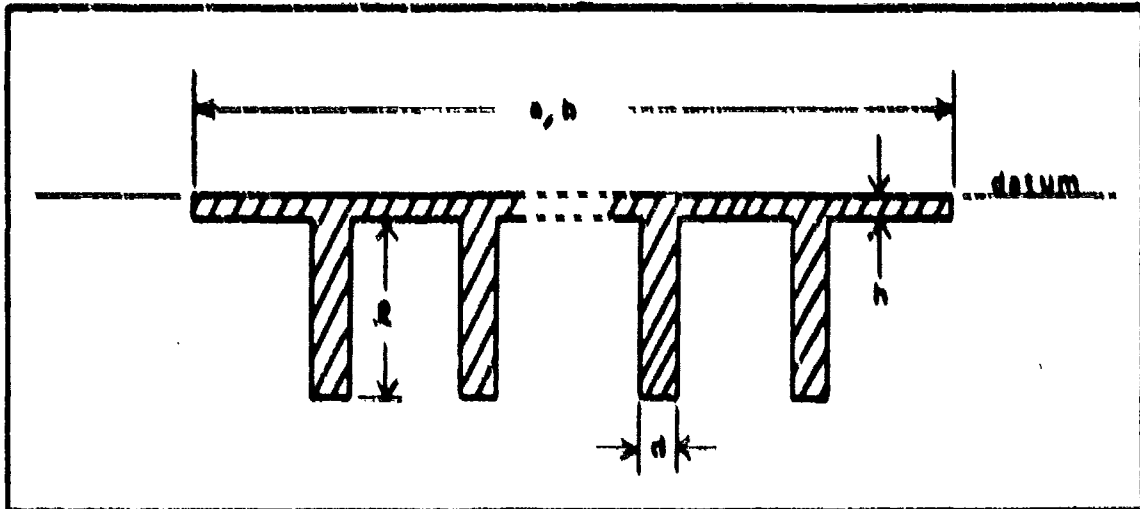


FIG. 2. The Stiffened Panel Cross-section

Examination of Eqs (18) and (19) reveals that the characterized stiffness of the panel structure using an equivalent plate model is dependent on the panel dimensions and the stringer and frame spacing; spacing being dependent on the number of stringers or frames present over the panel width.

It was determined that the response of a structure could be predicted using Eq (16), knowing the excitations, the characterized mass and stiffness parameters for the structure, and the function $C(f)$. It should be recognized that while the method for quantifying stiffness is not representative of actual panel stiffness, the derived stiffness parameter, D , can be expected to be proportional to actual stiffness in some manner. Because stiffness is such a difficult quantity to determine for a complex structure, the method does permit characterization of the stiffness in terms of the significant structural parameters. Differences which may exist between these characterized parameters and actual parameters can be accounted for by determining $C(f)$ from measured data taken from panel structures for which these parameters are known. Thus, unless an entirely different approach is taken, any minor modification

in the method for quantifying stiffness, or approximating any of the other frequency dependent parameters, would only change the value of $C(f)$ by some proportionate amount. The vibration prediction relation can be expected, therefore, to provide reasonable estimates of responses of structures using $C(f)$ in Eq (16), and the method for characterizing the mass and stiffness parameters from which $C(f)$ was determined.

III. Panel Construction

In determining the response of panels to variations in mass and stiffness parameters, it was desired to construct two sets of similar panels, one set varying in weight only, and one set varying only in stiffness. Panel configuration and fabrication was kept as simple as possible while a measure of similarity to actual aircraft structures in weight and construction was maintained.

Eleven aluminum, nine-bay panels were constructed. Stiffeners were made from stock angle aluminum and attached to the panel skin using one-eighth inch diameter aluminum rivets spaced one inch apart. All panels were constructed with identical overall dimensions and stiffener configuration in an attempt to keep variable effects in construction at a minimum. A constant skin thickness of 0.050 inches was used for all panels (See Fig. 3). Lead was added to the panels to vary total panel weight, and stiffener moment of inertia was varied to change panel stiffness. With one panel constructed as a baseline panel, five panels were varied in mass and five panels were varied in stiffness.

Variation in Panel Mass

Variation in mass for five panels was achieved with the addition of 3/4-inch square lead weights bonded between the stiffener rivets. A lumped mass approach was used, rather than using lead strips, to minimize increases in panel damping caused by the addition of the lead. Epoxy adhesive was used to bond the lead to the panels, epoxy being a relatively rigid adhesive material which affects damping very little (Ref 15:53). Total weight of the five panels was varied by a factor of approximately two times the baseline panel weight to cover the normal range of

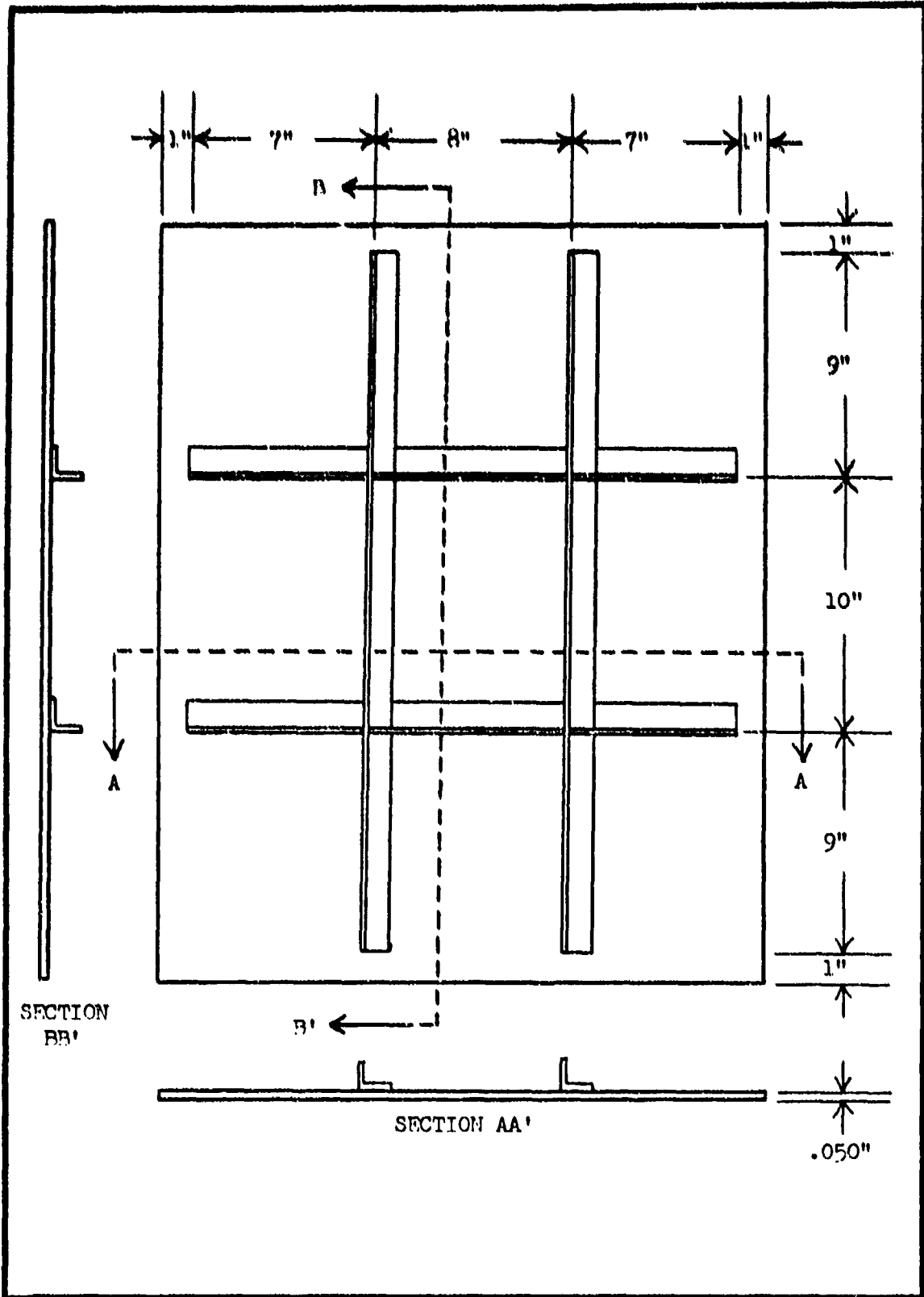


Fig. 3. Test Panel Configuration

structural weights encountered in typical aircraft structures. Figure 4 shows a typical panel with lead added to the stiffeners, and Table I lists the weights and dimensions for each of the eleven panels. Section IV of this report includes an analysis of damping effects caused by the addition of lead to the panels.

Variation in Panel Stiffness

Panel stiffness was varied by changing the moment of inertia of the aluminum stiffeners (See Appendix A). By keeping the cross-sectional area of the stiffeners constant, the weight of the panels was not altered from that of the baseline panel. Table I also includes the moment of inertia calculated for each stiffener type. As can be seen, the moment values for the five panels and the baseline panel varied by a factor of approximately sixteen, while mass was maintained within two per cent of the baseline panel mass. These small variations in weight were considered to be within tolerable limits for the constant mass panels.

Static Deflection Tests

A force/deflection test was performed on all panels to determine static stiffnesses. Each panel was simply supported at the boundaries, and static tests were taken at nine locations on the panel. These nine points corresponded to the same locations for attachment of accelerometers used in obtaining response data for the random noise tests (See Fig. 16, Sec. V). Table II lists the static stiffnesses calculated at each point on the panel. Deflections were measured only at the point of application of the load, hence, influence coefficients were not considered.

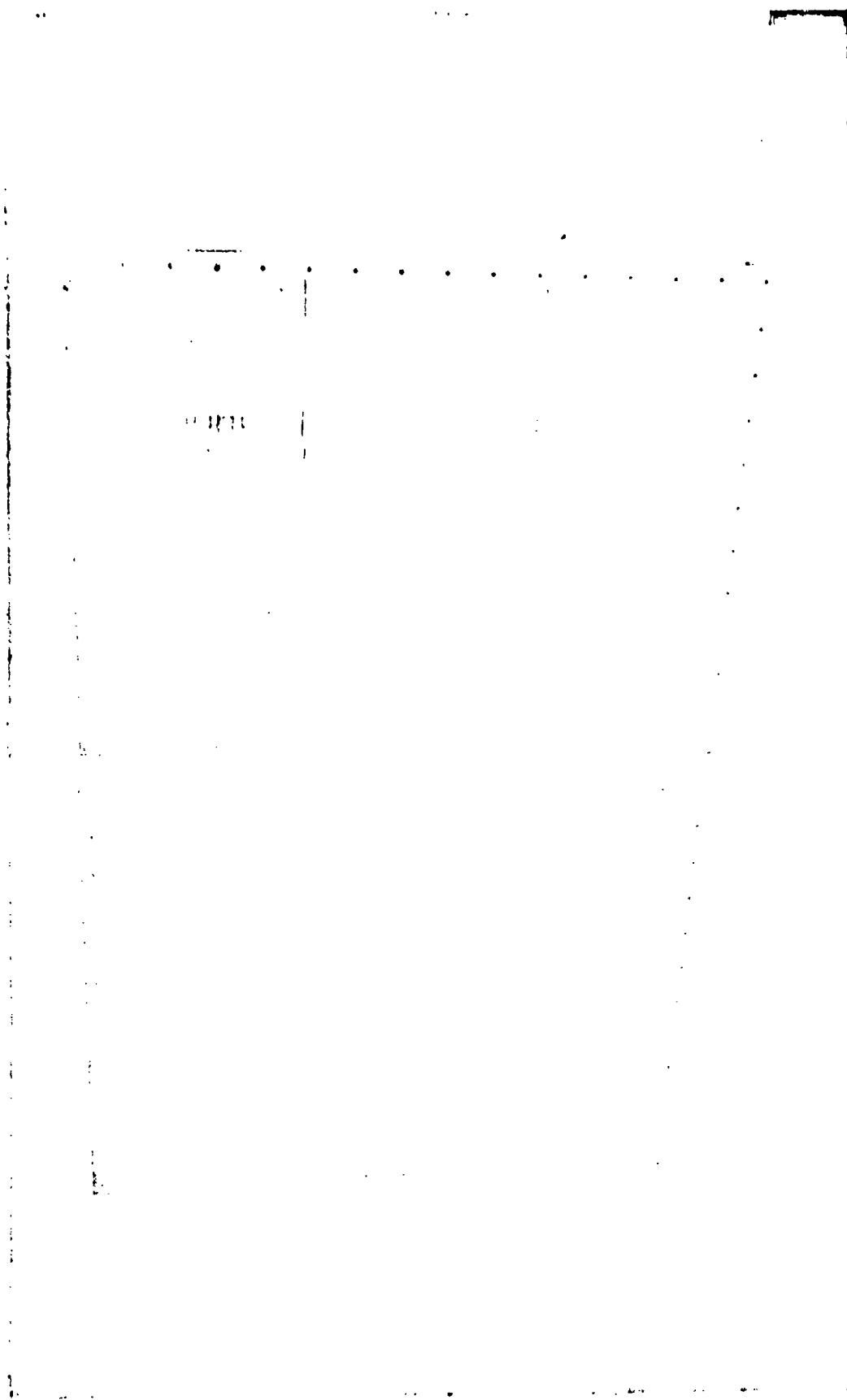


Fig. 4. Test Panel with Bonded Lead Weights

Table I. 24" by 30" Aluminum Panel Specifications

All panels were constructed with a skin thickness of .050"

Panel	Weight (lb)	Stiffener Dimensions ^a (in)			Stiffener Moment of Inertia (in ⁴)
		L ₁	L ₂	d	
A	5.44	1.00	1.00	.094	0.0171
B	5.38	0.75	1.25	.094	0.0045
C	5.53	0.75	0.80	.125	0.0096
D	5.50	1.25	0.75	.094	0.0288
E	5.50	1.50	0.50	.094	0.0510
F	5.38	2.20	0.75	.040	0.0680
G	6.22	1.00	1.00	.094	0.0171
H	6.94	1.00	1.00	.094	0.0171
I	7.75	1.00	1.00	.094	0.0171
J	9.00	1.00	1.00	.094	0.0171
K	9.97	1.00	1.00	.094	0.0171

^a Dimensions L₁, L₂ and d for the angle stiffener are given in Fig. 24, Appendix A

Table II. Test Panel Static Stiffnesses

Panel	Static Stiffness Calculated at Each Accelerometer Location (lb/in) ^a									Average Panel Stiffness (lb/in)	Stiffness Ratio w/r to Panel A
	Accelerometer Location (lb/in)										
	1	2	3	4	5	6	7	8	9		
A	347	328	331	421	399	238	290	318	380	350	1.00
B	273	212	142	267	252	237	170	158	233	216	0.62
C	307	249	233	296	286	274	222	230	352	272	0.78
D	243	237	293	318	495	447	472	490	389	376	1.07
E	462	420	348	340	451	428	538	497	542	448	1.28
F	515	467	340	442	503	386	495	600	582	481	1.37
G	398	363	316	467	455	386	366	366	451	396	1.13
H	374	333	299	373	416	362	387	442	502	387	1.11
I	354	315	270	343	411	379	372	387	452	364	1.04
J	361	335	317	439	554	542	432	443	463	395	1.13
K	364	340	309	455	600	560	432	414	463	437	1.25

^aReference Fig. 16, Sec. V for test locations 1-9.

Various weights were used for performing the tests, ranging from 2-5 pounds. In all cases the force/deflection curve proved to be linear; the slope representing the stiffness at the tested point. A wide range of values was obtained for these point stiffnesses primarily due to the boundary condition variance from one panel to the next, the atmospheric conditions, and the degree of prestressing present in a particular test. For this reason, the stiffness values listed in Table II represent an average of several tests performed on each panel.

As can be seen from Table II, a variation in stiffener moment of inertia by a factor of sixteen resulted in a total panel stiffness variation of approximately two times the lowest stiffness for the six constant mass panels. For the constant stiffness panels, Table II shows that stiffness did not remain constant, and in some cases, varied as much as 25 per cent from the baseline panel stiffness. Since the only variable in these panels, other than small variations in construction techniques, was the bonded lead weights, it must be assumed that the addition of the lead had considerable effect on panel stiffness. While this large variation does not appear to be intuitively representative of changes in panel stiffness due to the addition of lumped masses, these variations must be taken into account in analysis of the data taken in the random tests.

IV. Sinusoidal Sweep Experimentations

Purpose of the Experiment

This experimentation was performed to examine the resonant modes of the panels and to determine the effect on damping of adding lead weights to the panel stiffeners. An automatic frequency-sweep oscillator generating a sinusoidal force was used to obtain acceleration plots for the panels. Acceleration measurements were taken normal to the panel stringers at the same locations used to mount accelerometers in performing the random vibration tests. While the use of the automatic sweep oscillator precluded obtaining exact values for resonant peaks, this method proved suitable for locating the modal frequencies of the panels. Once the modal frequencies were identified, the resonant peaks were tuned manually to obtain exact force and acceleration readings. Point impedance was then calculated at these resonances from which panel damping was determined.

Description of Test Apparatus

Figure 5 depicts a block diagram of the experimental apparatus used in the sinusoidal sweep testing. A Bruel and Kjaer Level Recorder was used to record the acceleration response of the panels by plotting acceleration voltages on a logarithmic graph. The recorder was connected to a Bruel and Kjaer Beat Frequency Oscillator by a mechanical drive to keep the oscillator and graph paper synchronized in frequency. A sinusoidal voltage generated by the oscillator was fed to a console containing a Ling-Temco-Vought DC Power Amplifier and Field Source, where the signals were amplified and passed to a Ling-Temco-Vought

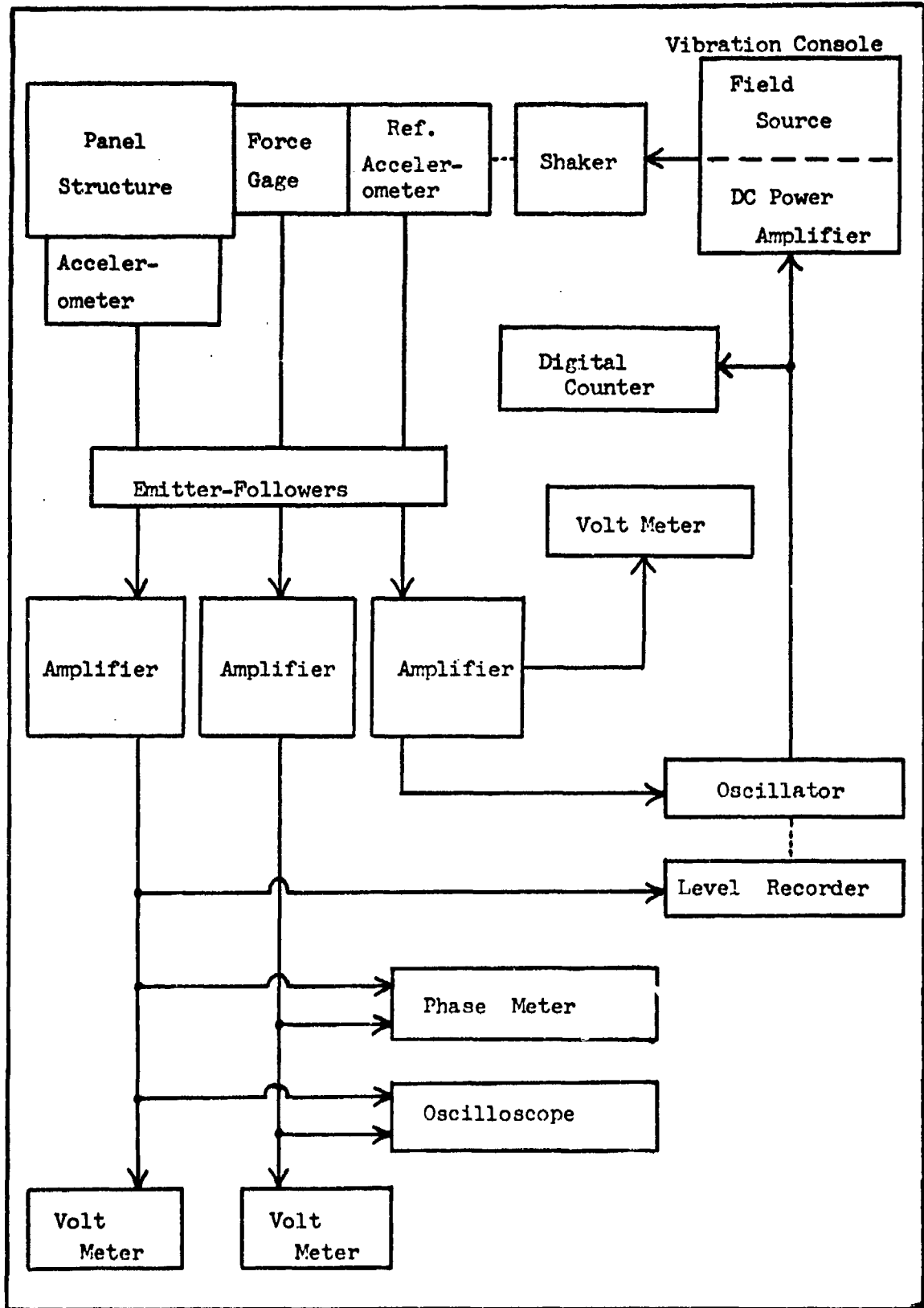


Fig. 5. Block Diagram of Test Apparatus

Electro-Magnetic Shaker. The force was picked up with a Wilcoxon L-10 Force Gage attached to the shaker head, and acceleration was picked up with a Columbia 606-2 Accelerometer mounted on the panel opposite the force gage. The force signal was passed to a Bruel and Kjaer Microphone Amplifier containing a voltmeter to monitor response; the acceleration signal was amplified by a Bruel and Kjaer Audio Frequency Spectrometer, also containing a voltmeter, and then fed to the level recorder. Both force and acceleration signals were first passed through in-line Bruel and Kjaer Emitter-Followers to condition the signals.

An additional accelerometer was used to provide a constant acceleration input to the system throughout the frequency range. A Columbia 902-H Accelerometer was attached to the shaker head. The signal from the accelerometer was amplified and fed back to the oscillator where the reference signal was used to control the voltage level of the oscillator output. A voltmeter attached to the amplifier provided a continuous reading of the reference accelerometer signal.

Other Apparatus. Additional apparatus was necessary to permit precise measurement of signal values and to monitor response levels. A Hewlett-Packard Electronic Digital Counter was connected to the oscillator to permit precise frequency control. The force and acceleration signals were measured for phase difference with the use of a Technology Instruments Phase Angle Meter. The signals were also monitored on a Hewlett-Packard Oscilloscope as a check on the waveform of the sinusoidal signals (See Figs. 6-7).

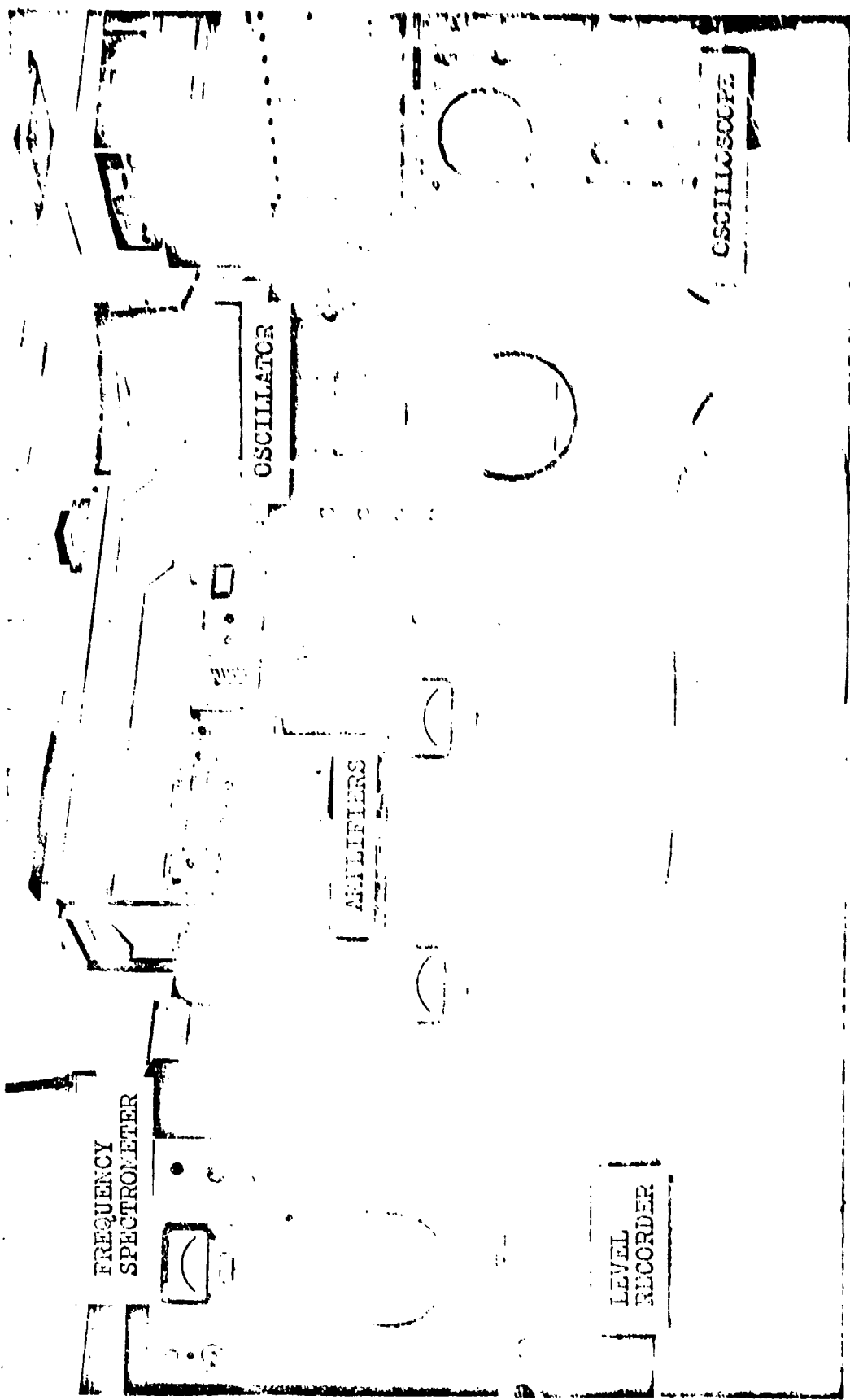


Fig. 6. Experimental Apparatus

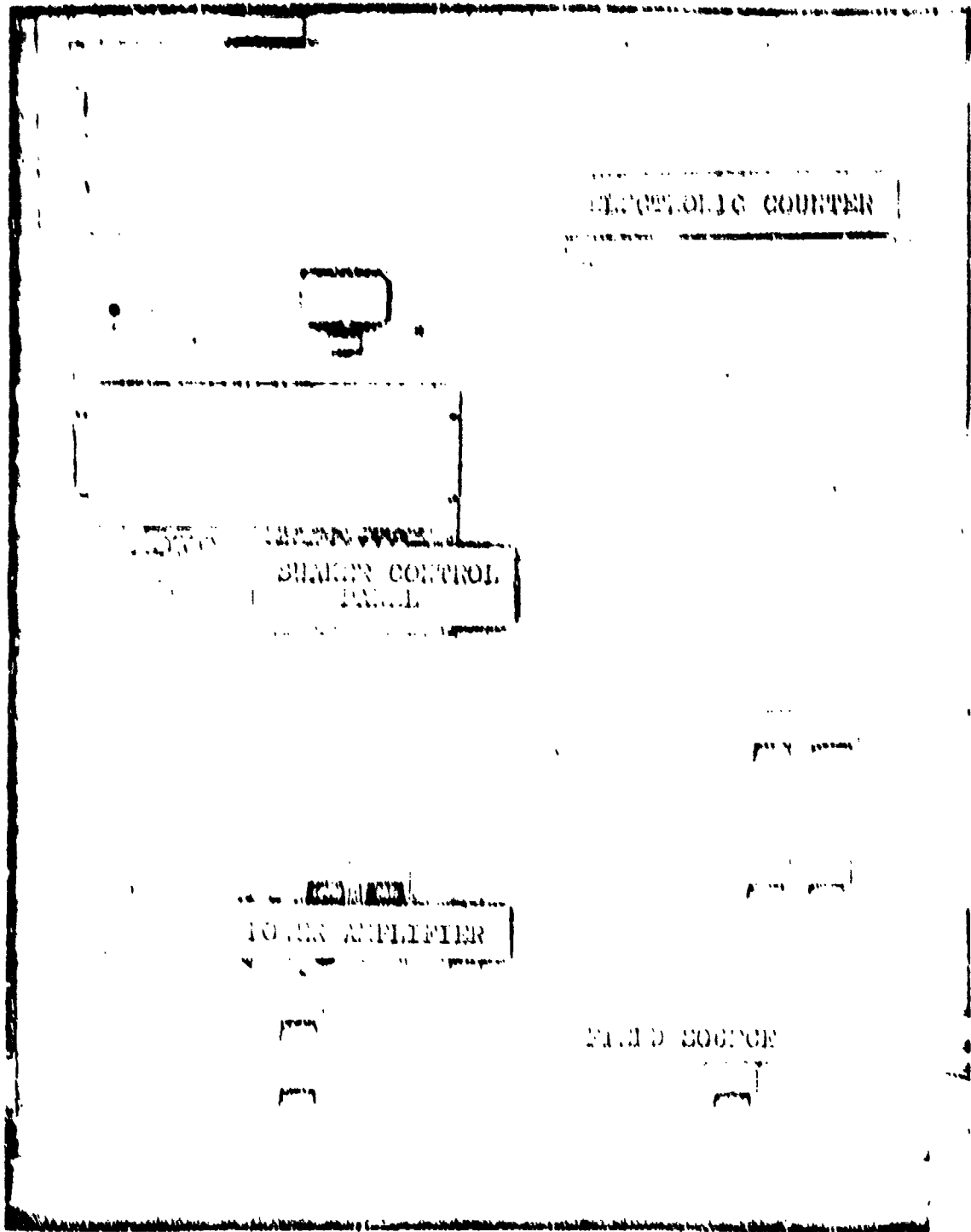


Fig. 7. Ling-Tempeo-Vought Vibration Console

Calibration of the Accelerometers

The accelerometers were mounted on a Bruel and Kjaer Calibration Shaker and shaken at one "g." The acceleration amplifiers were then adjusted until a convenient voltage was read on each voltmeter. A one pound mass was then mounted on the shaker and an accelerometer was affixed to the mass. The amplitude of the shaker was increased until the accelerometer indicated one "g," and the force amplifier was adjusted to a convenient voltage on the voltmeter.

Experimental Techniques

Each test panel was clamped in a rigid frame which was bolted to a massive test bed as shown in Fig. 8. The natural frequency of the structure was low enough (below 40 Hz) not to interfere with the response of the panels.

The shaker was attached to the structure through the force gage at one of the points to be investigated. The reference accelerometer was then mounted on the shaker head next to the force gage and used as a feedback to the oscillator in maintaining a constant acceleration input (See Fig. 9). The Columbia 606-2 Accelerometer was then mounted on the opposite side of the panel at the point of application of the shaker (See Fig. 10). Double-backed adhesive tape was used to attach the accelerometer and shaker to the panel.

Modal Tests. Five panels were tested to examine the resonant modes and to determine the damping. Panels A, H, I and K were selected to account for the full weight range of the constant stiffness panels. In addition, Panel D was tested as a check on the damping present in the constant mass panels where no load was used. Each panel was tested at

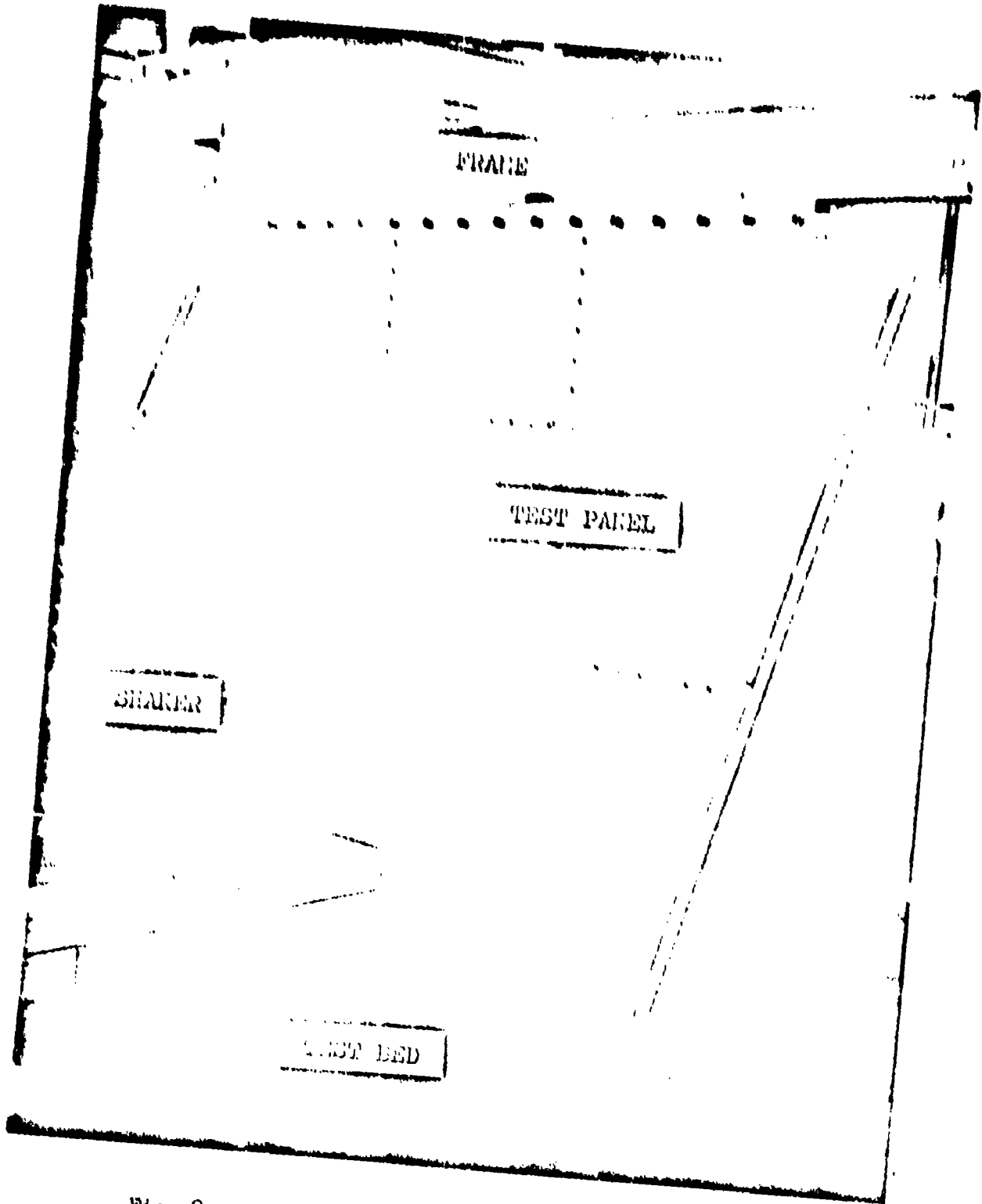


Fig. 8. Test Panel and Shaker Mounted to Test Bed

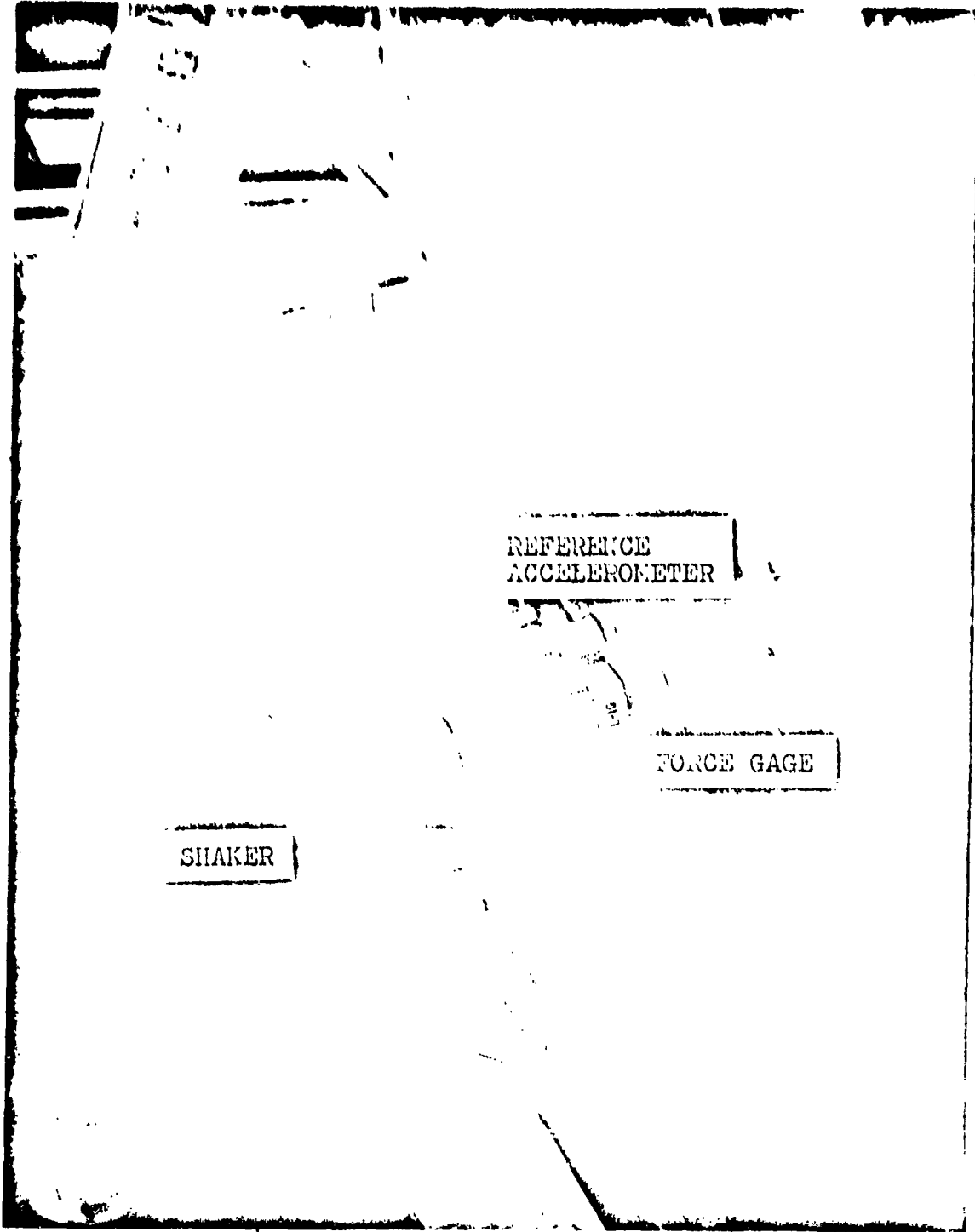


Fig. 9. Reference Accelerometer and Force Gage Attachment

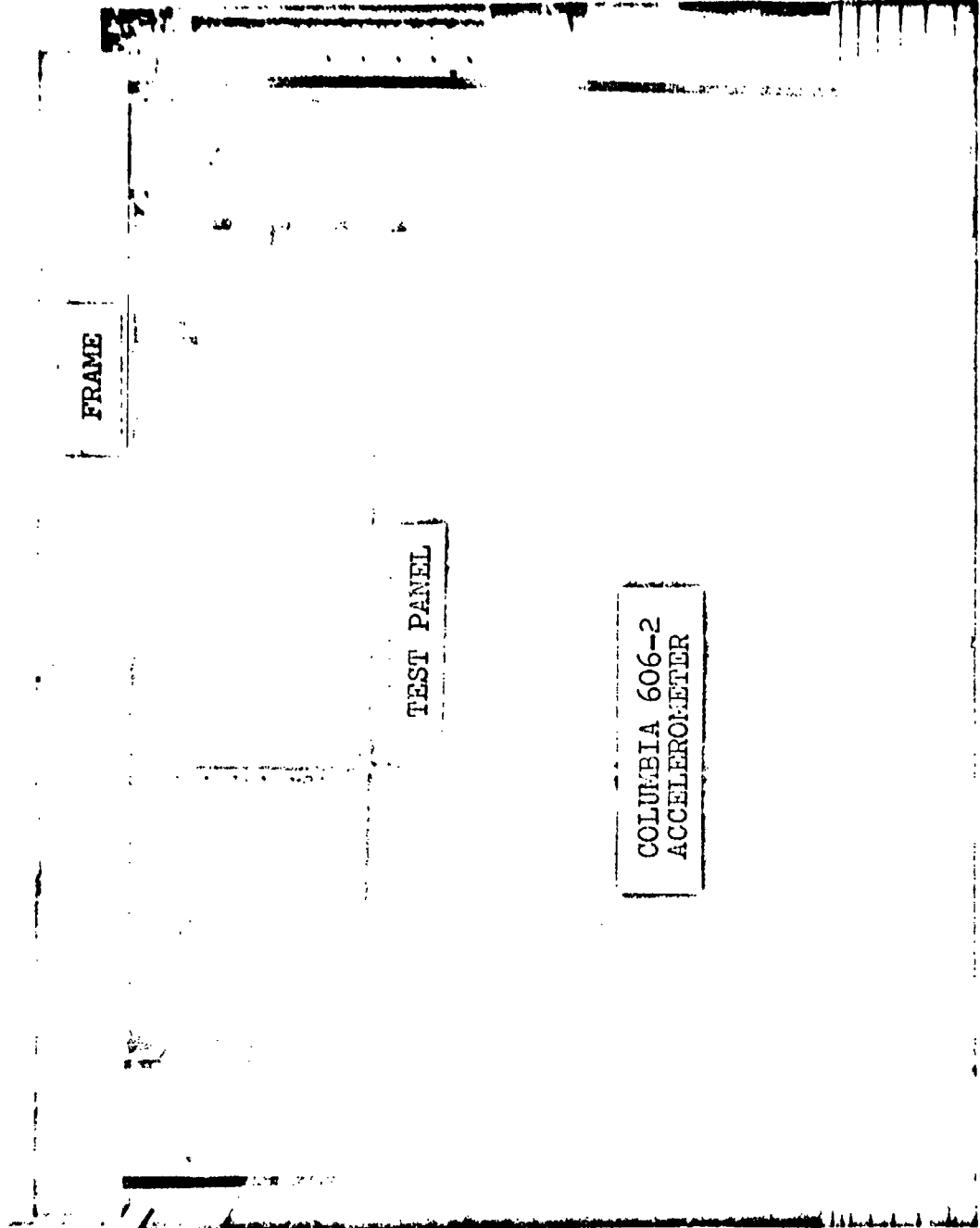


Fig. 10. Accelerometer Attachment for Sinusoidal Tests

three different locations; these locations were selected to coincide with accelerometer locations 3, 4 and 7 to be used in the random vibration experimentation (See Fig. 16, Sec. V). Additional consideration was given to shaker positions to insure that modes which may have nodal lines located at the shaker position for one test would show up with the shaker located at another testing position.

With the accelerometer attached opposite the shaker head, the oscillator amplitude was increased until the desired force was being transmitted to the structure. The oscillator frequency and graph paper were set to 40 Hz, the oscillator was clutched to the recorder, and the recorder drive was started. When the frequency reached 2000 Hz, the recorder was stopped. This procedure was then used for the other two shaker locations.

Impedance Measurements. Force and acceleration measurements were taken at the same shaker locations used in the modal tests. With the recorder disengaged, resonant peaks observed from the acceleration plots were tuned manually using the phase meter and digital frequency counter. When a 90 degree phase shift was observed, the frequency, force and acceleration values were recorded. The technique was applied to approximately 12 to 15 resonant peaks from 100 to 1200 Hz.

Results of the Experiment

Figures 11 and 12 show representative plots of resonant conditions for the five panels. Comparison of all the plots indicated that the fundamental frequencies of the panels varied from approximately 105 - 120 Hz. Although a few panels exhibited small peaks in the range from 65 - 80 Hz, these peaks were assumed to be caused by localized skin or stringer vibrations, and not panel modes.

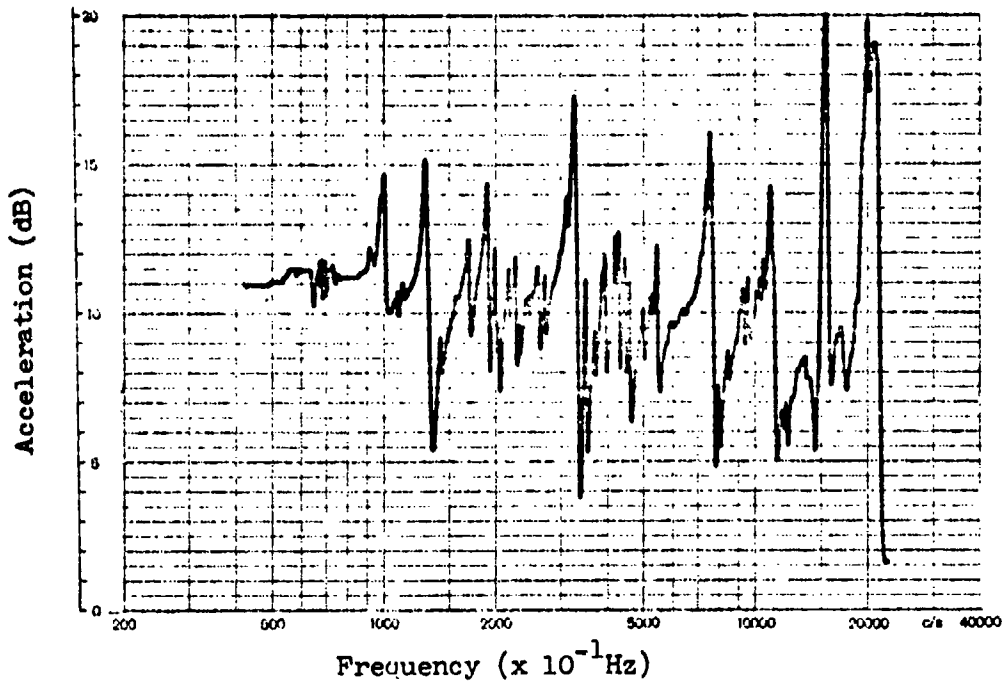


Fig. 11. Acceleration Response, Panel A, Accelerometer 4

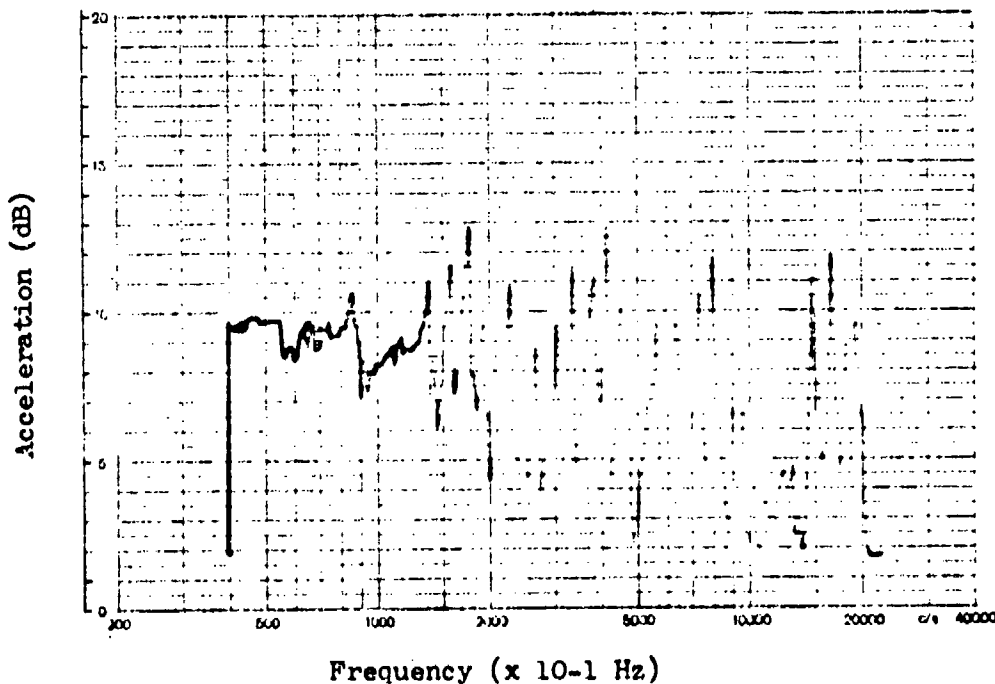


Fig. 12. Acceleration Response, Panel K, Accelerometer 4

With force and acceleration values obtained by tuning resonant peaks manually, the impedance of each panel was calculated at the resonant peaks, and the damping ratio was determined (See Theory Section). While the damping ratio varied as much as thirty per cent from peak to peak, an average of all damping ratios for each panel showed a variance of less than three per cent among panels. The average damping ratio determined by averaging the damping ratios for each mode, for all five panels ranged from 0.0082 to 0.0084, which would classify the panels as being in the low to medium damped range. With this small variance, the addition of lead to the panels was considered to have negligible effect on panel damping, hence, variations in damping were not considered in analysis of the data taken in the random vibration experimentation (See Sec. VI).

V. Random Vibration Experimentation

Purpose of the Experiment

Random vibration tests on the panels were conducted by the Wide Band Acoustic Facility, Air Force Flight Dynamics Laboratory, Wright-Patterson AFB, Ohio. The purpose of the experiment was to determine the effects of local mass and stiffness parameters on the response characteristics of the panels when subjected to a random acoustic excitation. The panels were subjected to a reverberant acoustic field and excited at five different sound pressure levels. Responses were monitored and plotted in 1/3-octave frequency band plots over a range from 3.15 - 4000 Hz.

Description of the Wide Band Acoustic Facility

Figure 13 shows the Wide Band Acoustic Facility, consisting of a 16 by 11 by 11 foot reverberation chamber and a wide band siren and horn assembly. A floor plan of the test facility is shown in Fig. 14. A 12 Kw wide band siren is utilized capable of providing a continuous spectrum from 50 - 10000 Hz, and a maximum overall sound pressure level (SPL) of 160 dB (re 0.0002 dynes/cm²). This von Gierke type siren produces a random noise spectrum which closely approximates the sound spectrum of a jet engine. A segmented horn with variable cutoff of 125 dB is used in the test chamber.

Test specimens are rigidly mounted in an enclosed steel fixture capable of holding up to five panels (See Fig. 15). For this experimentation, the test fixture was positioned in the chamber such that the panel surface was normal to the incident excitation. Sound absorbing

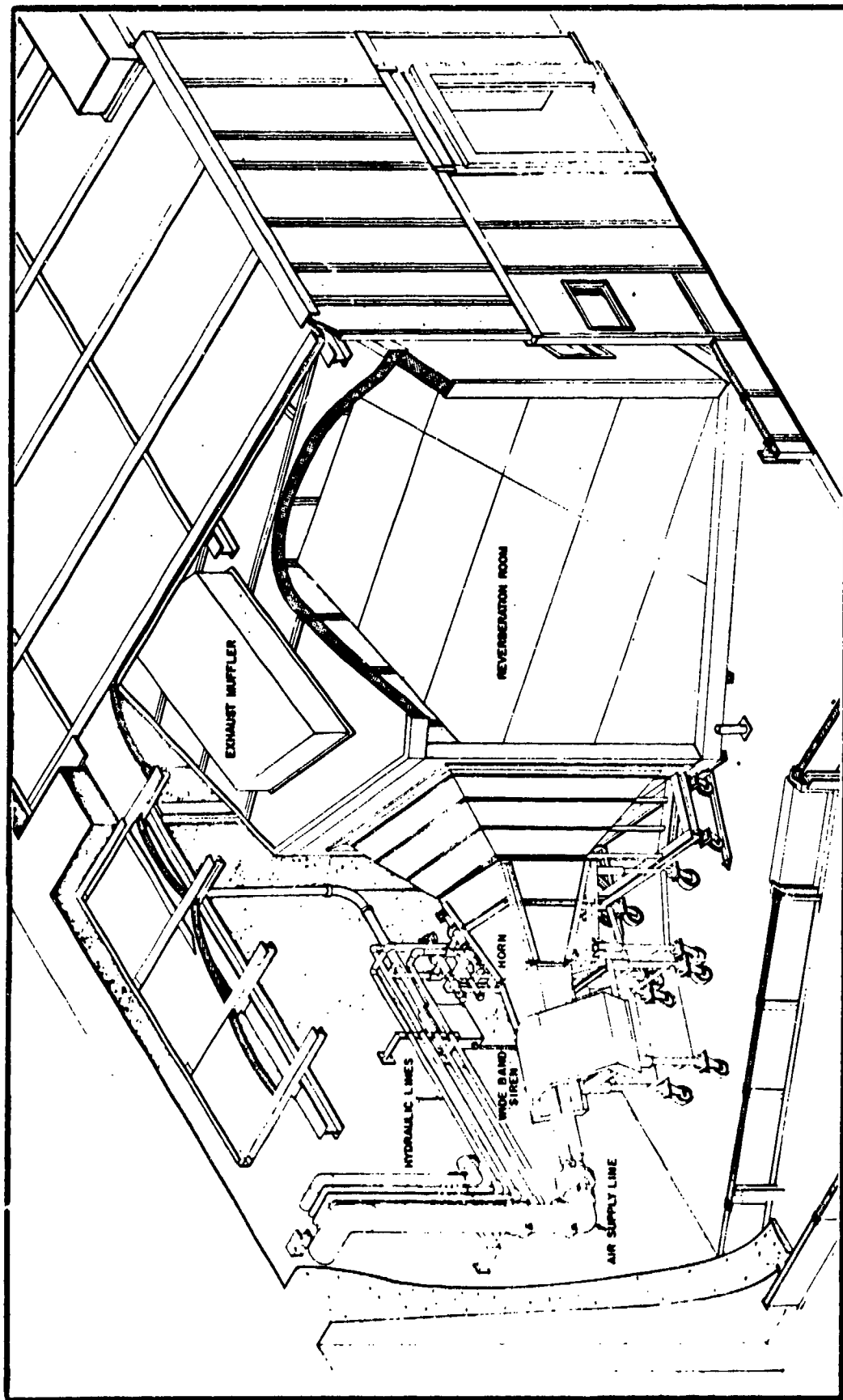


Fig. 13. Wide Band Acoustic Facility

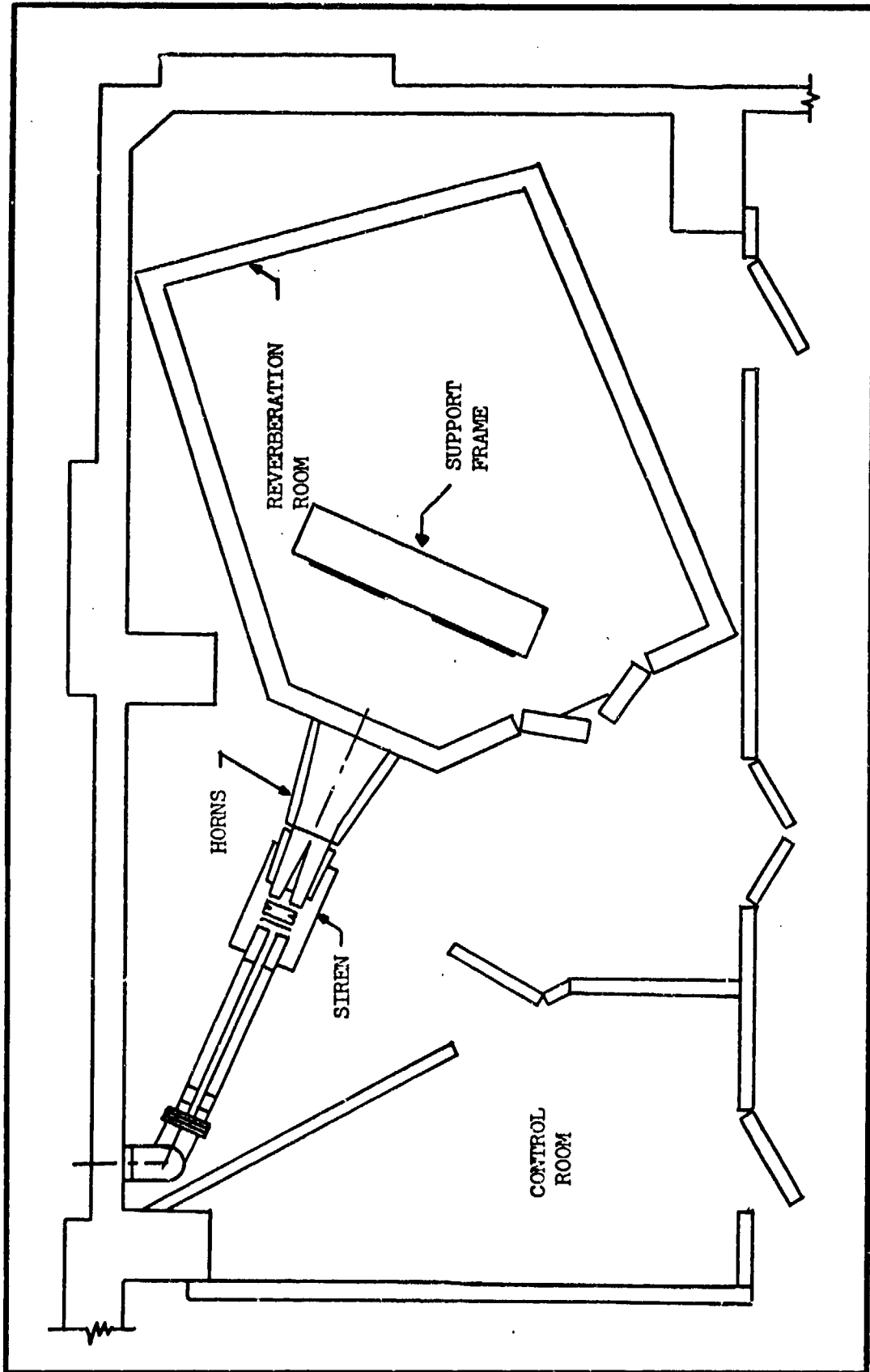


Fig. 14. Floor Plan of Test Facility

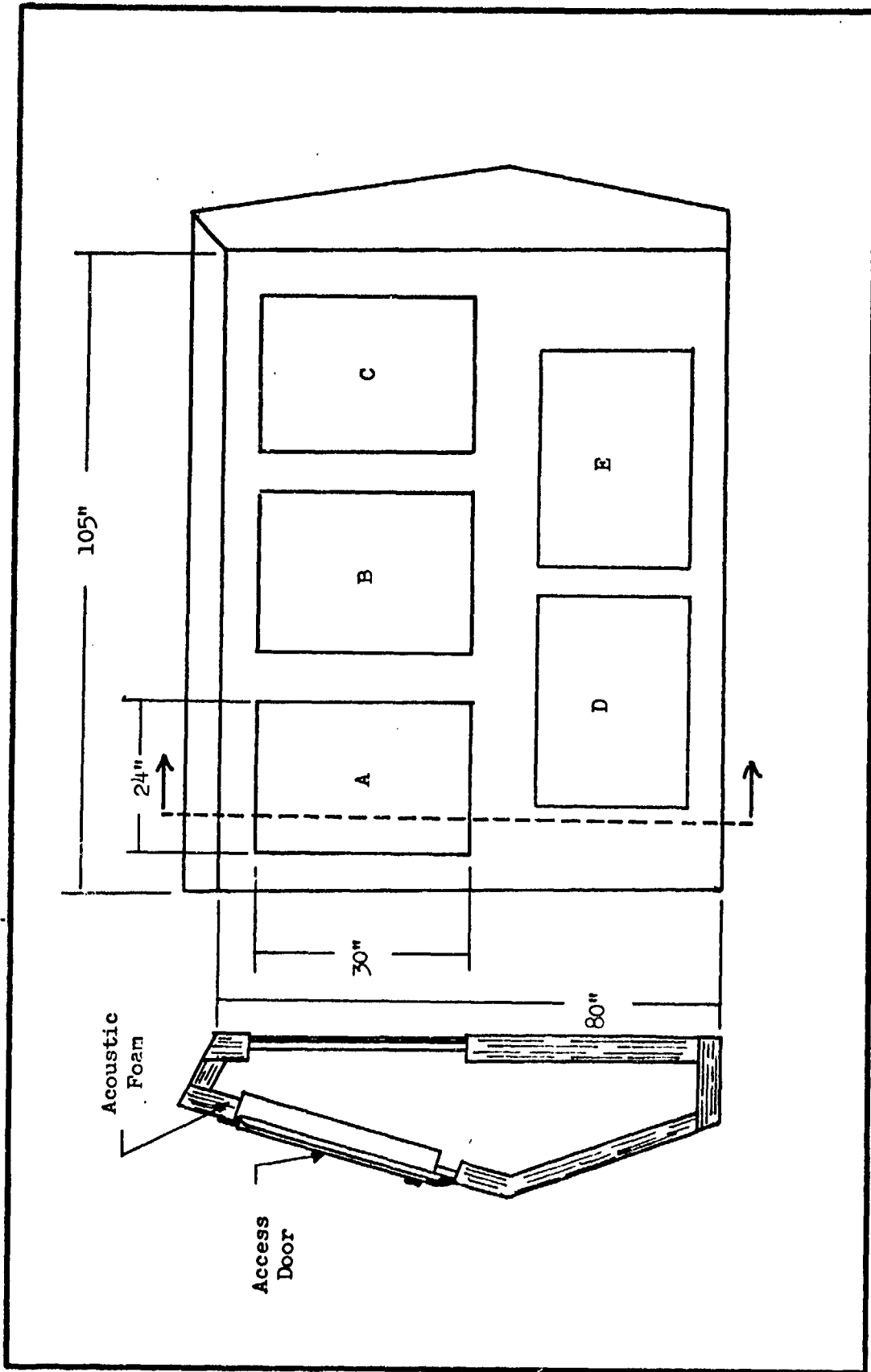


Fig. 15. Test Fixture

material is contained in the test fixture to prevent formation of standing waves and, once installed, access to the rear of the panels is provided by removable covers. By proper positioning of the test fixture, a variance of ± 1 dB in overall sound pressure level over the fixture can be achieved (Ref 16:4).

Experimental Techniques

Facility instrumentation permits a maximum of 72 channels of data to be recorded at one time on six 14-channel tape recorders. For this test, only 24 channels were available for recording data, and it was determined that a minimum of 10 channels would be needed for each panel to adequately describe the excitation and response characteristics of the test specimens. This allowed for a maximum of two panels to be tested at one time. The panels were mounted in locations B and C of the test fixtures for each run with the panel skin facing the excitation. One microphone was located at the center of each panel and nine accelerometers were mounted on the panel stringers normal to the panel surface. Figure 16 shows the locations of the nine accelerometers used for each panel. The 22 channels of data were fed to two tape recorders with channels 13 and 14 of each recorder being used to record identification and timing signals. Figures 17 and 18 show front and rear views of the mounted test panels with microphone and accelerometers in place.

Testing was performed at five sound pressure level settings ranging from approximately 143 dB to 155 dB, with intermediate values at 3 dB intervals. Data were recorded for two minutes at each SPL. At the beginning of each testing period, the noise spectrum was shaped by

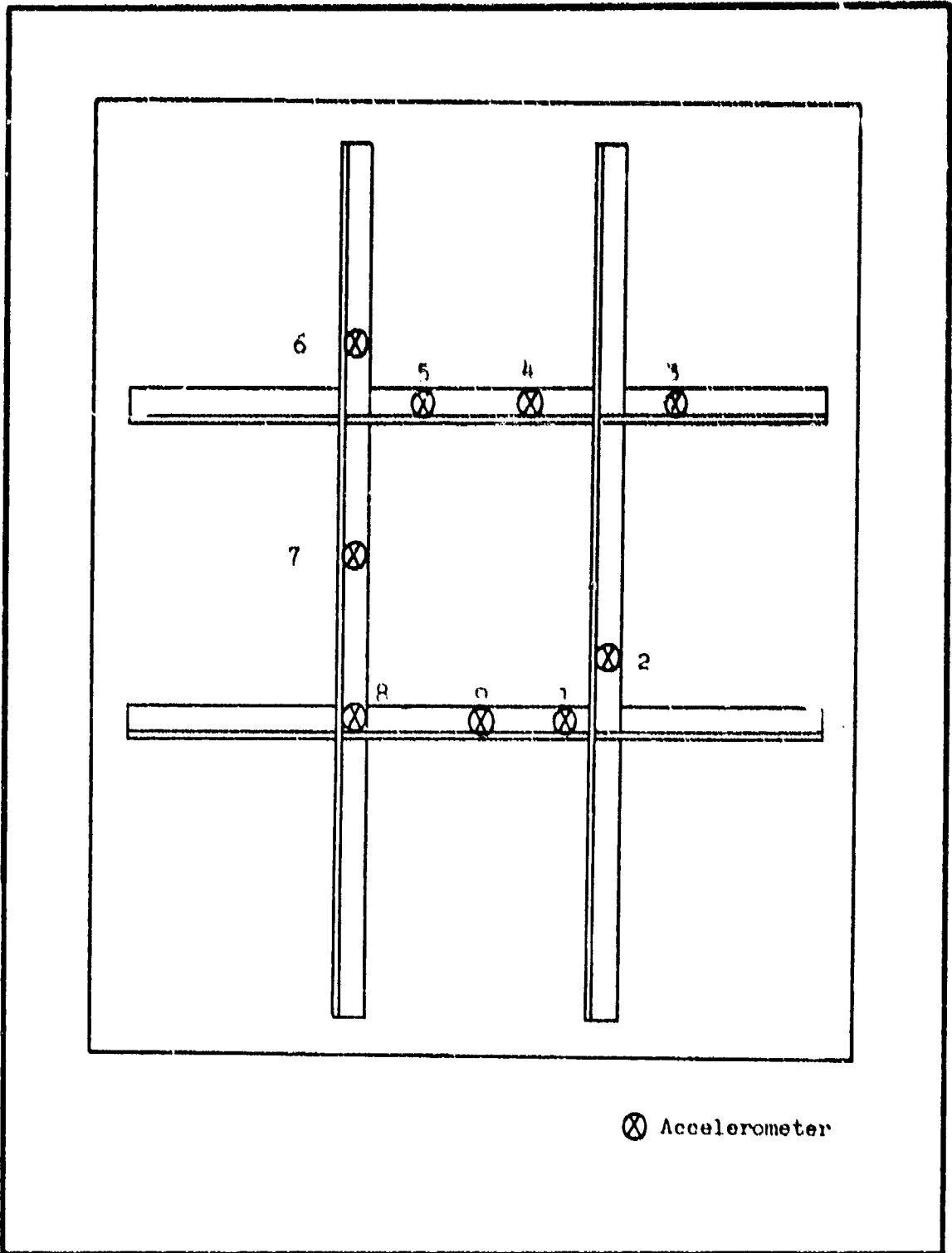


Fig. 16. Accelerometer Positions for Random Tests

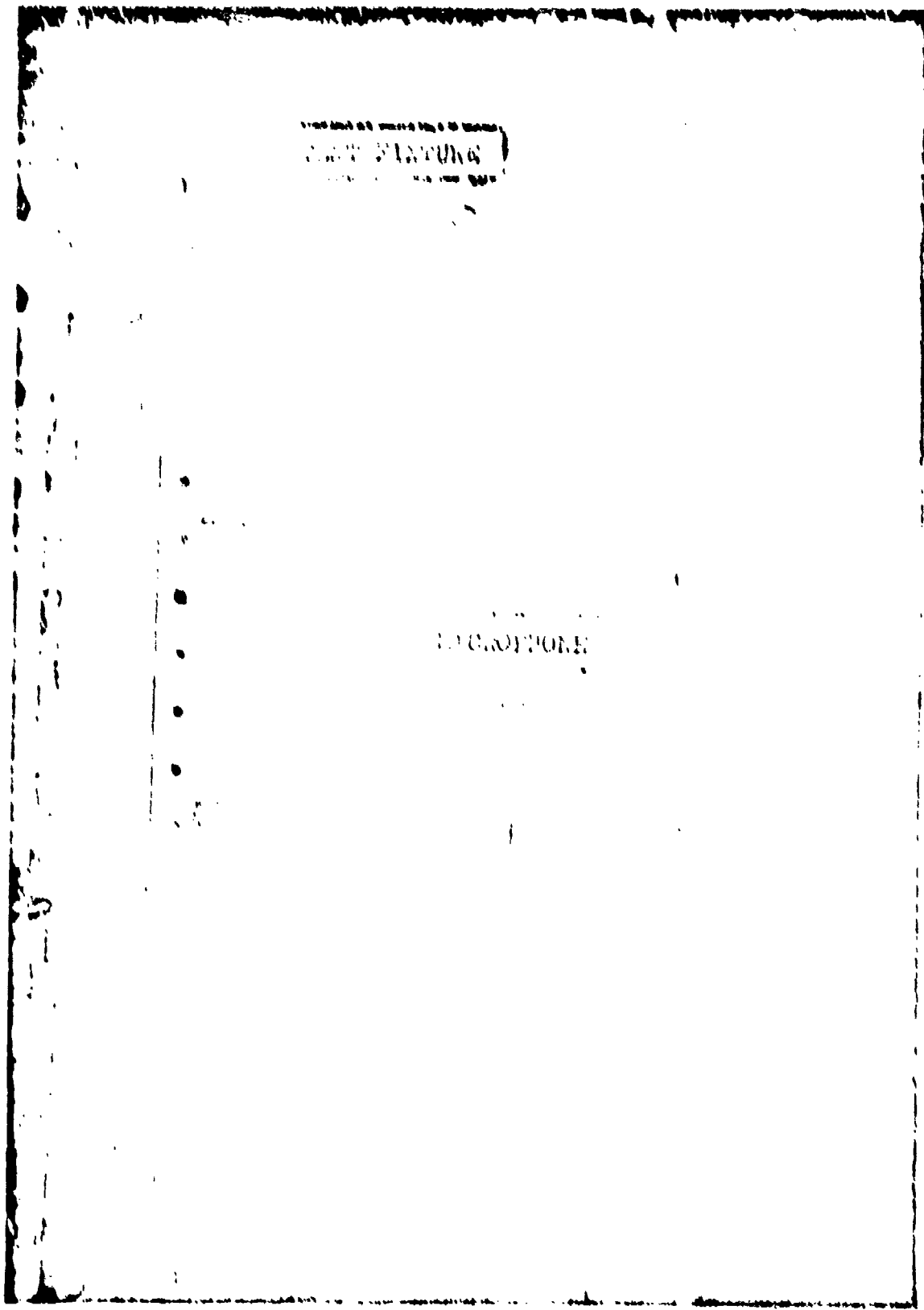


FIG. 17. Front View of Pounted Test Panel

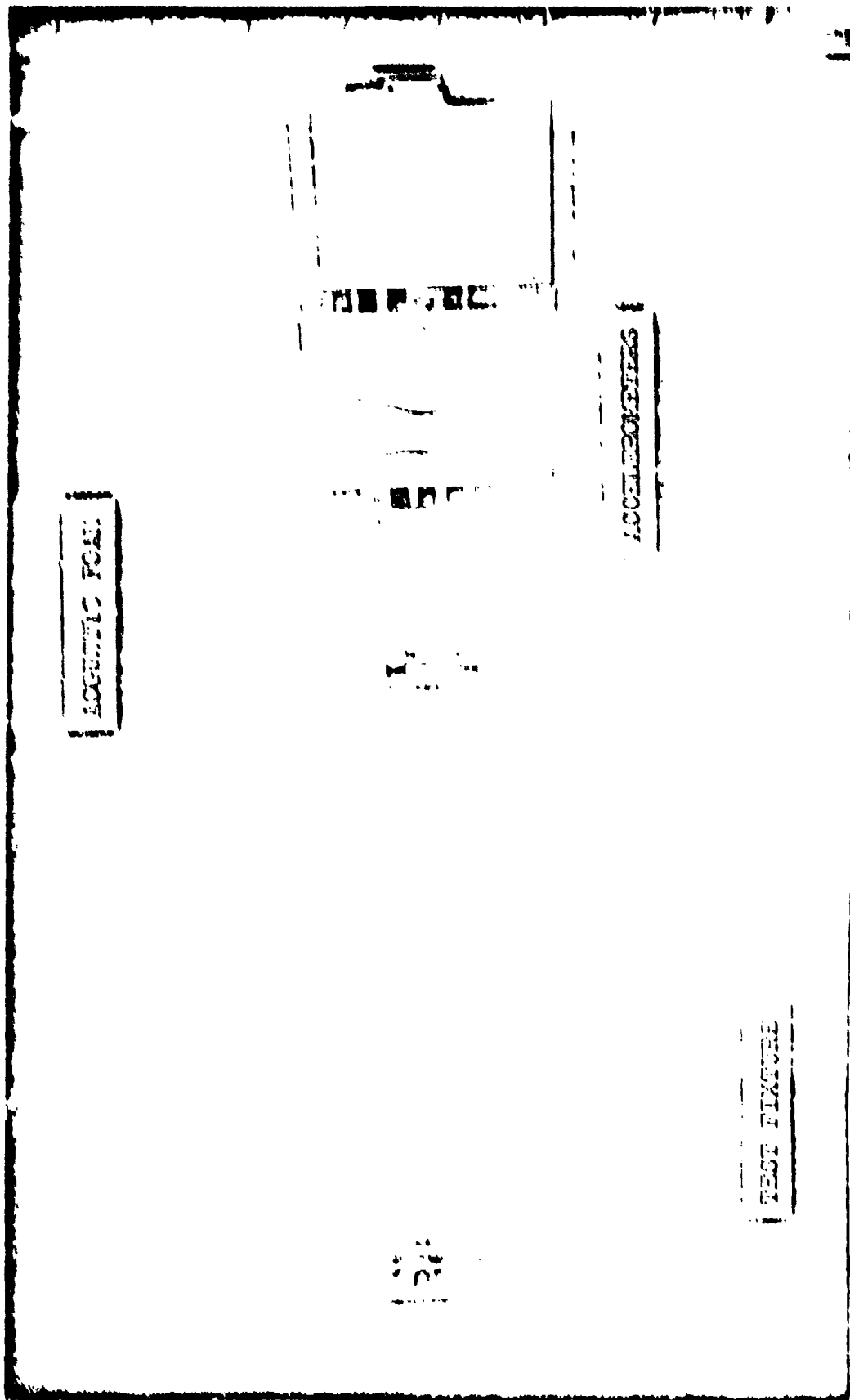


Fig. 18. Rear View of Mounted Test Panel

adjusting the siren rotor speeds to achieve the desired spectrum over the entire frequency range.

Facility Instrumentation

Noise levels in the test chamber were measured with Gulton MVA 2100 microphones, and accelerometers were BEN Model 501 miniature crystal transducers, utilizing lightweight microdot cables. Transducers were calibrated prior to the beginning of each test and normalized to produce the same selected output voltage for the same physical input. Signal conditioning was necessary before the data were suitable for recording in FM frequency ranges. Amplification was provided and fixed at some optimal setting during normal operation. An automatic attenuation system was used to enable the wide range of signal levels encountered in facility operation to be raised or lowered to the input signal range required by the tape recorders. Attenuation was possible in 10 dB increments over a 60 dB range. An identification system was used to identify commutator and attenuator positions for each data channel. An oscillograph, spectrum analyzer, filters, rms meters, an oscilloscope, and one-third octave band analyzers were available to monitor signals going on tape during a test. Figure 19 shows a simplified block diagram of the data collection and monitoring system. Additional information on the Acoustic Facility and the data collection process can be found in Ref 17:17-41 and Ref 18.

Data Analysis

Data reduction was performed by the Dynamics Technology Applications Branch of the Air Force Flight Dynamics Laboratory. The acoustic FM data recorded on magnetic tape by the Acoustic Test Facility were

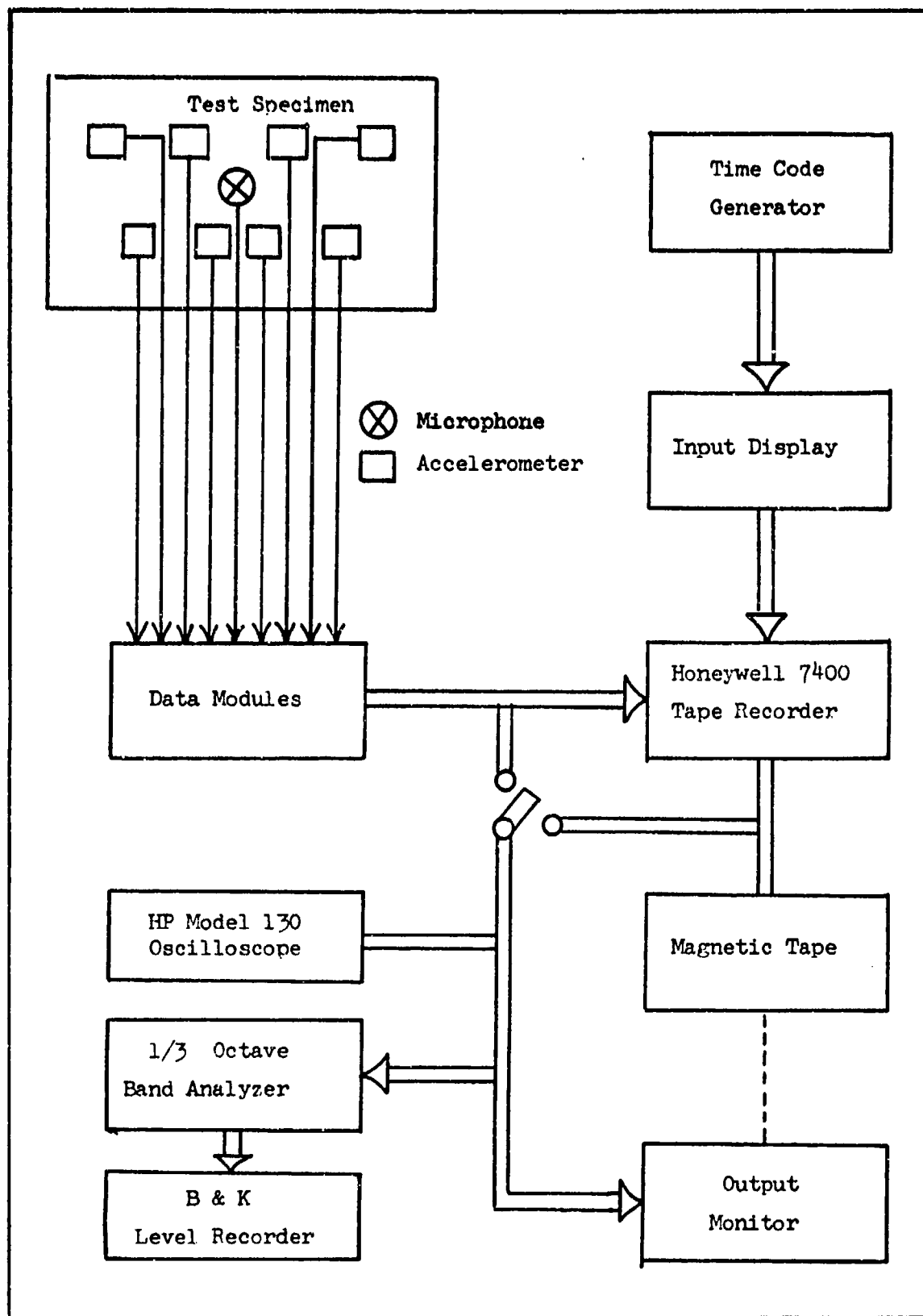


Fig. 19. Data Collection and Monitoring System

played back and edited on a Honeywell Model 7600 tape record/reproduce system. The accelerometer and microphone data were processed with a General Radio Model 1921 One-Third Octave Band Analyzer. An integration time of 32 seconds was used. The acoustic values were converted to sound pressure levels (dB), and the accelerometer values to acceleration amplitudes (g-rms) using the Raytheon 704 computer system. The resulting one-third octave band data were plotted in report form with an Information Technology Inc. Model 4900 computer controlling a CALCOMP Model 563 Plotter. A digital readout of the one-third octave band data was also obtained from the Raytheon computer. Figure 20 gives a schematic of the one-third octave band analysis system. Representative accelerometer and sound pressure level data in plotted form are given in Appendix B.

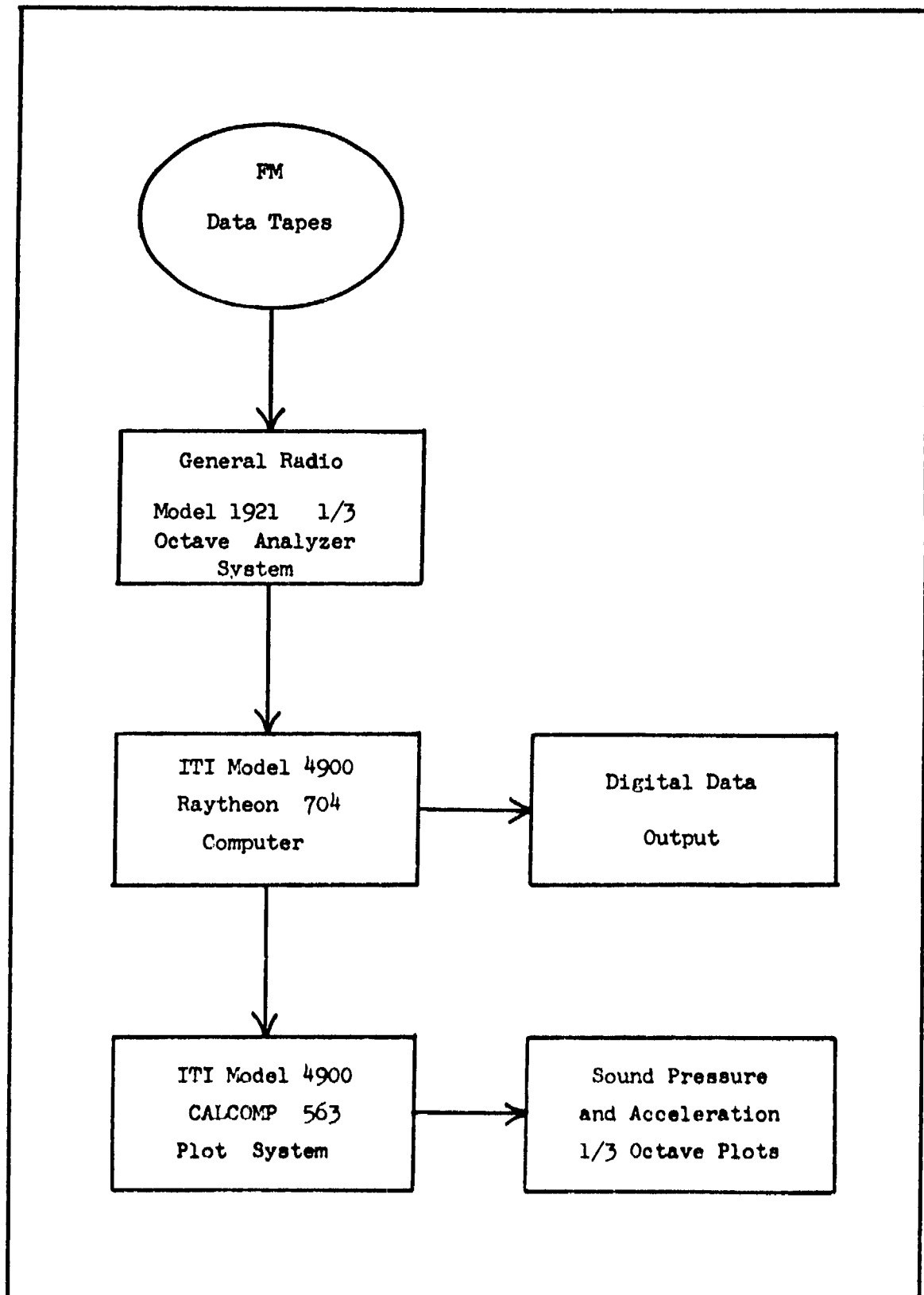


Fig. 20. One-Third Octave Band Analysis System

VI. Data Reduction and Results

The data and results taken from the static, sinusoidal, and acoustic tests were analyzed and used to correlate mass and stiffness parameters of the eleven tested panels with the measured acoustic response and excitation levels. These results were then presented in the form of vibration prediction curves to show the dependence of response levels, as a function of frequency, on mass and stiffness. In addition, the random acoustic data was incorporated into a vibration prediction model derived in the THEORY section of this report.

Effects of Panel Damping

It was determined from the forced harmonic testing of the panels that addition of lead had very little effect on the overall damping of the panels (See Sec. IV). The average damping ratio for the five constant mass and constant stiffness panels tested, ranged from 0.0082 to 0.0084. This variance of less than two per cent was considered small enough to be able to treat all panels as having constant damping in the analysis of the acoustic data.

Correlation of Static Stiffness Data

An attempt was made to correlate static stiffness measurements taken for each panel with the response/excitation levels measured in the acoustic testing. No meaningful results could be obtained, however, due primarily to an inability to maintain consistent boundary conditions from one static test to the next. Although each panel was clamped at the boundaries, the apparatus did not permit monitoring of the clamping force. Thus, it was not possible to apply the same

boundary conditions when panels were changed in the apparatus. For the six constant mass panels, correlation of individual stiffnesses between panels showed no definite trends which could be analyzed, although overall averages indicated an increasing stiffness for Panels B through F (See Table II, Sec. III). In addition, it was concluded that the mass loading effect due to addition of lead to the five constant stiffness panels only increased this inherent boundary error. For these five panels, it was felt that a variation in stiffness up to 25 per cent would not be possible since the lumped mass lead was the only variable among these panels. Because of the unreliability of the measured values, the data were used only as a general indicator of panel stiffness, and Panels G-K were assumed to have a constant stiffness for purposes of analyzing the data from the acoustic tests.

Determination of Mass and Stiffness Parameters

In order to develop vibration prediction curves as a function of mass and stiffness, it was desirable to represent the mass and stiffness parameters in common engineering terms, easily calculated and recognizable by the design engineer. The most convenient parameter to quantify mass was chosen to be total panel weight per unit area, W/A. The stiffness parameter, however, was more difficult to characterize. Because of the complexity involved in analytically determining the stiffness of a multi-bay panel structure in terms of structural parameters, a representative stiffness parameter was derived. An equivalent plate stiffness parameter, D, was used to represent the panel stiffness as derived and explained in the THEORY section;

$$D = \frac{3E}{12(a+b)(1-\nu^2)} \left[I_a + I_b \right] \quad (19)$$

Table III lists the parameters, W/A and D, calculated for each panel.

Construction of Vibration Prediction Curves

Having once determined appropriate mass and stiffness parameters, plots were obtained as a function of frequency for each parameter versus excitation/response levels. Figures 35-43 contained in Appendix C show plots for the constant stiffness panels A, G, H, I, J and K as the parameter W/A varies. The parameter, $L_a - L_p$, represents the difference of the response and excitation levels respectively in dB, where

$$L_a = 20 \log_{10} \left(\frac{g}{g_o} \right) \quad (20)$$

and

$$L_p = 20 \log_{10} \left(\frac{P}{P_o} \right) \quad (21)$$

and L_a is the acceleration level in dB

L_p is the sound pressure level in dB

g is the root-mean-square acceleration in "g"s

g_o is the reference root-mean-square acceleration, equal to one "g"

P is the root-mean-square pressure acting on the structure in psi

P_o is the reference pressure, equal to 0.0002 microbar

Plots were made for nine accelerometer locations used to record response levels of the panels (See Fig. 16, Sec. V). For each accelerometer location, data were plotted for 15 band center frequencies from 100 Hz to 2500 Hz; each data point represents an average of the parameter, $L_a - L_p$, calculated at five tested sound pressure level settings.

Table III. Characterized Mass and Stiffness Parameters

Panel	W/A (10^{-3} lb/in ²)	D (10^{-3} lb-in)
A	7.55	7.83
B	7.46	3.68
C	7.68	4.79
D	7.64	14.55
E	7.64	24.44
F	7.46	31.71
G	8.64	7.83
H	9.64	7.83
I	10.76	7.83
J	12.50	7.83
K	13.84	7.83

Since 15 frequency band curves were needed for each accelerometer location, two plots were used, one for frequencies from 100 Hz to 500 Hz, and one for frequencies from 630 Hz to 2500 Hz.

Figures 44 - 52 contained in Appendix D, show plots made for the constant mass panels A, B, C, D, E, and F as the stiffness parameter, D, varies. The same technique described for plotting the constant stiffness panels was applied to these plots.

In addition to the individual plots of excitation/response levels for each accelerometer location and frequency band, plots of overall excitation and response levels were constructed for the frequency range 100 - 2500 Hz (See Figs. 21 and 22). These plots were used to indicate general overall trends in response/excitation levels as mass and stiffness of the panels were varied.

Application of the Empirical Prediction Model

In addition to the vibration prediction curves, it was desired that it be possible to determine response levels when structural parameters differ from those presented by the curves. For this reason, an empirical relation was derived and applied to the measured data (See THEORY Section). It was found that the response of a structure to a random acoustic excitation could be determined using

$$g_{rms} = C(f) (a^2 + b^2)^{\frac{1}{2}} \left[\frac{D}{(W/A)^5} \right]^{1/4} \frac{P(f)}{A} \quad (16)$$

where g_{rms} is the root-mean-square acceleration of the structure in "g's"

a, b are the overall dimensions of the panel in inches

P(f) is the mean-square pressure in psi per Hz

- ACCELEROMETER 1
- ACCELEROMETER 2
- △ ACCELEROMETER 3
- + ACCELEROMETER 4
- x ACCELEROMETER 5
- ◆ ACCELEROMETER 6
- † ACCELEROMETER 7
- ⊗ ACCELEROMETER 8
- z ACCELEROMETER 9

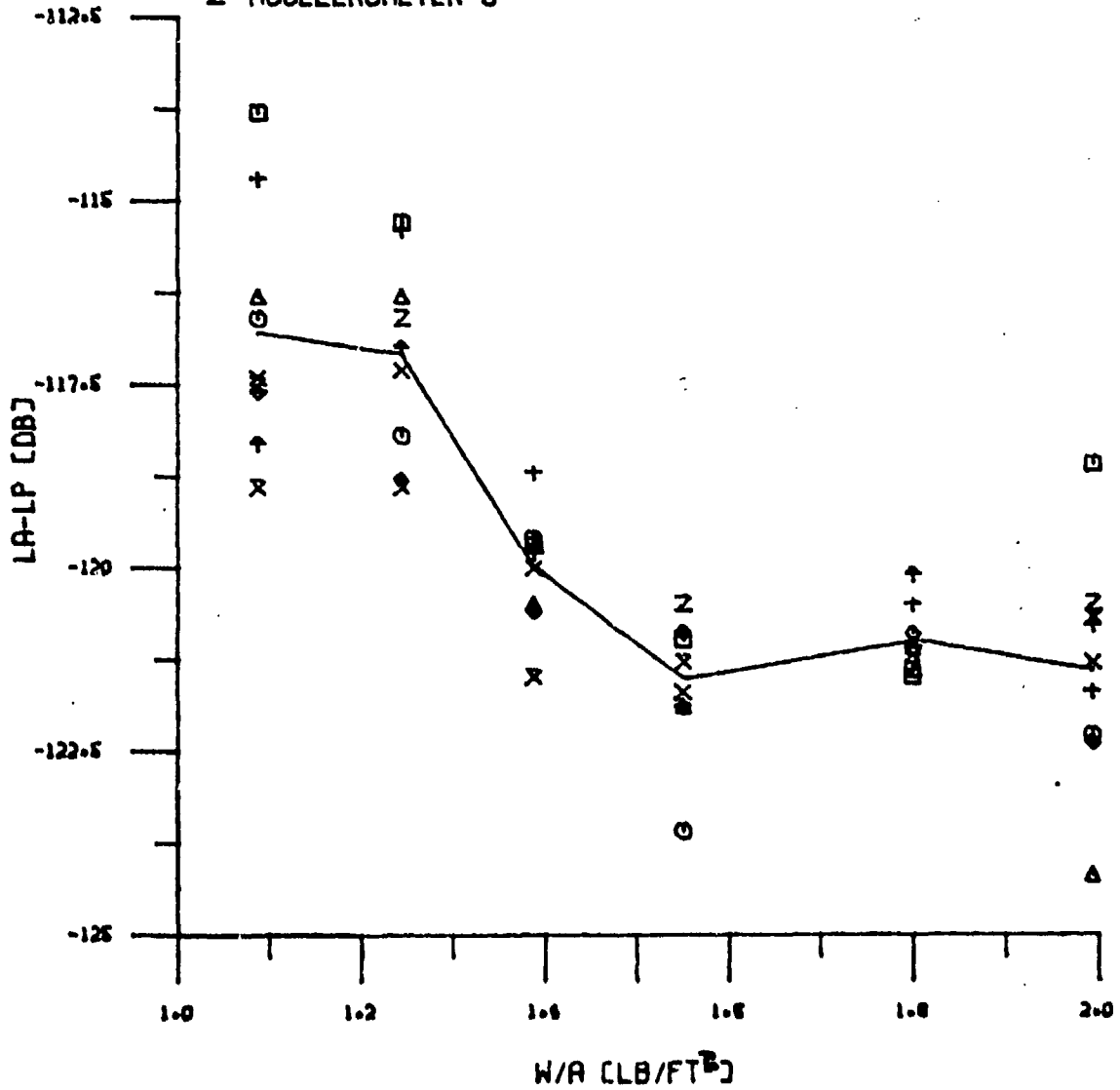


Fig. 21. Mean Overall Response Level for Variation of Mass

- ACCELEROMETER 1
- ⊙ ACCELEROMETER 2
- △ ACCELEROMETER 3
- + ACCELEROMETER 4
- × ACCELEROMETER 5
- ◆ ACCELEROMETER 6
- ↑ ACCELEROMETER 7
- × ACCELEROMETER 8
- z ACCELEROMETER 9

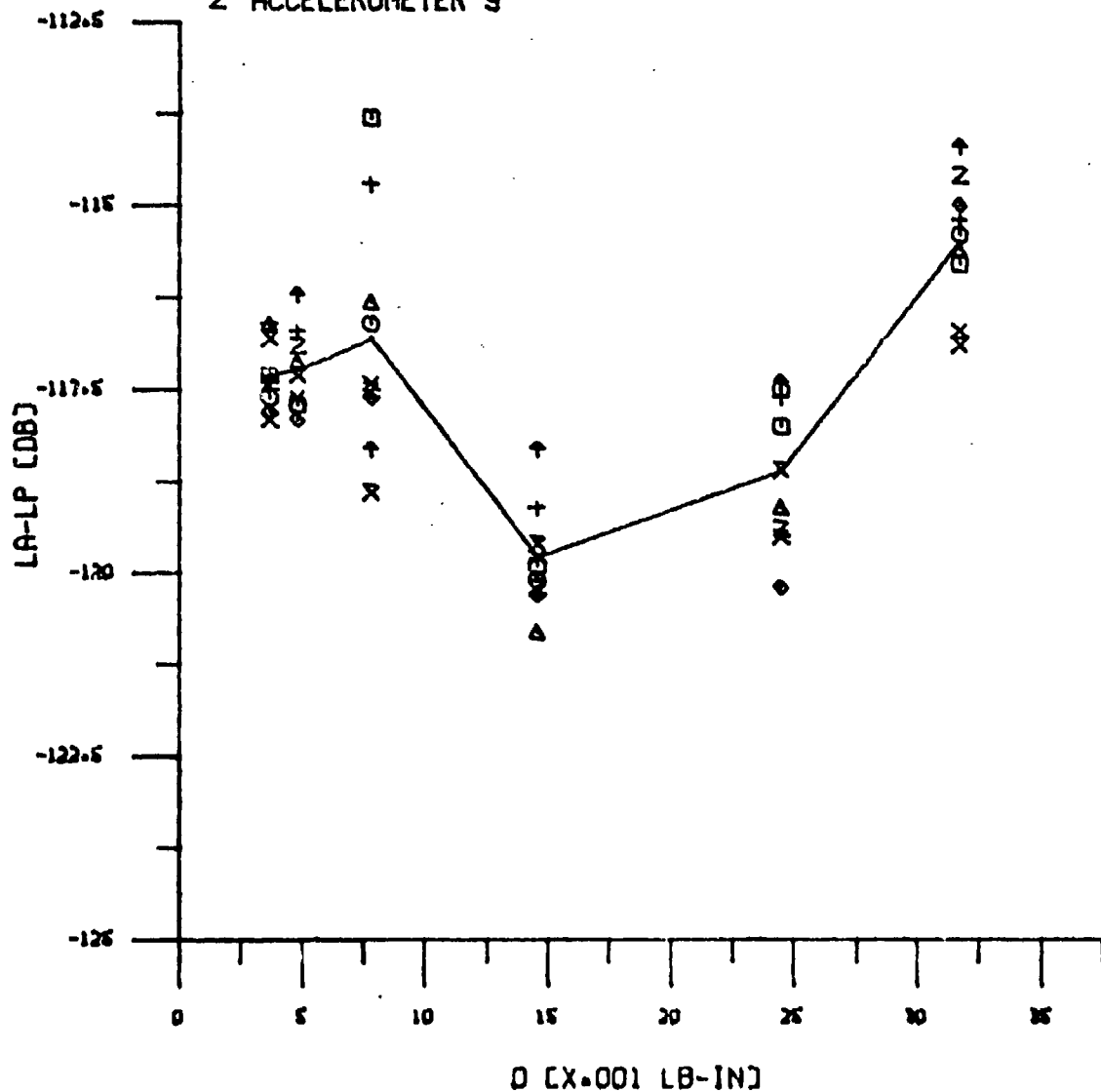


Fig. 22. Mean Overall Response Level for Variation of Stiffness

- W is the total panel weight in pounds
- A is the total panel area, in²
- D is the characterized stiffness parameter in pounds-inches
- C(f) is a frequency-dependent variable determined empirically from measured data

Using the measured excitation and response levels, the weights and dimensions, and the characterized mass and stiffness parameters of the panels, Eq (16) was solved for the function C(f). This function was then plotted versus frequency for each of the nine accelerometer locations used in the acoustic testing (See Fig. 16, Sec. V), as shown in Figure 23. To obtain a data point for a particular band center frequency, the ratio of the acceleration and pressure levels were first averaged for the five sound pressure level settings. Acceleration proved to be quite linear with sound pressure level so that this averaging technique resulted in very little error. Eq (16) was then solved for C(f) for each accelerometer location and each of the eleven panels. The final value was then obtained by averaging the C(f) functions for each panel. As shown in Figure 23, the plot of the data points resulted in a fairly narrow band, and considerable crossing of individual curves for each accelerometer was evident as frequency varied. For this reason, a mean value curve was fitted to the data. Presenting C(f) in this manner permits a range of values to be used in the prediction model such that a maximum response can be predicted for a particular frequency band. Since C(f) represents an average of many data points for all eleven panels, there exists an inherent error in the

- ACCELEROMETER 1
- ACCELEROMETER 2
- ▲ ACCELEROMETER 3
- + ACCELEROMETER 4
- × ACCELEROMETER 5
- ACCELEROMETER 6
- ▽ ACCELEROMETER 7
- × ACCELEROMETER 8
- × ACCELEROMETER 9

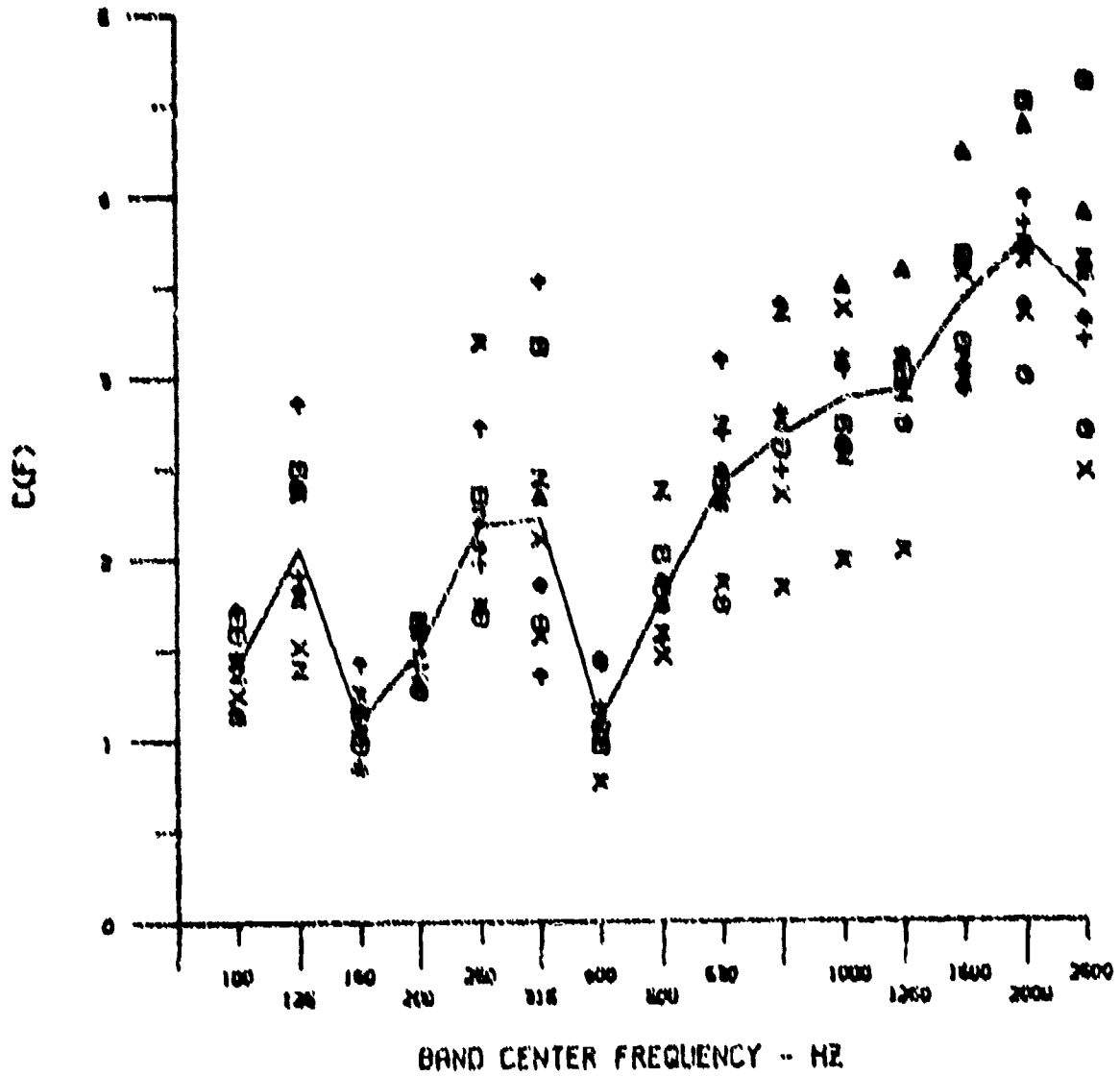


Fig. 23. Frequency Dependent Variable, $C(f)$, for Empirical Model

model as was indicated by using $G(f)$ to predict responses for the same data from which it was determined. However, if it is required that only a reasonable estimate is needed to predict the response of a structure without regard to exact location, the use of $G(f)$ in the prediction equation should provide sufficient accuracy.

Summary of Results

Discussion of the Prediction Curves. The vibration prediction curves as shown in Appendices C and D show the effects of mass and stiffness on the response levels of the tested panel structures. The curves show considerable frequency dependence of response levels as mass and stiffness are varied. For instance, it is apparent that a frequency shift in panel modes occurs as mass and stiffness change, and that there exists a marked degree of cross-over of the frequency curves. In general, the curves show that the response decreases as mass increases. As stiffness varies, however, no definite trends can be recognized. The plots of overall response-excitation levels as shown in Figures 21 and 22 further illustrates these same general results.

Discussion of the Empirical Prediction Model. To predict response levels of entire panel structures, the prediction relation as derived in Eq (16) can be used, knowing the characterized mass and stiffness parameters of the structure, the excitations, and the quantity $G(f)$. In order to use these results, however, certain observations should be made concerning the assumptions and limitations placed on the mathematical model. First, to derive the prediction relation, panel response was approximated by applying certain assumptions

0A/MG/7/2A-1

to the known response of a single mass excited by a random force. While these assumptions concerning the independence of panel modal responses and the linearity of excitations and responses have been shown to be quite representative of actual conditions at higher frequency regimes, it should be recognized that no conclusion can be drawn about the motion of the panel. Only resonant conditions are considered, and to determine vibration characteristics other than acceleration levels, it would be necessary to know the uncoupled generalized motion of each panel mode.

Assumptions were also made concerning the frequency dependence of certain structural parameters. The relation expressed by Eq (8) represents the response of a panel mode as a function of the frequency, modal weight and area. Eq (10) was used to approximate the frequency of a mode as a function of the wave number, or effective half-wave length, and the panel dimensions. In order to remove the frequency dependence of these parameters from the relation, a frequency dependent variable $C(f)$ was defined, which was then determined from empirical data. These assumptions may place some limitations on the usefulness of the results obtained in this study. For geometrically similar panels, the mode shapes and natural frequencies are proportional to some aspect ratio of the panels, and it would be expected that the derived model and prediction curves are quite adequate. When panel structures differ significantly in configuration and construction from those tested, accurate predictions would be somewhat questionable until further testing is done on a broad class of panel structures.

Lastly, certain simplifications were made in order to quantify stiffness of the panels. In reality it must be recognized that panel

stiffness is a function of many parameters, including frequency of vibration and modal mass. The use of an equivalent plate model to determine the stiffness parameter D should not be construed as anything more than a method for accounting for the significant structural parameters which contribute to stiffness, and not representative of actual panel stiffness. The method does offer a degree of validity, however, when one considers that it does account for configurational and structural differences, which for panels of similar construction, can be assumed to have properties proportional to actual stiffnesses. Again, only further testing will determine the degree to which this method of characterizing stiffness is valid for a broad class of structures.

An additional observation may be warranted concerning the use of the empirical model and the prediction curves. It was determined from the panel tests that damping remained constant. For this reason, the damping term in the prediction equation was included as part of the variable $C(f)$. Thus, allowance for variations in damping were not explicitly included in the results. For panels which differ markedly from those tested, some error would be expected in using the model. It would therefore be necessary to adjust the prediction curves by some appropriate factor based on the ratio of tested and desired panel damping factors. Of course, since $C(f)$ is a function of damping, it also would require a method of adjustment.

VII. Conclusions and RecommendationsConclusions

Analysis of data and a summary of the results were presented in the previous section. Based on these results, the following conclusions were made:

1. Since present prediction methods do not account for the effects of local structural parameters, the techniques and results presented in this study should provide a valuable tool in improving existing vibration prediction methods.
2. When using these techniques to predict responses of panel structures which differ significantly in configuration from those tested, certain limitations and assumptions should be recognized until further testing is accomplished to determine their validity for a broad class of structures.
3. The method used to characterize mass and stiffness of the panels accounts for the significant structural parameters of the panels, however, further study may show that more suitable methods are appropriate.
4. Because of the assumptions made, the results can be expected to give more accurate predictions at higher frequencies, far above the fundamental modes of the panels.
5. Overall response levels indicate that, in general, response decreases as mass increases. However, no observable trends in response levels for variations in stiffness could be identified.

Recommendations

At the present state of the art, the effect of local structural parameters on the vibration response of multi-bay panel systems subjected to random excitation is extremely difficult to predict with accuracy. It is recommended that further testing be conducted to verify the techniques and results presented in this study, especially for structures differing from those tested.

In addition, further analysis of the empirical prediction model derived in this study is recommended to determine if the single-mass-oscillator model representation and the method of quantifying mass and stiffness, are adequate to predict panel responses with accuracy. It may be that a more complicated model is required, or that methods more suitable for quantifying mass and stiffness can be found.

Finally, an analytical investigation should be conducted to compare with the results obtained through empirical analysis. The use of energy methods, the solution of the differential equations of motion, or a finite element approach could be used to study the effects of local structural parameters under random excitation.

Bibliography

1. Unger, E. E., R. Madden, R. H. Lyon and E. K. Bender. A Guide for Predicting the Vibrations of Fighter Aircraft in the Preliminary Design Stages. AFFDL-TR-71-63. Wright-Patterson Air Force Base, Ohio: Air Force Flight Dynamics Laboratory, May 1972.
2. White, R. W., D. J. Bozich and K. M. Elred. Empirical Correlation of Excitation Environment and Structural Parameters with Flight Vehicle Vibration Response. AFFDL-TR-64-160. Wright-Patterson Air Force Base, Ohio: Air Force Flight Dynamics Laboratory, December 1964.
3. Blackman, D. R., D. M. Clark, G. J. McNulty and J. F. Wilby. Boundary Layer Pressure Fluctuations and Structural Response. AFFDL-TR-67-97. Wright-Patterson Air Force Base, Ohio: Air Force Flight Dynamics Laboratory, October 1967.
4. Jacobs, L. D., R. Lagerquist and F. L. Gloyna. Response of Complex Structures to Turbulent Boundary Layers. AIAA Paper No. 69-20, 1969.
5. Ballentine, J. R., F. F. Rudder, Jr., J. T. Mathis and H. E. Plumblee, Jr. Refinement of Sonic Fatigue Structural Design Criteria. AFFDL-TR-67-156. Wright-Patterson Air Force Base, Ohio: Air Force Flight Dynamics Laboratory, 1968.
6. Clarkson, B. L., and F. Cicci. Methods of Reducing the Response of Internally Stiffened Structures to Random Pressures. American Society of Mechanical Engineers, ASME Paper No. 69-26, 1969.
7. Maidanik, G. "Response of Ribbed Panels to Reverberant Acoustic Fields." Journal of the Acoustical Society of America, Vol 34, No. 6, June 1962.
8. Cot, R. J., H. J. Parry and J. Clough. A Study of the Characteristics of Modern Engine Noise and the Response Characteristics of Structures. WADD-TR-60-220. Wright-Patterson Air Force Base, Ohio: Air Force Flight Dynamics Laboratory, December 1961.
9. Unger, E. E., N. Koronaios and J. E. Manning. Application of Statistical Energy Analysis to Vibrations of Multi-Panel Structures. AFFDL-TR-67-79. Wright-Patterson Air Force Base, Ohio: Air Force Flight Dynamics Laboratory, August 1967.
10. Olson, M. D., and G. M. Lindberg. Free Vibrations and Random Response of an Internally-Stiffened Panel. Aeronautical Technical Report No. LR-544. Ottawa, Canada: National Research Council of Canada, October 1970.

11. Roberts, W. H. "Empirical Correlation of Flight Vehicle Vibration Response." The Shock and Vibration Bulletin, No. 37, Part 7. Washington, D. C.: The Shock and Vibration Information Center, U. S. Naval Research Lab., January 1968.
12. Crandall, S. H., et al. Random Vibration. Notes from the M. I. T. Special Program On. Cambridge, Mass.: The Technology Press of the Massachusetts Institute of Technology, 1958.
13. Elred, K. M. "Empirical Prediction of Space Vehicle Vibration." The Shock and Vibration Bulletin, No. 29, Part 4. Washington, D. C.: The Shock and Vibration Information Center, U. S. Naval Research Lab., June 1961.
14. Excerpt from unpublished status report, submitted to the Air Force Flight Dynamics Laboratory, Wright-Patterson Air Force Base, by the Lockheed-Georgia Company, Marietta, Georgia, dated 18 September 1973.
15. Heckl, M. A., R. H. Lyon, G. Maidanik and E. E. Ungar. New Approaches to Flight Vehicle Structural Vibration Analysis and Control. ASD-TDR-62-237. Wright-Patterson Air Force Base, Ohio: Flight Dynamics Laboratory, Aeronautical Systems Division, October 1962.
16. Kolb, A. W. and R. C. W. van der Heyde. Sonic Fatigue Resistance of Lightweight Aircraft Structures. Unpublished Report, Wright-Patterson Air Force Base, Ohio: Air Force Flight Dynamics Laboratory, December 1972.
17. Kolb, A. W., and H. A. Magrath. "RTD Sonic Fatigue Facility, Design and Performance Characteristics." The Shock and Vibration Bulletin, No. 37, Supplement. Washington, D. C.: The Shock and Vibration Information Center, U. S. Naval Research Lab., January 1968.
18. Hankel, K. M., and J. P. Henderson. Design and Performance of a 15 KW Wide Band Acoustic Facility. AFFDL-TR-66-8. Wright-Patterson Air Force Base, Ohio: Air Force Flight Dynamics Laboratory, March 1966.

Appendix ADerivation of Angle Section Moment of Inertia
and Area Equations

The stiffness of a structural element can be shown to be a function of the moment of inertia of the element. An increase in the moment of inertia in the desired direction will correspondingly increase the stiffness in that direction, provided all other parameters remain unchanged.

The area moment of inertia of an angle section can be shown to be

$$I_{xx} = \frac{1}{3} \left[d(L_1 - \bar{y})^3 + L_2 \bar{y}^3 - (L_2 - d)(\bar{y} - d)^3 \right] \quad (22)$$

where

$$\bar{y} = \frac{L_1^2 + L_2^2 - d^2}{2(L_1 + L_2 - d)} \quad (23)$$

and L_1 and L_2 are the lengths of the section legs, d is the thickness and \bar{y} is the location of the centroidal axis referenced to the datum plane (See Fig. 24). Substituting Eq (23) into Eq (22) and grouping terms

$$I_{xx} = \frac{1}{24(L_1 + L_2 - d)^3} \left[d(L_1^2 + 2L_1L_2 - 2L_1d - L_2d + d^2)^3 + L_2(L_1^2 + L_2d - d^2)^3 - (L_2 - d)(L_1^2 - L_2d - 2L_1d + d^2)^3 \right] \quad (24)$$

Eq (24) represents the moment of inertia of the angle section with respect to the datum plane in terms of L_1 , L_2 and d .

If it is desired to change the moment of inertia of the section, and thus stiffness, and keep weight per unit area constant, the area of

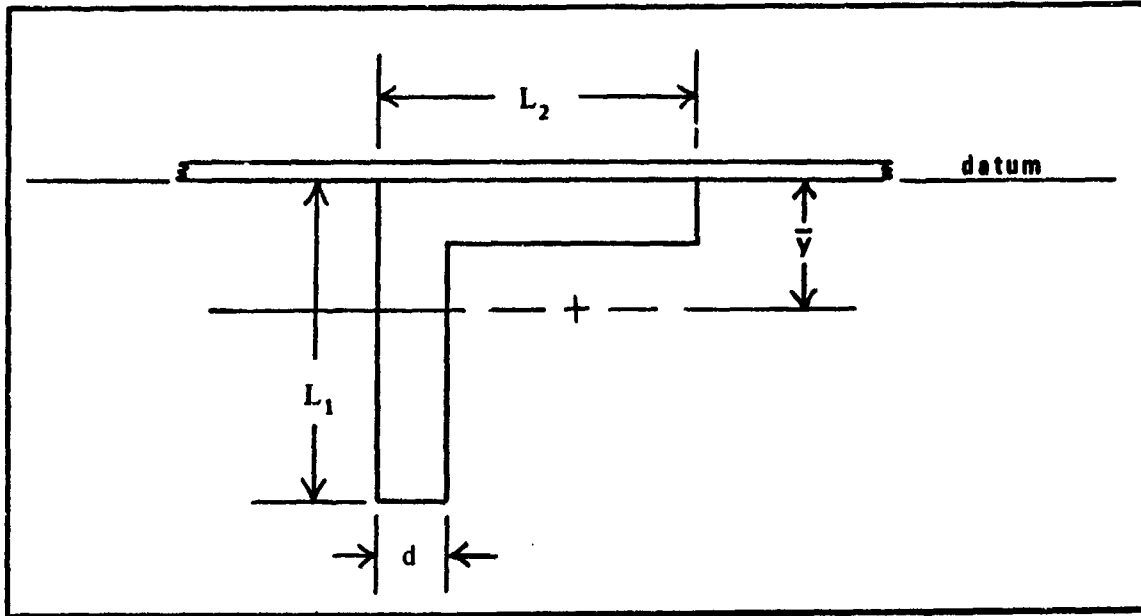


Fig. 24. Angle Stiffener Configuration

the section must remain constant, providing material properties do not change. Thus, the area of the angle section can be calculated to be

$$A = d (L_1 + L_2 - d) \quad (25)$$

Here again, Eq (25) is represented by the angle lengths and the thickness, L_1 , L_2 and d respectively.

Using Eq (25) it is possible to select values for any two parameters and compute the third to maintain constant area, and thus weight. These values can then be used in Eq (24) to determine the moment of inertia of the section. Values of the parameters can then be adjusted until the desired moment of inertia is achieved.

Appendix BExcitation and Response Levels
from the Random Vibration Tests

The following graphs are plots of the sound pressure level (SPL) and acceleration vibration data for nine accelerometers in acoustic tests performed on Panel A. Similar plots for the remaining ten panels were obtained. All data were digitized and stored on magnetic tape for future use. Sound pressure levels are given in dB and acceleration is given in g-rms. Actual overall SPL values are given in the extreme right-hand column of each plot. The following information is contained in the key for each plot:

- a. Panel - identification of the panel
- b. Location (Loc.) - location of the panel in the test fixture (See Fig. 15, Sec. V)
- c. Transducer (PUID) - identification of microphone of accelerometer position (See Fig. 16, Sec. V)
- d. Record (Rec.) - identification of each two minute test run; each run corresponding to an overall input SPL of approximately

- (1) 143 dB
- (2) 146 dB
- (3) 149 dB
- (4) 152 dB
- (5) 155 dB

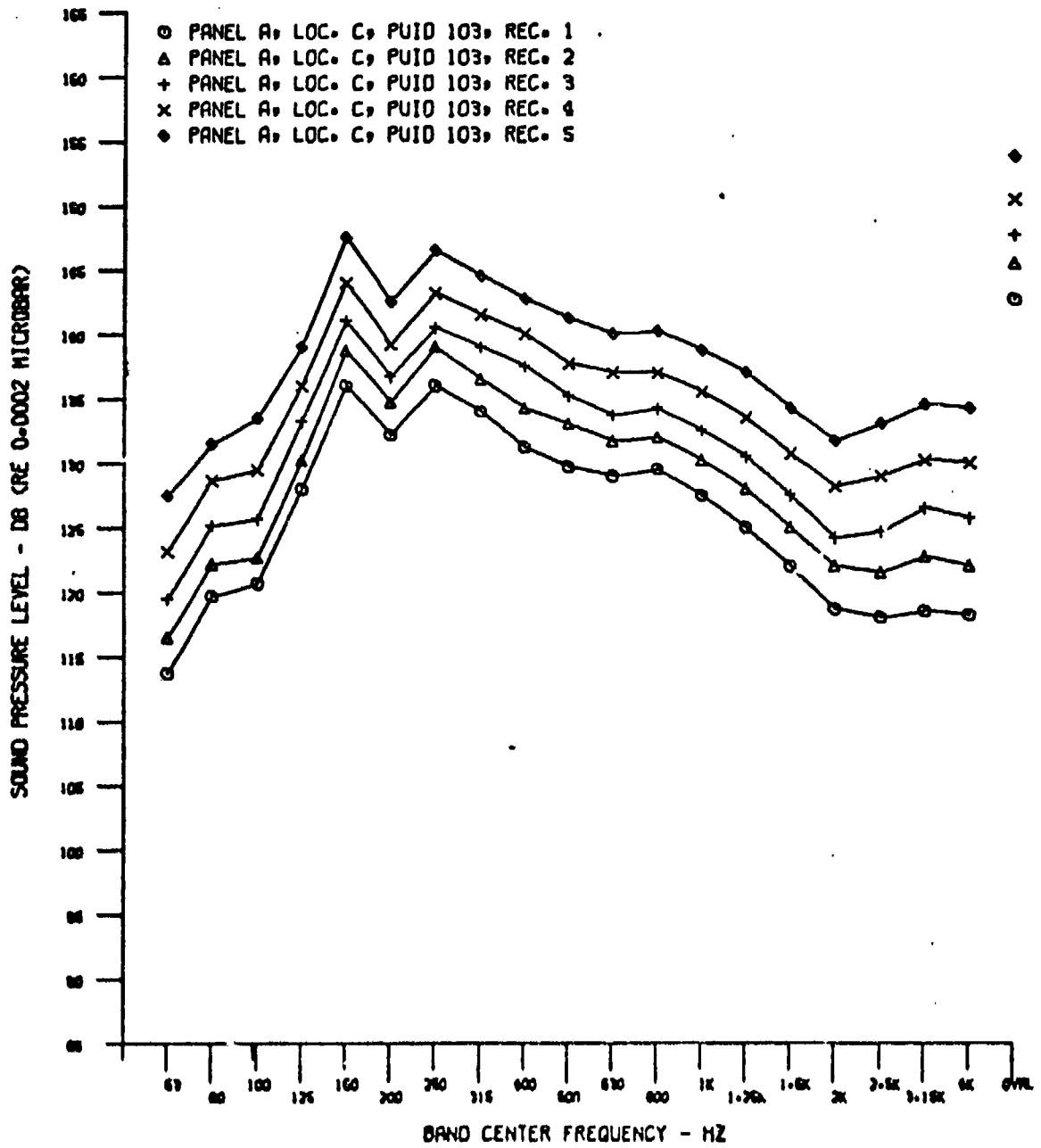


Fig. 25. Acoustic Sound Pressure Levels, Panel A

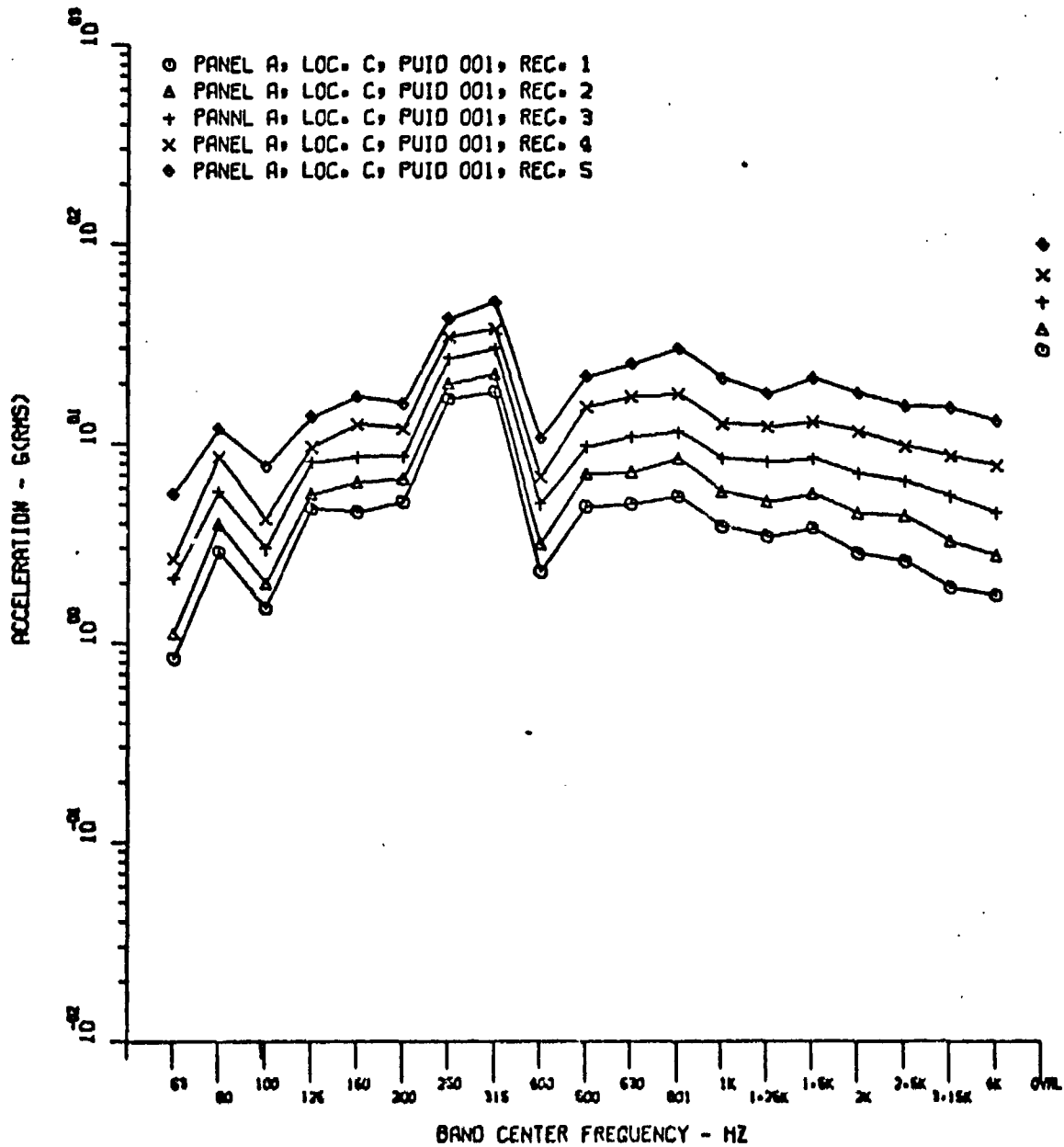


Fig. 26. Acceleration Response, Panel A,
Accelerometer 1

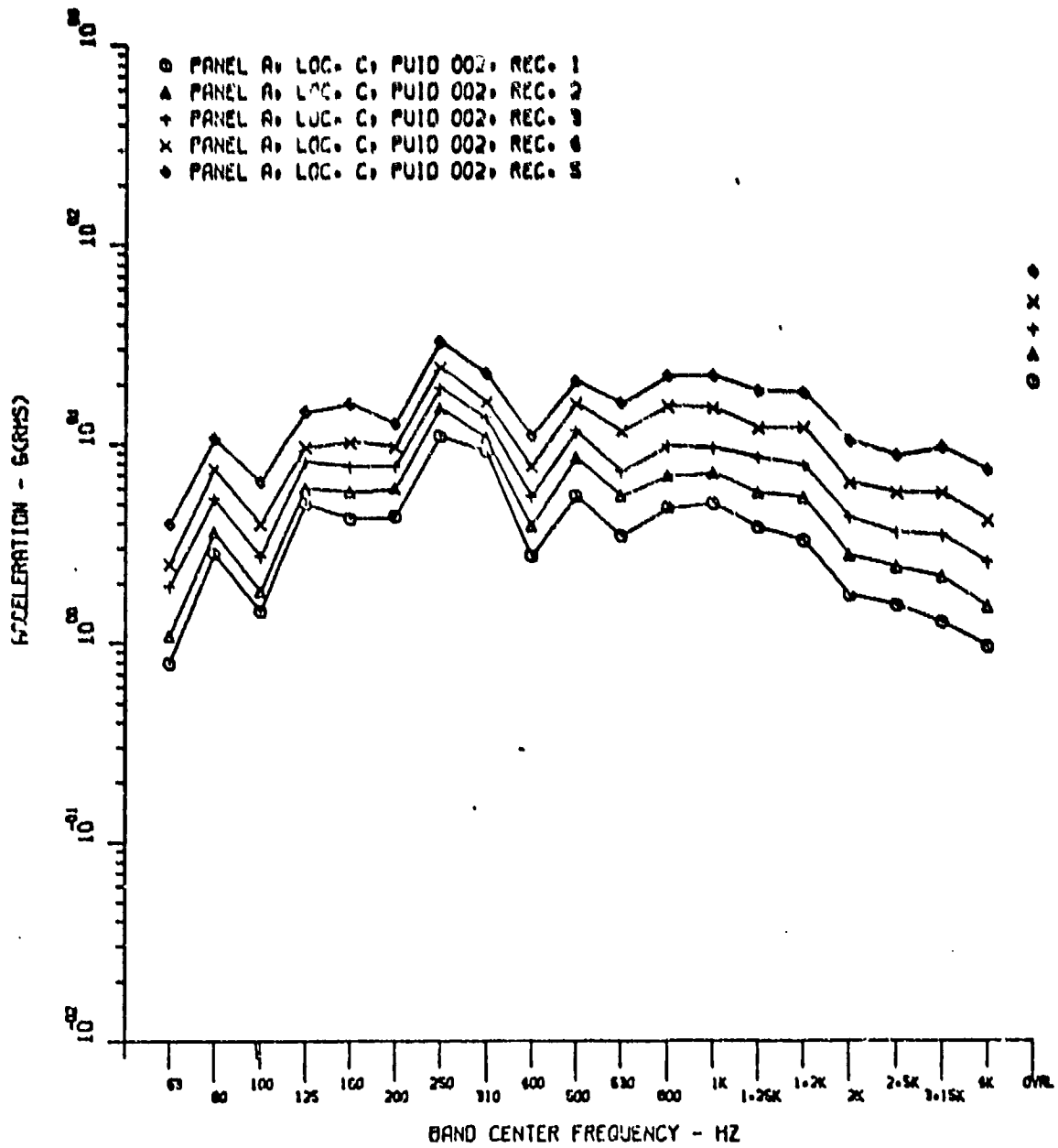


Fig. 27. Acceleration Response, Panel A
Accelerometer 2

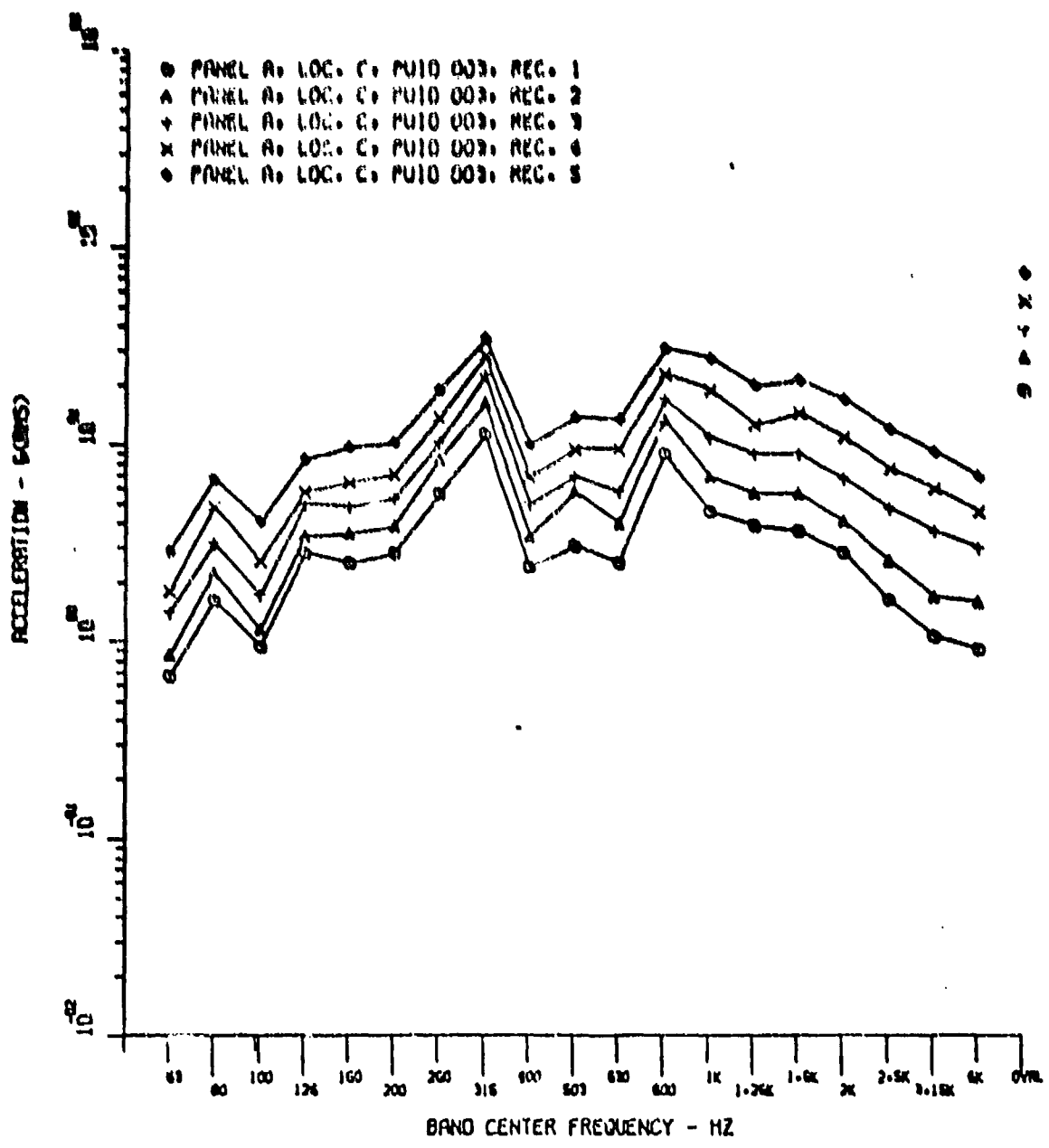


Fig. 28. Acceleration Response, Panel A,
Accelerometer 3

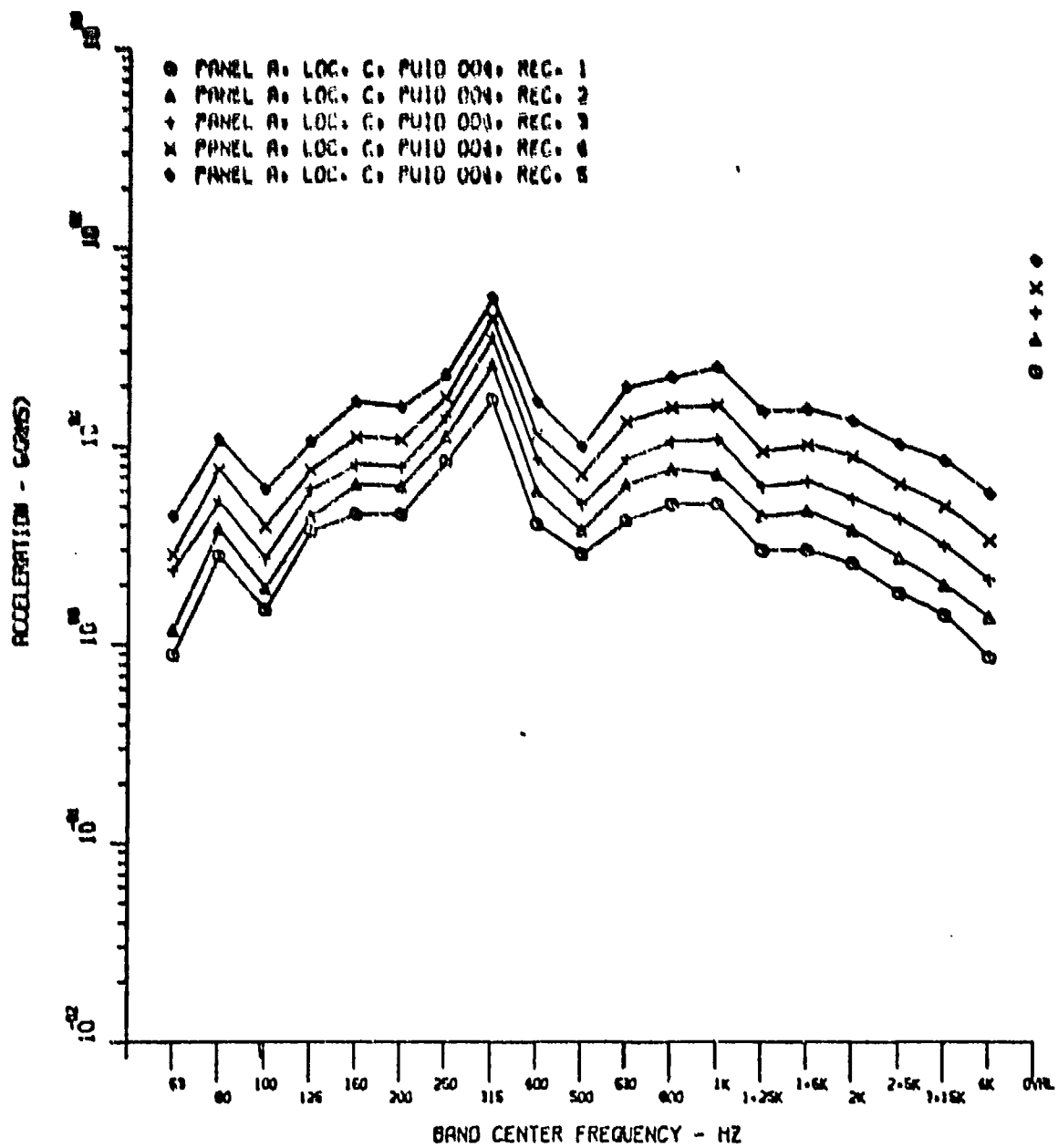


Fig. 29. Acceleration Response, Panel A,
Accelerometer 4

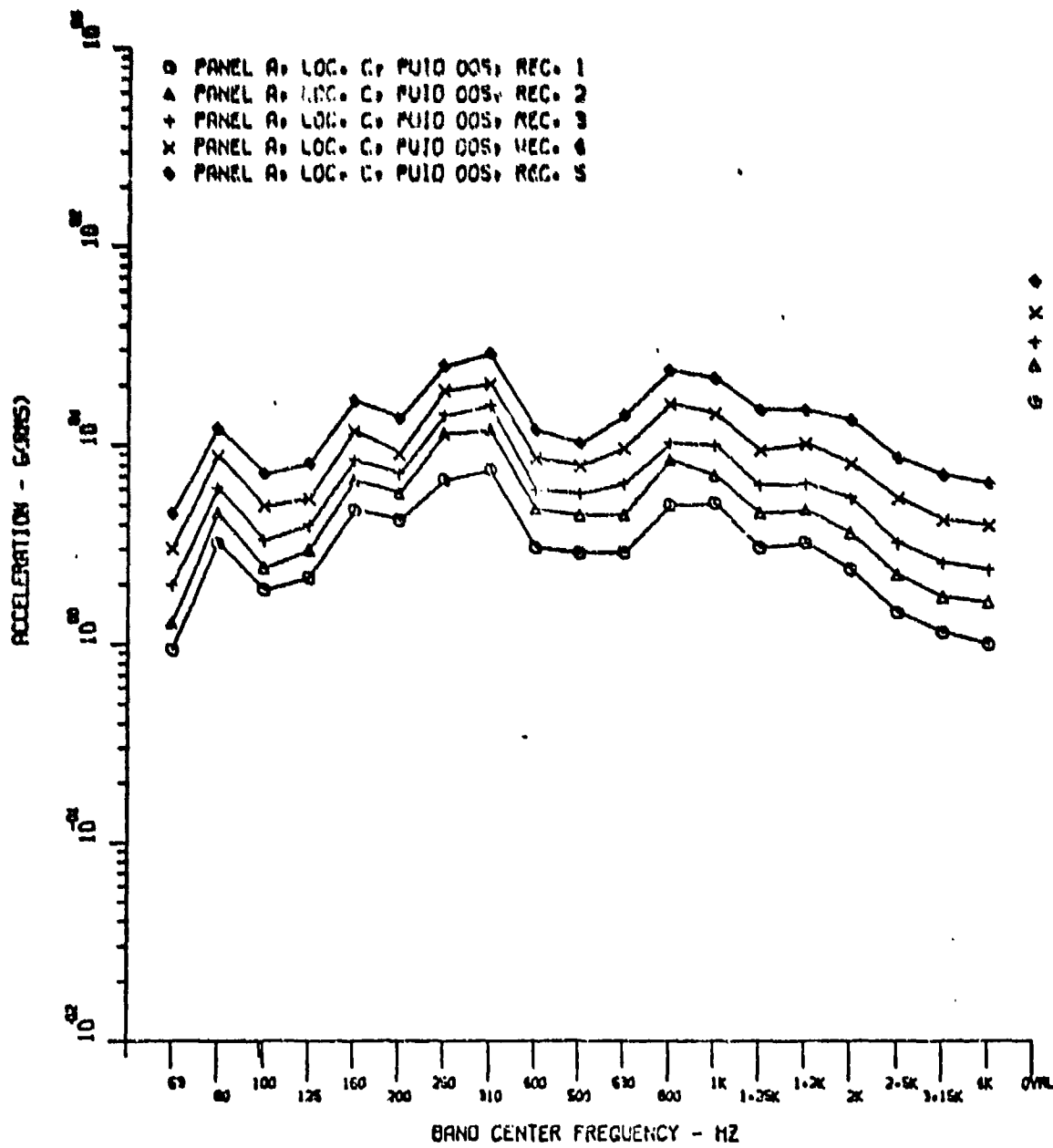


Fig. 30. Acceleration Response, Panel A, Accelerometer 5

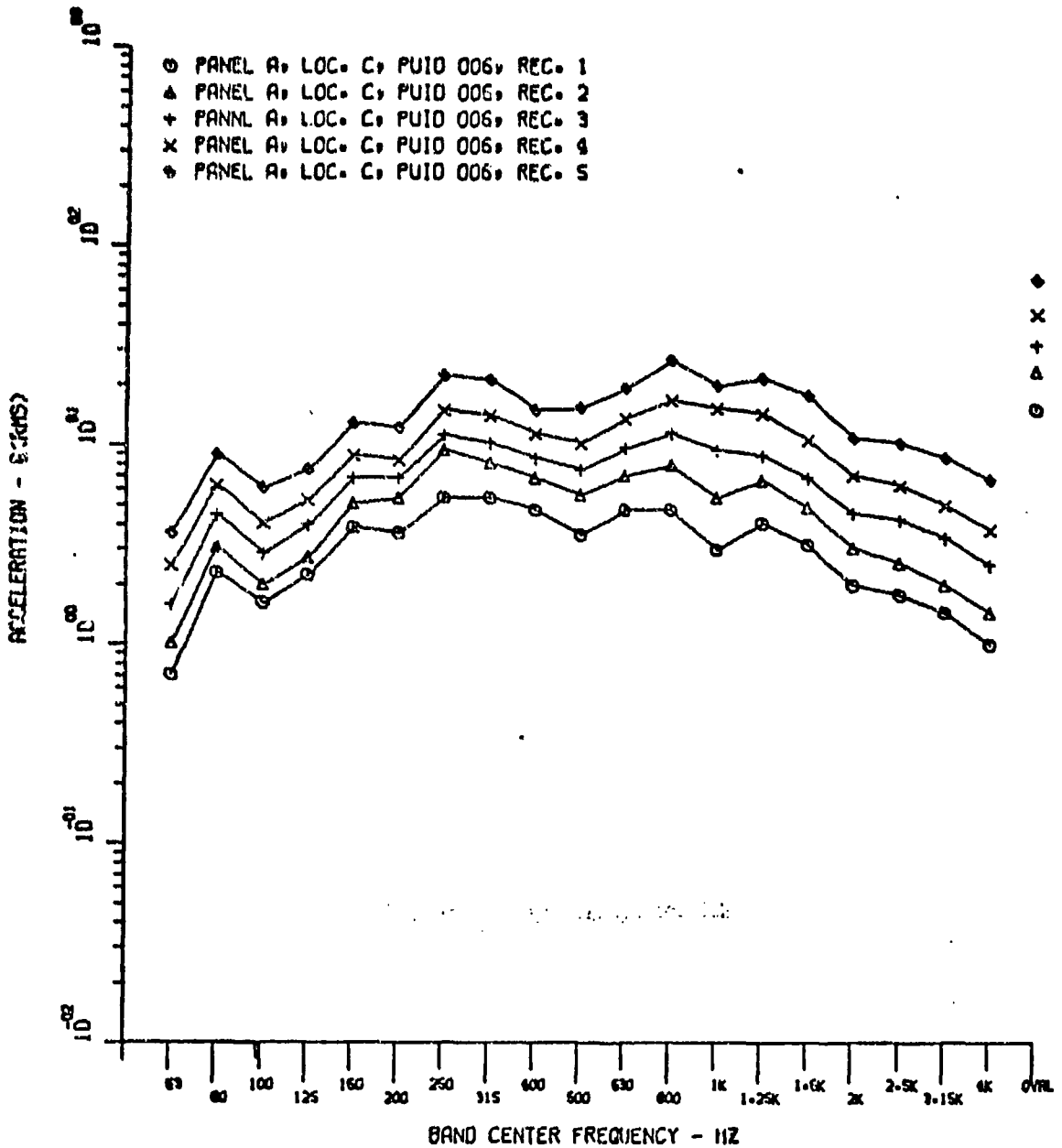


Fig. 31. Acceleration Response, Panel A, Accelerometer 6

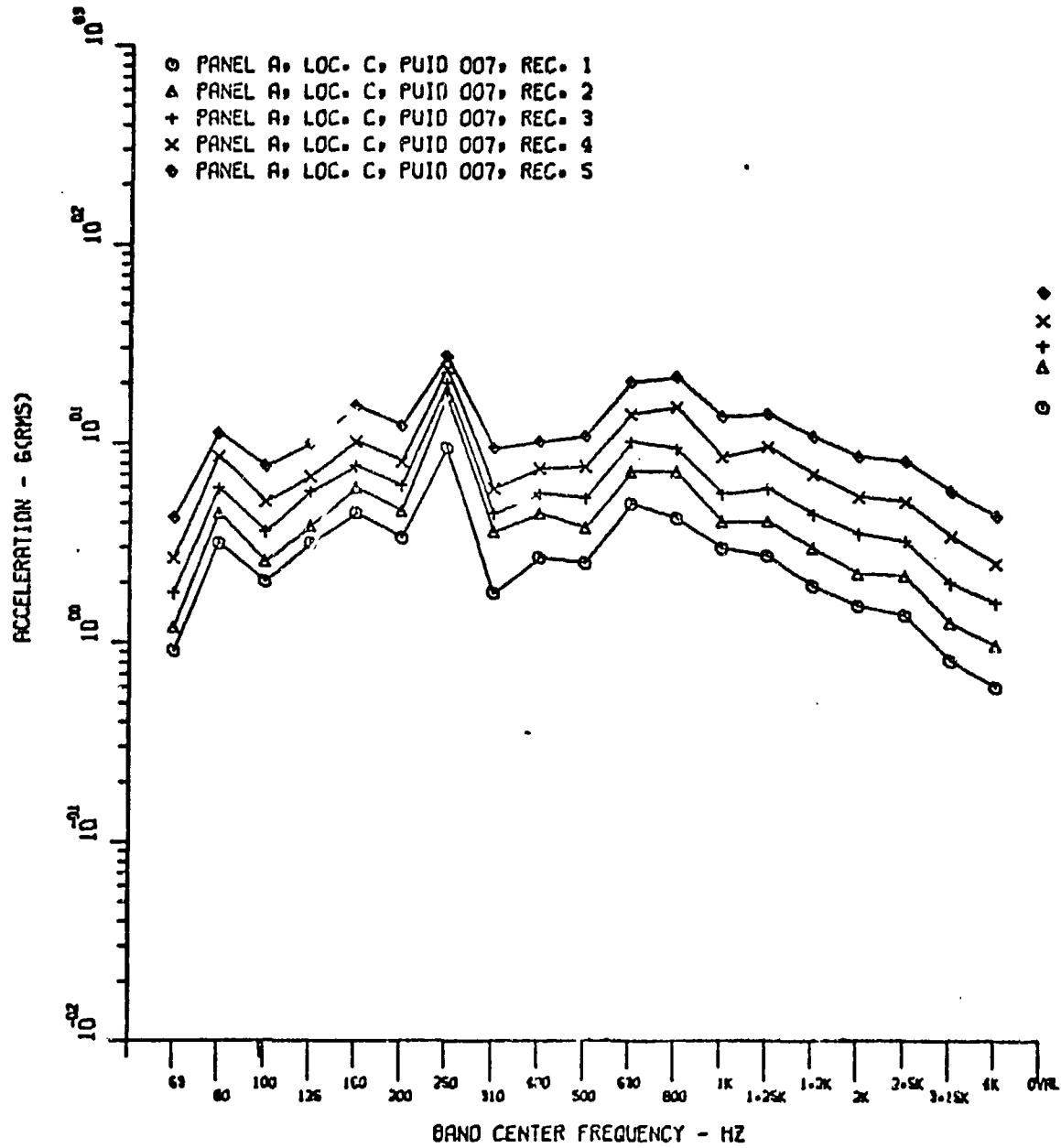


Fig. 32. Acceleration Response, Panel A, Accelerometer 7

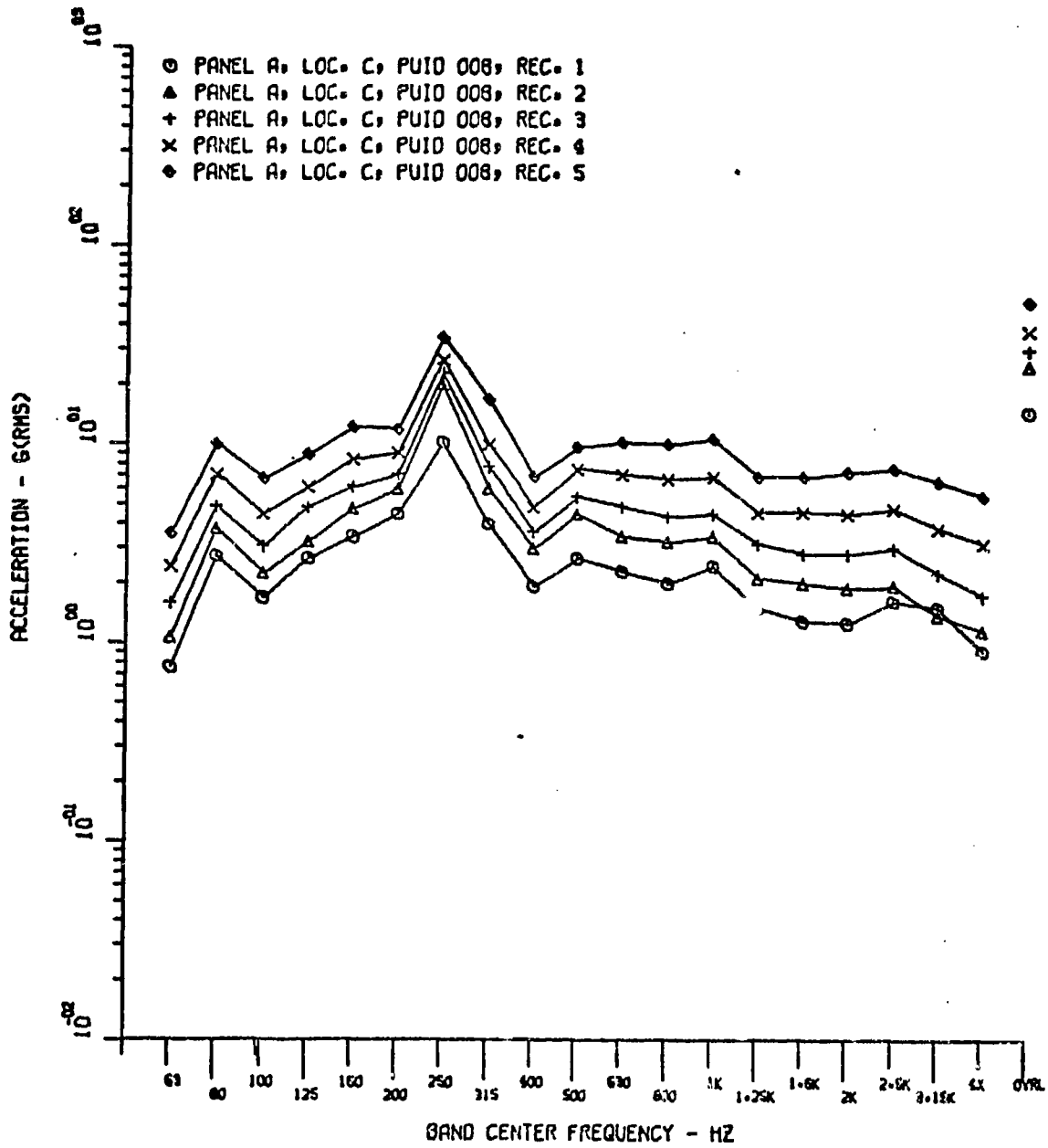


Fig. 33. Acceleration Response, Panel A, Accelerometer 8

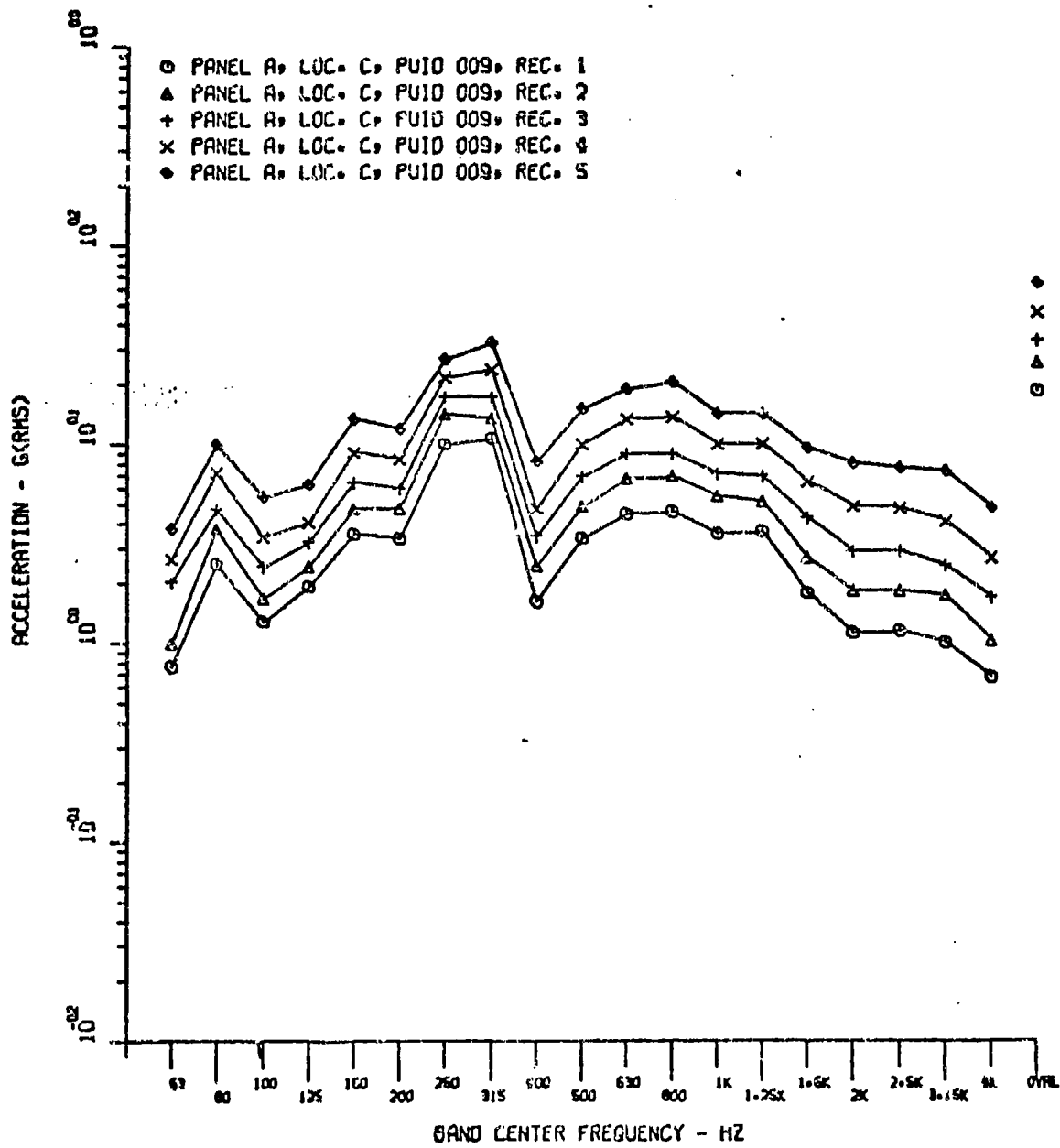
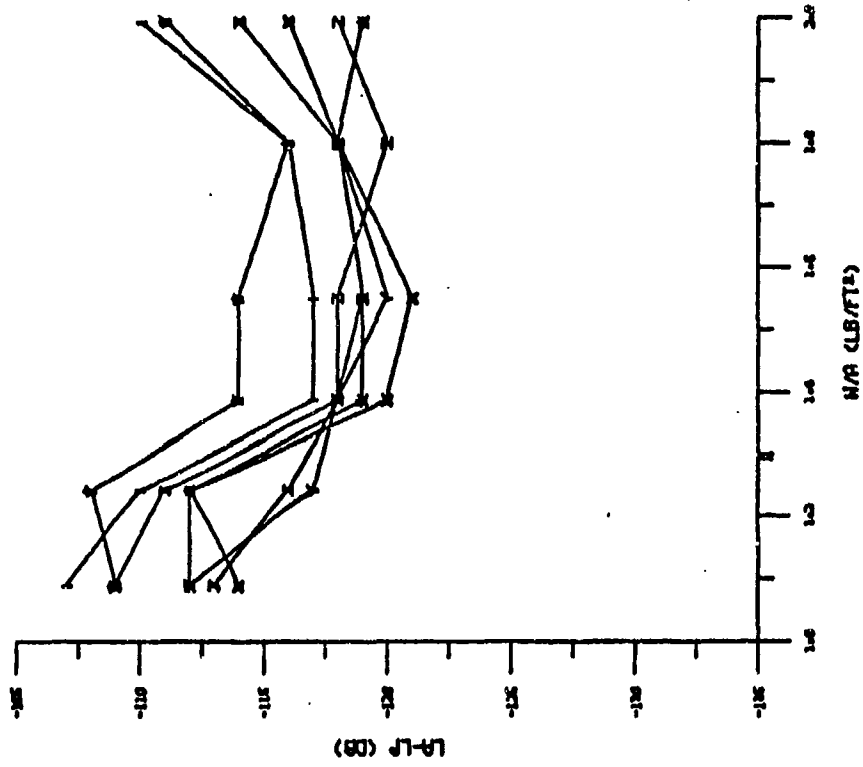


Fig. 34. Acceleration Response, Panel A, Accelerometer 9

Appendix CEmpirical Prediction Curves;
Response Versus Variation in Mass

The following plots represent the excitation/response levels measured for the six constant stiffness panels as the mass was varied. The parameter, $L_a - L_p$, represents the difference in acceleration and sound pressure values, expressed in dB. W/A represents the total weight per unit area of the panels. Two plots are used for each of nine accelerometer locations; one for band center frequencies from 100-500 Hz, and one for frequencies from 620-2500 Hz. The key for each plot contains the symbol identification for each frequency curve, the band center frequency, and the accelerometer location as referenced to Fig. 16, Section V. The plots contained for accelerometer number 5 contain three data points for each frequency curve for which no data existed. These points were arbitrarily set to some value for purposes of plotting.

- Z CENTER BAND FREQ. 620 HZ, ACC. 1
- Y CENTER BAND FREQ. 800 HZ, ACC. 1
- X CENTER BAND FREQ. 1000 HZ, ACC. 1
- W CENTER BAND FREQ. 1250 HZ, ACC. 1
- V CENTER BAND FREQ. 1600 HZ, ACC. 1
- U CENTER BAND FREQ. 2000 HZ, ACC. 1
- T CENTER BAND FREQ. 2500 HZ, ACC. 1



- Q CENTER BAND FREQ. 100 HZ, ACC. 1
- P CENTER BAND FREQ. 125 HZ, ACC. 1
- O CENTER BAND FREQ. 160 HZ, ACC. 1
- N CENTER BAND FREQ. 200 HZ, ACC. 1
- M CENTER BAND FREQ. 260 HZ, ACC. 1
- L CENTER BAND FREQ. 315 HZ, ACC. 1
- K CENTER BAND FREQ. 400 HZ, ACC. 1
- J CENTER BAND FREQ. 500 HZ, ACC. 1

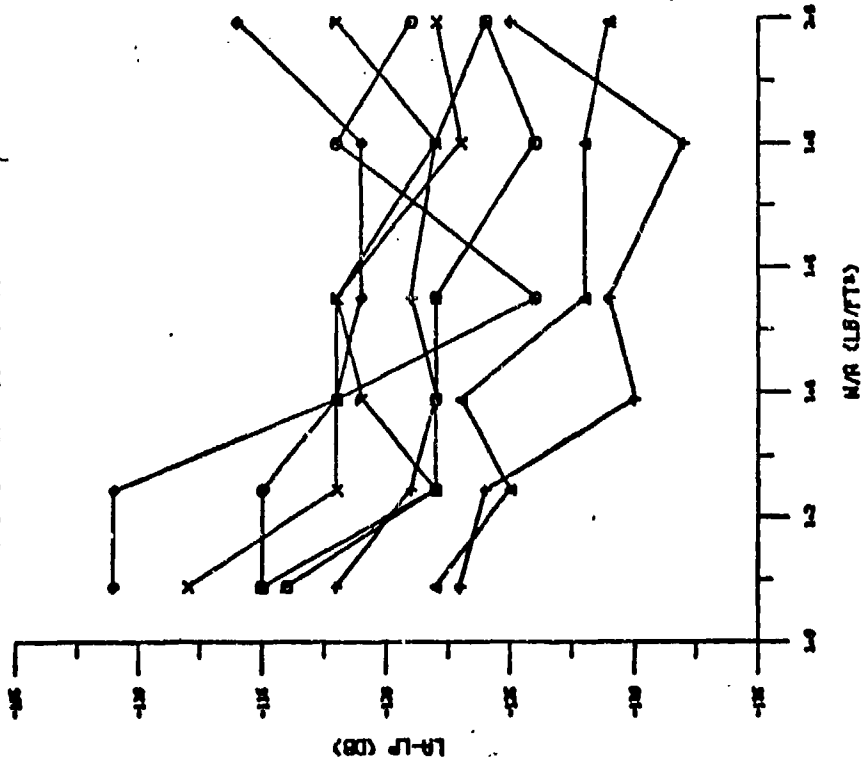
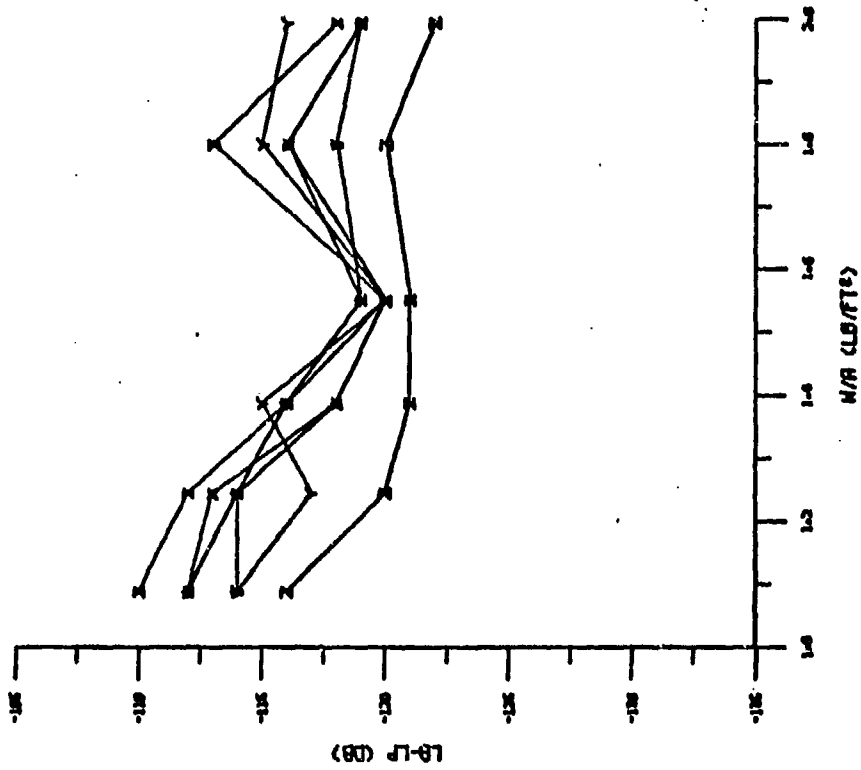


Fig. 35. Prediction Curve, Accelerometer 1, Variation in Mass

- Z CENTER BAND FREQ. 520 HZ, ACC. 2
- Y CENTER BAND FREQ. 600 HZ, ACC. 2
- X CENTER BAND FREQ. 1000 HZ, ACC. 2
- W CENTER BAND FREQ. 1250 HZ, ACC. 2
- V CENTER BAND FREQ. 1600 HZ, ACC. 2
- U CENTER BAND FREQ. 2000 HZ, ACC. 2
- T CENTER BAND FREQ. 2500 HZ, ACC. 2



- Q CENTER BAND FREQ. 100 HZ, ACC. 2
- P CENTER BAND FREQ. 125 HZ, ACC. 2
- O CENTER BAND FREQ. 160 HZ, ACC. 2
- N CENTER BAND FREQ. 200 HZ, ACC. 2
- M CENTER BAND FREQ. 260 HZ, ACC. 2
- L CENTER BAND FREQ. 315 HZ, ACC. 2
- K CENTER BAND FREQ. 400 HZ, ACC. 2
- J CENTER BAND FREQ. 500 HZ, ACC. 2

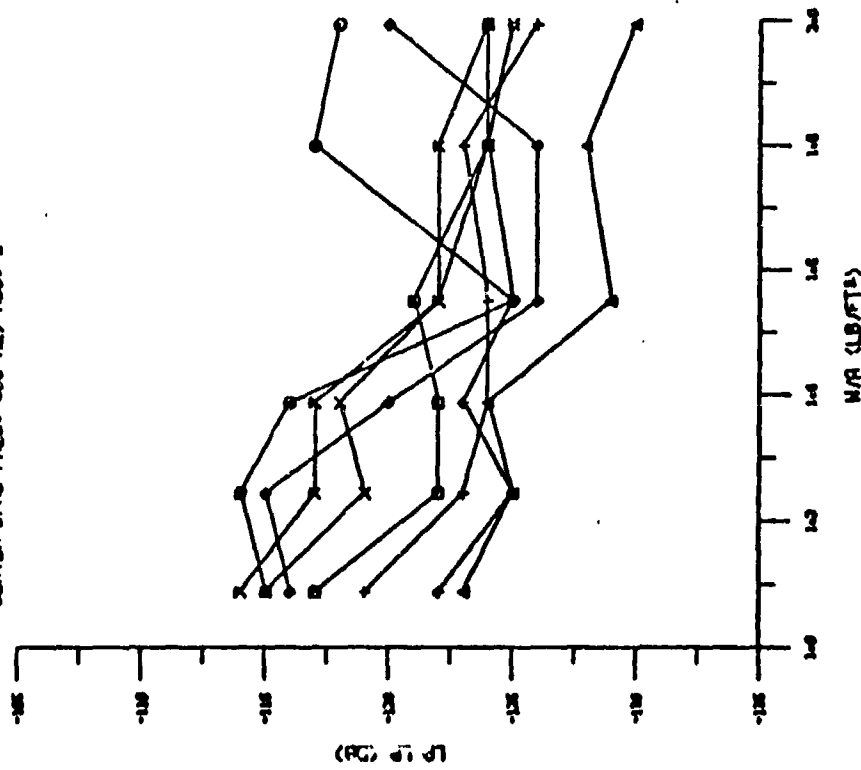
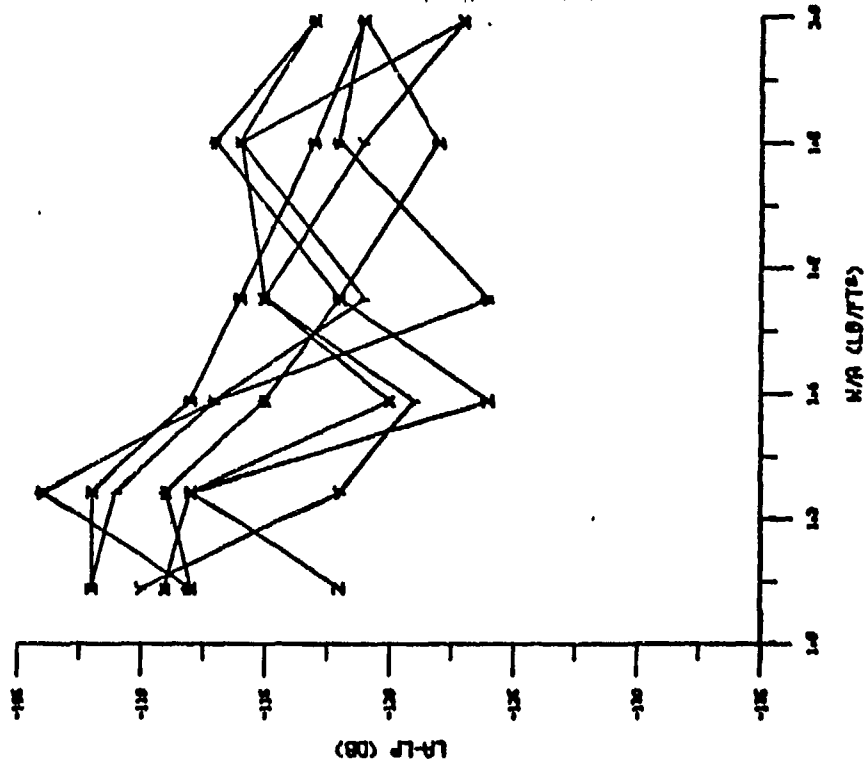


Fig. 36. Prediction Curve, Accelerometer 2, Variation in Mass

- Z CENTER BAND FREQ. 620 HZ, ACC. 3
- Y CENTER BAND FREQ. 800 HZ, ACC. 3
- X CENTER BAND FREQ. 1000 HZ, ACC. 3
- W CENTER BAND FREQ. 1250 HZ, ACC. 3
- V CENTER BAND FREQ. 1600 HZ, ACC. 3
- I CENTER BAND FREQ. 2000 HZ, ACC. 3
- S CENTER BAND FREQ. 2500 HZ, ACC. 3



- Q CENTER BAND FREQ. 100 HZ, ACC. 3
- P CENTER BAND FREQ. 125 HZ, ACC. 3
- A CENTER BAND FREQ. 160 HZ, ACC. 3
- J CENTER BAND FREQ. 200 HZ, ACC. 3
- K CENTER BAND FREQ. 260 HZ, ACC. 3
- L CENTER BAND FREQ. 315 HZ, ACC. 3
- M CENTER BAND FREQ. 400 HZ, ACC. 3
- N CENTER BAND FREQ. 500 HZ, ACC. 3

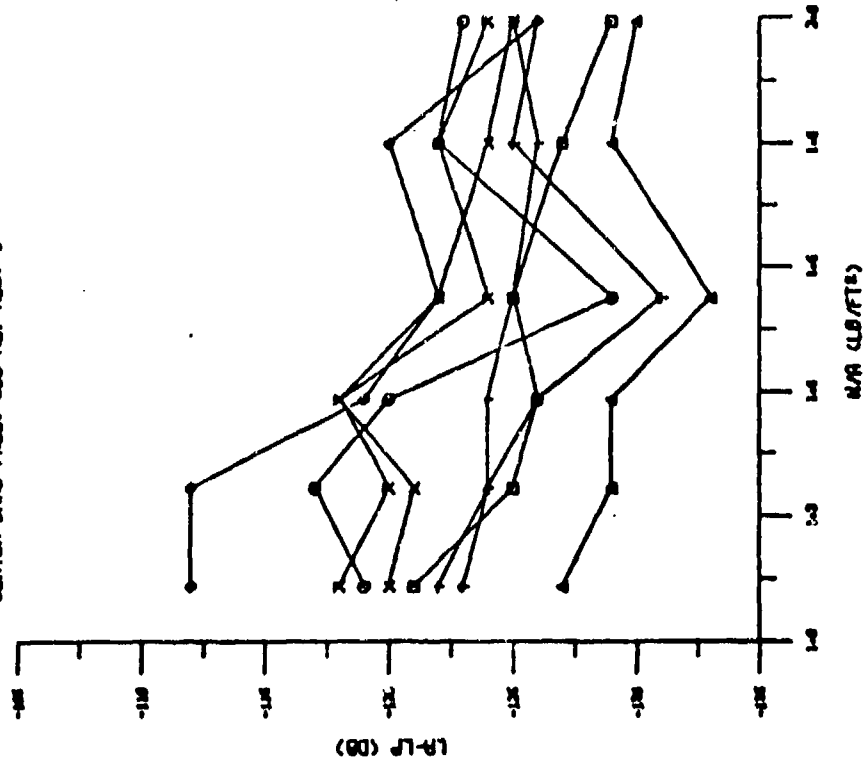
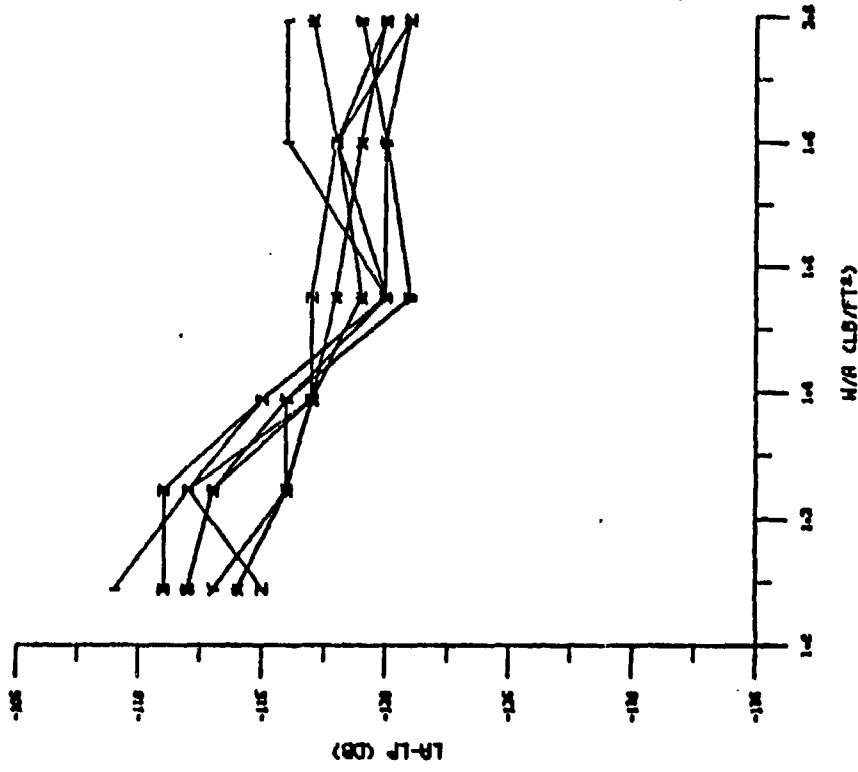


Fig. 37. Prediction Curve, Accelerometer 3, Variation in Mass

Z CENTER BAND FREQ. 620 HZ, ACC. 6
 Y CENTER BAND FREQ. 800 HZ, ACC. 6
 X CENTER BAND FREQ. 1000 HZ, ACC. 6
 W CENTER BAND FREQ. 1250 HZ, ACC. 6
 V CENTER BAND FREQ. 1600 HZ, ACC. 6
 U CENTER BAND FREQ. 2000 HZ, ACC. 6
 T CENTER BAND FREQ. 2500 HZ, ACC. 6



B CENTER BAND FREQ. 100 HZ, ACC. 6
 C CENTER BAND FREQ. 125 HZ, ACC. 6
 D CENTER BAND FREQ. 160 HZ, ACC. 6
 E CENTER BAND FREQ. 200 HZ, ACC. 6
 F CENTER BAND FREQ. 260 HZ, ACC. 6
 G CENTER BAND FREQ. 315 HZ, ACC. 6
 H CENTER BAND FREQ. 400 HZ, ACC. 6
 I CENTER BAND FREQ. 500 HZ, ACC. 6

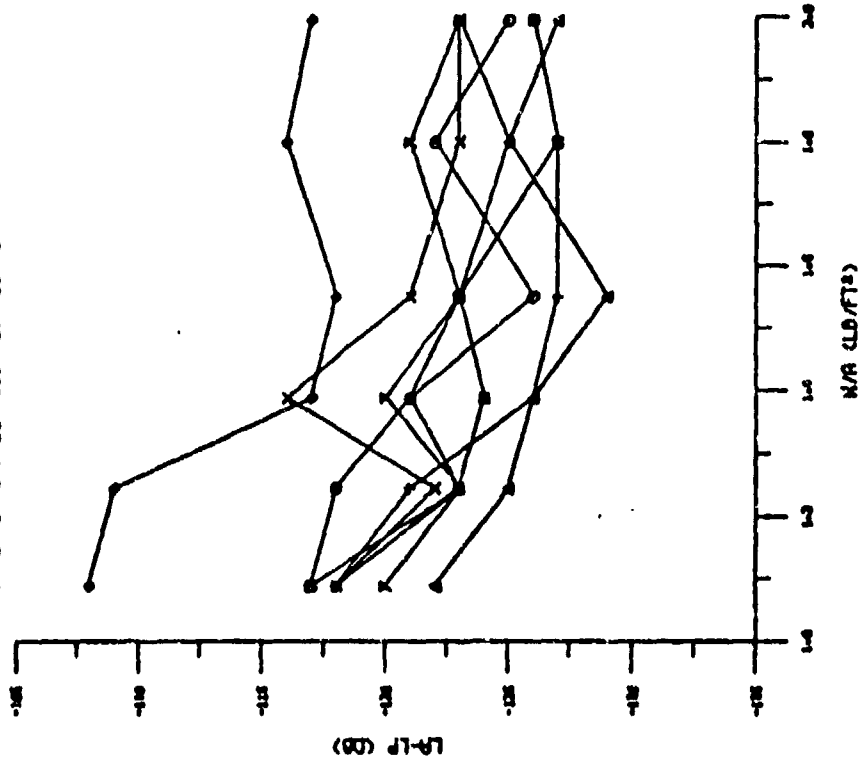
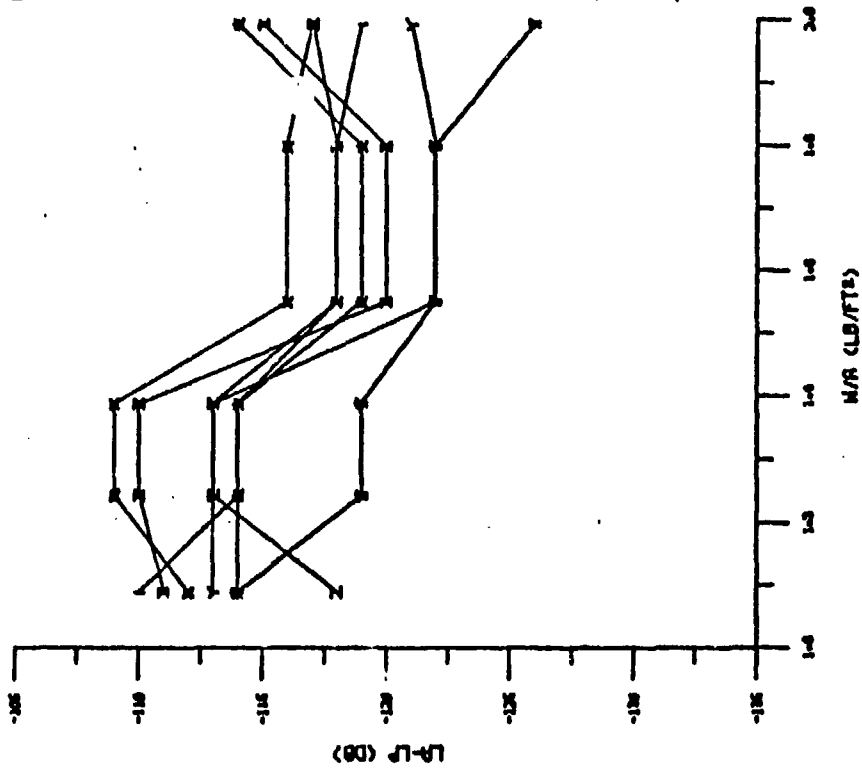


Fig. 38. Prediction Curve, Accelerometer 4, Variation in Mass

- 2 CENTER BAND FREQ. 620 HZ, ACC. 5
- Y CENTER BAND FREQ. 800 HZ, ACC. 5
- X CENTER BAND FREQ. 1000 HZ, ACC. 5
- ▲ CENTER BAND FREQ. 1250 HZ, ACC. 5
- ⊗ CENTER BAND FREQ. 1600 HZ, ACC. 5
- ! CENTER BAND FREQ. 2000 HZ, ACC. 5
- ⊠ CENTER BAND FREQ. 2500 HZ, ACC. 5



- CENTER BAND FREQ. 100 HZ, ACC. 5
- CENTER BAND FREQ. 125 HZ, ACC. 5
- ▲ CENTER BAND FREQ. 160 HZ, ACC. 5
- △ CENTER BAND FREQ. 200 HZ, ACC. 5
- ⊗ CENTER BAND FREQ. 260 HZ, ACC. 5
- CENTER BAND FREQ. 315 HZ, ACC. 5
- ⊠ CENTER BAND FREQ. 400 HZ, ACC. 5
- ⊗ CENTER BAND FREQ. 500 HZ, ACC. 5

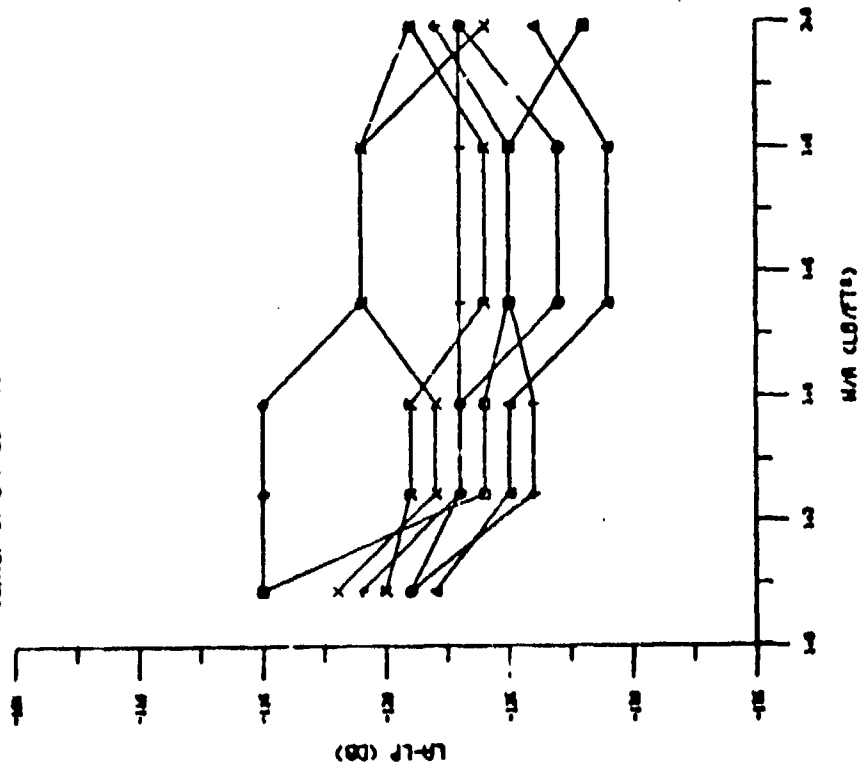
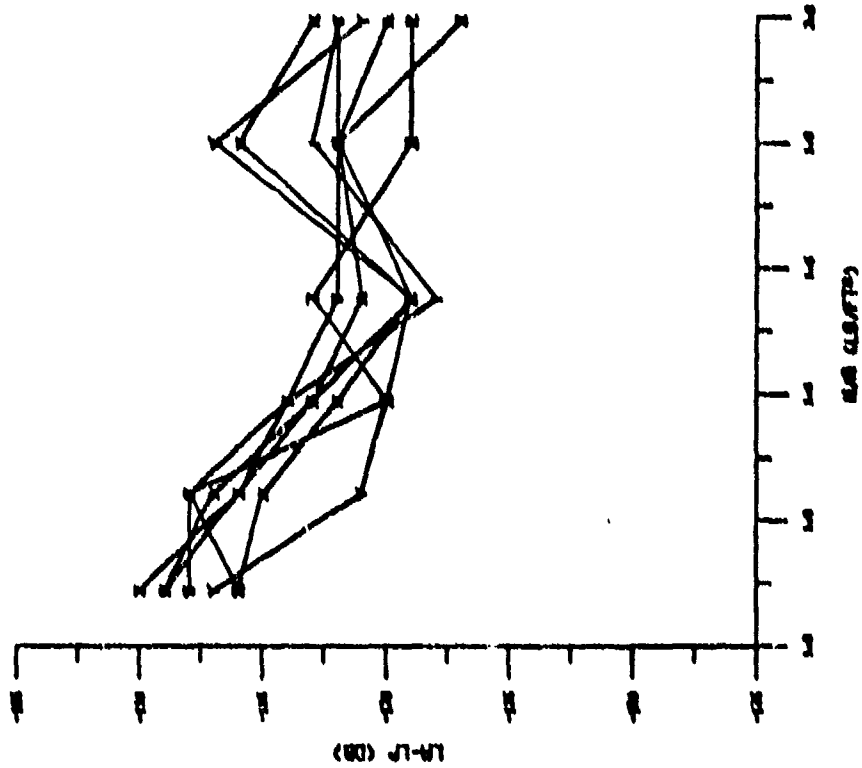


Fig. 39. Prediction Curve, Accelerometer 5, Variation in Mass

Z CENTER BAND FREQ. 600 HZ, ACC. 6
 Y CENTER BAND FREQ. 800 HZ, ACC. 6
 X CENTER BAND FREQ. 1000 HZ, ACC. 6
 W CENTER BAND FREQ. 1250 HZ, ACC. 6
 V CENTER BAND FREQ. 1600 HZ, ACC. 6
 U CENTER BAND FREQ. 2000 HZ, ACC. 6
 T CENTER BAND FREQ. 2500 HZ, ACC. 6



B CENTER BAND FREQ. 100 HZ, ACC. 6
 C CENTER BAND FREQ. 125 HZ, ACC. 6
 D CENTER BAND FREQ. 160 HZ, ACC. 6
 E CENTER BAND FREQ. 200 HZ, ACC. 6
 F CENTER BAND FREQ. 250 HZ, ACC. 6
 G CENTER BAND FREQ. 315 HZ, ACC. 6
 H CENTER BAND FREQ. 400 HZ, ACC. 6
 I CENTER BAND FREQ. 500 HZ, ACC. 6

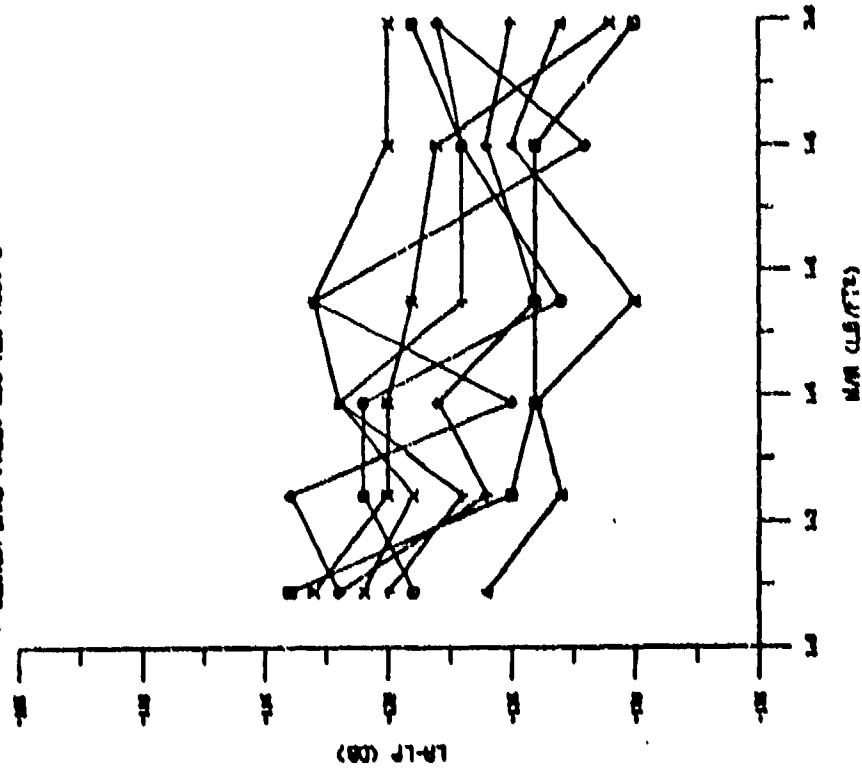
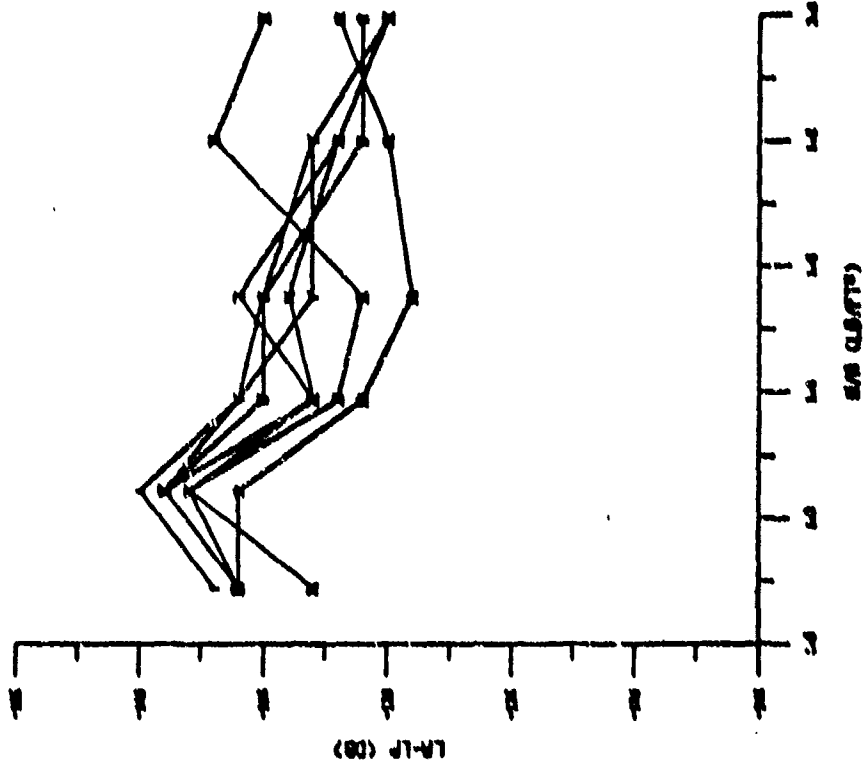


Fig. 40. Prediction Curve, Accelerometer 6, Variation in Mass

2 CENTER BAND FREQ. 820 HZ, ACC. 7
 V CENTER BAND FREQ. 800 HZ, ACC. 7
 7 CENTER BAND FREQ. 1000 HZ, ACC. 7
 8 CENTER BAND FREQ. 1250 HZ, ACC. 7
 3 CENTER BAND FREQ. 1600 HZ, ACC. 7
 1 CENTER BAND FREQ. 2000 HZ, ACC. 7
 6 CENTER BAND FREQ. 2500 HZ, ACC. 7



0 CENTER BAND FREQ. 100 HZ, ACC. 7
 6 CENTER BAND FREQ. 125 HZ, ACC. 7
 4 CENTER BAND FREQ. 160 HZ, ACC. 7
 + CENTER BAND FREQ. 200 HZ, ACC. 7
 x CENTER BAND FREQ. 250 HZ, ACC. 7
 o CENTER BAND FREQ. 315 HZ, ACC. 7
 + CENTER BAND FREQ. 400 HZ, ACC. 7
 3 CENTER BAND FREQ. 500 HZ, ACC. 7

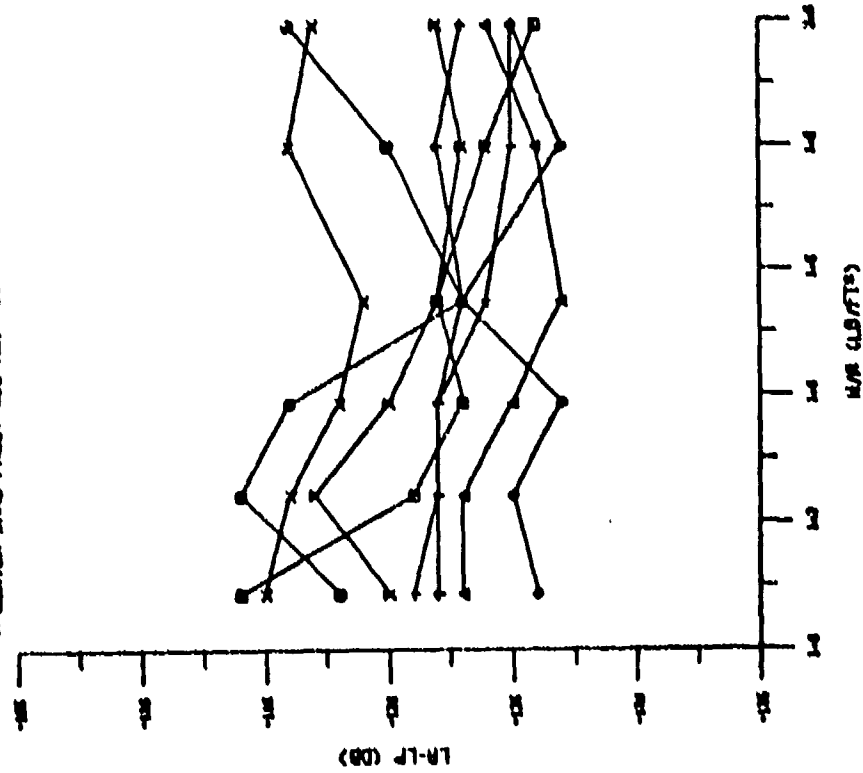
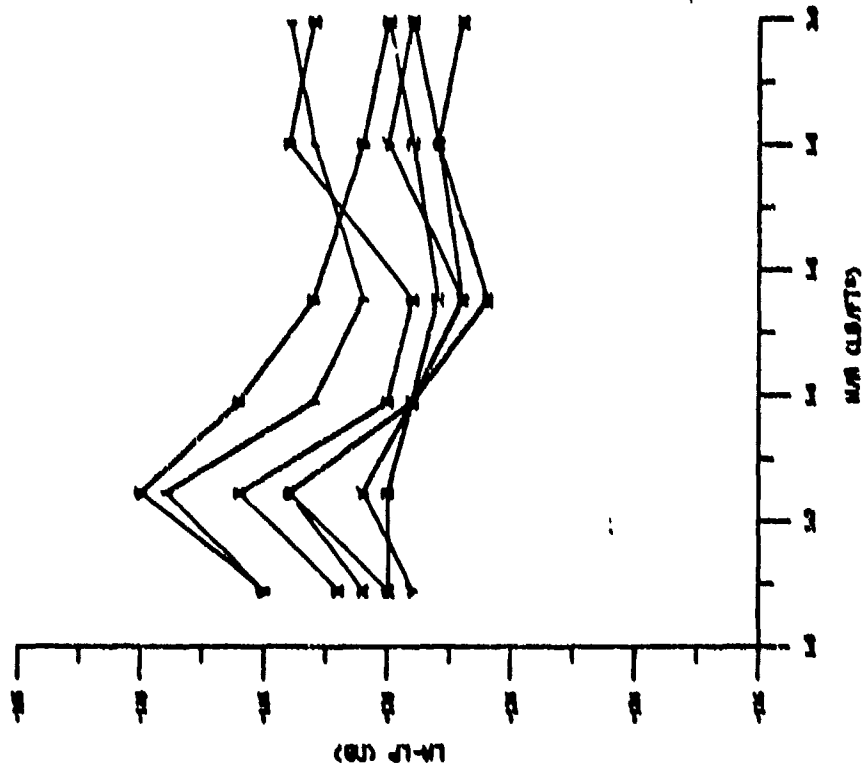


Fig. 41. Prediction Curve, Accelerometer 7, Variation in Pz.ss

Z CENTER BAND FREQ. 620 HZ, ACC. 8
 Y CENTER BAND FREQ. 800 HZ, ACC. 8
 X CENTER BAND FREQ. 1000 HZ, ACC. 8
 W CENTER BAND FREQ. 1250 HZ, ACC. 8
 V CENTER BAND FREQ. 1600 HZ, ACC. 8
 U CENTER BAND FREQ. 2000 HZ, ACC. 8
 T CENTER BAND FREQ. 2500 HZ, ACC. 8



O CENTER BAND FREQ. 100 HZ, ACC. 8
 ● CENTER BAND FREQ. 125 HZ, ACC. 8
 ▲ CENTER BAND FREQ. 160 HZ, ACC. 8
 ◆ CENTER BAND FREQ. 200 HZ, ACC. 8
 × CENTER BAND FREQ. 250 HZ, ACC. 8
 † CENTER BAND FREQ. 315 HZ, ACC. 8
 ‡ CENTER BAND FREQ. 400 HZ, ACC. 8
 § CENTER BAND FREQ. 500 HZ, ACC. 8

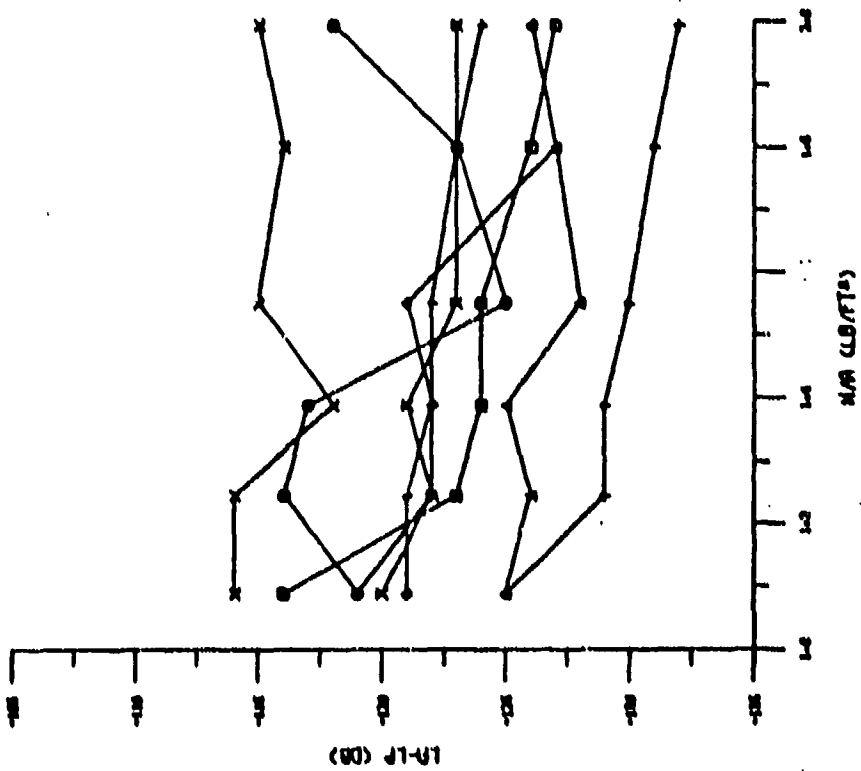
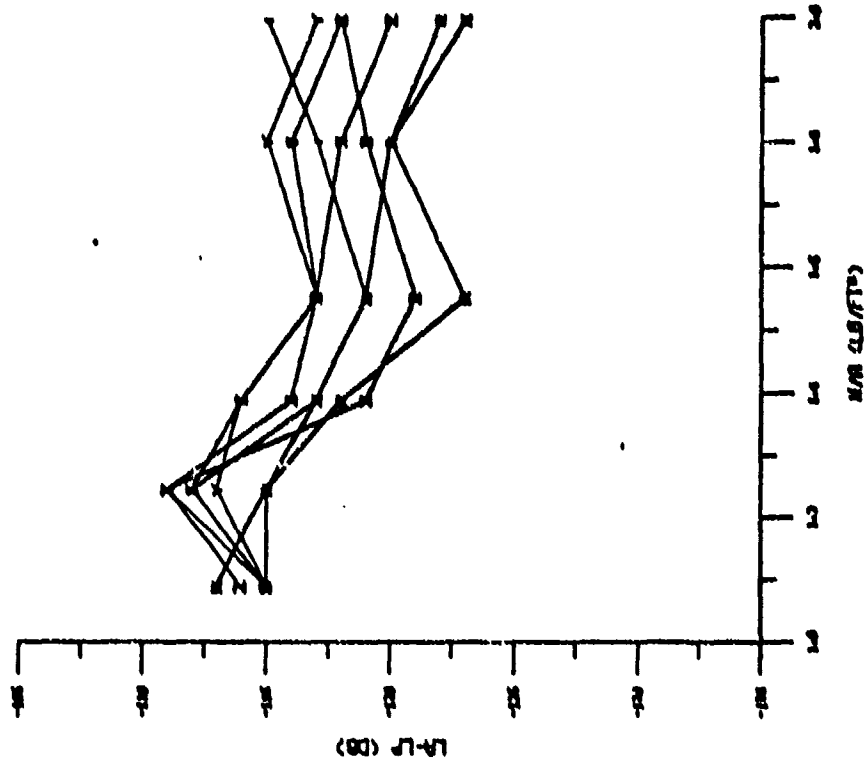


Fig. 42. Prediction Curve, Accelerometer 8, Variation in Mass

Z CENTER BAND FREQ. 520 HZ, ACC. 9
 Y CENTER BAND FREQ. 800 HZ, ACC. 9
 X CENTER BAND FREQ. 1000 HZ, ACC. 9
 W CENTER BAND FREQ. 1250 HZ, ACC. 9
 V CENTER BAND FREQ. 1600 HZ, ACC. 9
 U CENTER BAND FREQ. 2000 HZ, ACC. 9
 T CENTER BAND FREQ. 2500 HZ, ACC. 9



O CENTER BAND FREQ. 100 HZ, ACC. 9
 Q CENTER BAND FREQ. 125 HZ, ACC. 9
 A CENTER BAND FREQ. 160 HZ, ACC. 9
 + CENTER BAND FREQ. 200 HZ, ACC. 9
 X CENTER BAND FREQ. 260 HZ, ACC. 9
 ● CENTER BAND FREQ. 315 HZ, ACC. 9
 † CENTER BAND FREQ. 400 HZ, ACC. 9
 * CENTER BAND FREQ. 500 HZ, ACC. 9

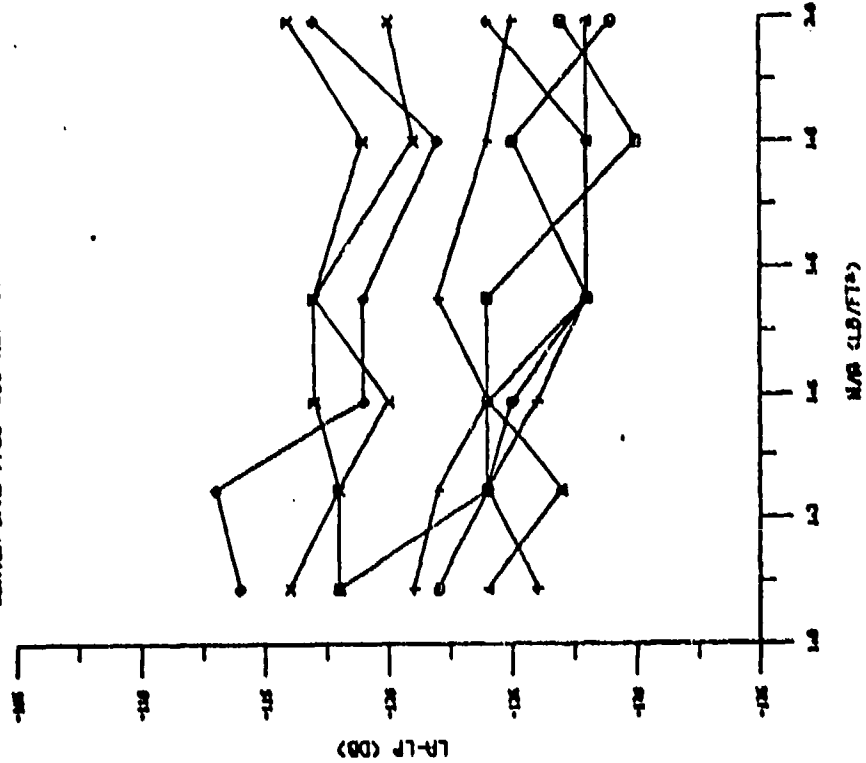
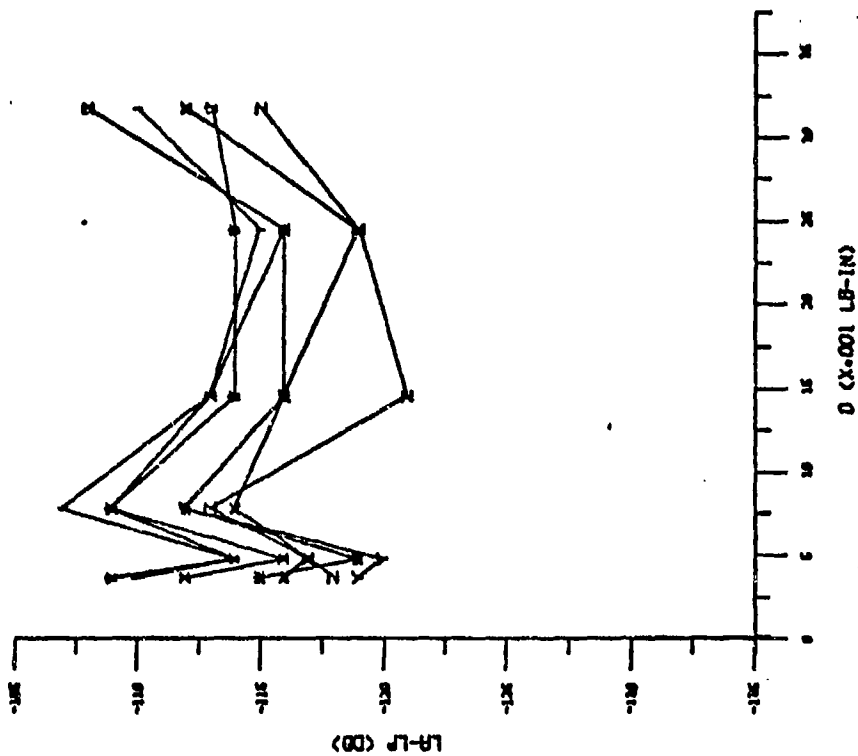


Fig. 43. Prediction Curve, Accelerometer 9, Variation in Mass

Appendix DEmpirical Prediction Curves;Response Versus Variation in Stiffness

The following plots represent the excitation/response levels measured for the six constant mass panels as the stiffness was varied. The parameter, $L_a - L_p$, represents the difference in acceleration and sound pressure values, expressed in dB. D represents the characterized stiffness parameter of the panels. Two plots are used for each of nine accelerometer locations; one for band center frequencies from 100-500 Hz, and one for frequencies from 620-2500 Hz. The key for each plot contains the symbol identification for each frequency curve, the band center frequency, and the accelerometer location as referenced in Fig. 16, Section V.

Z CENTER BAND FREQ. 620 HZ, ACC. 1
 Y CENTER BAND FREQ. 800 HZ, ACC. 1
 X CENTER BAND FREQ. 1000 HZ, ACC. 1
 W CENTER BAND FREQ. 1250 HZ, ACC. 1
 V CENTER BAND FREQ. 1600 HZ, ACC. 1
 U CENTER BAND FREQ. 2000 HZ, ACC. 1
 T CENTER BAND FREQ. 2500 HZ, ACC. 1



Q CENTER BAND FREQ. 100 HZ, ACC. 1
 P CENTER BAND FREQ. 125 HZ, ACC. 1
 A CENTER BAND FREQ. 160 HZ, ACC. 1
 + CENTER BAND FREQ. 200 HZ, ACC. 1
 X CENTER BAND FREQ. 260 HZ, ACC. 1
 O CENTER BAND FREQ. 315 HZ, ACC. 1
 * CENTER BAND FREQ. 400 HZ, ACC. 1
 Z CENTER BAND FREQ. 500 HZ, ACC. 1

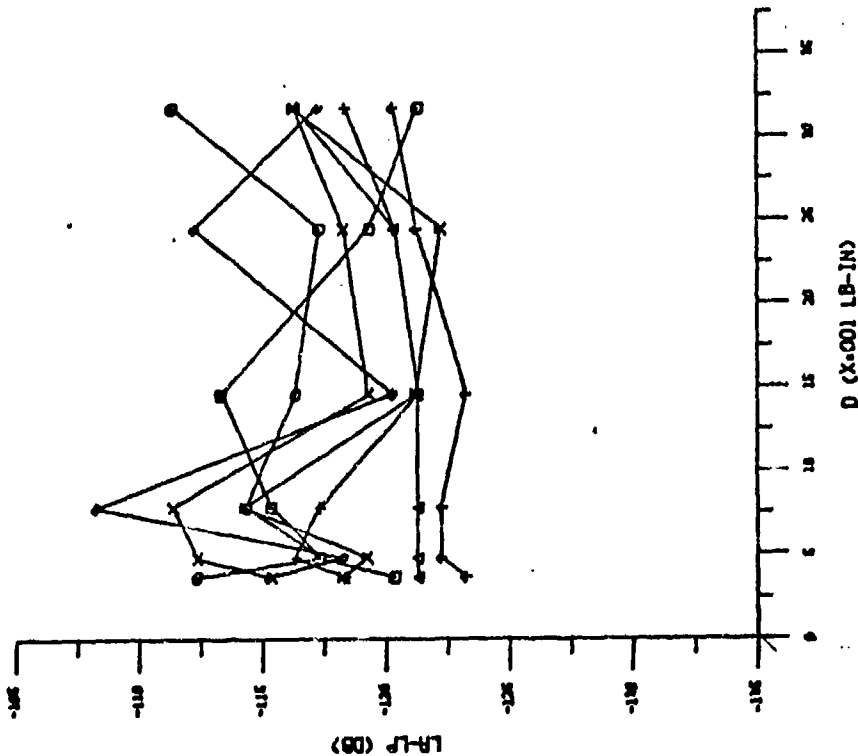
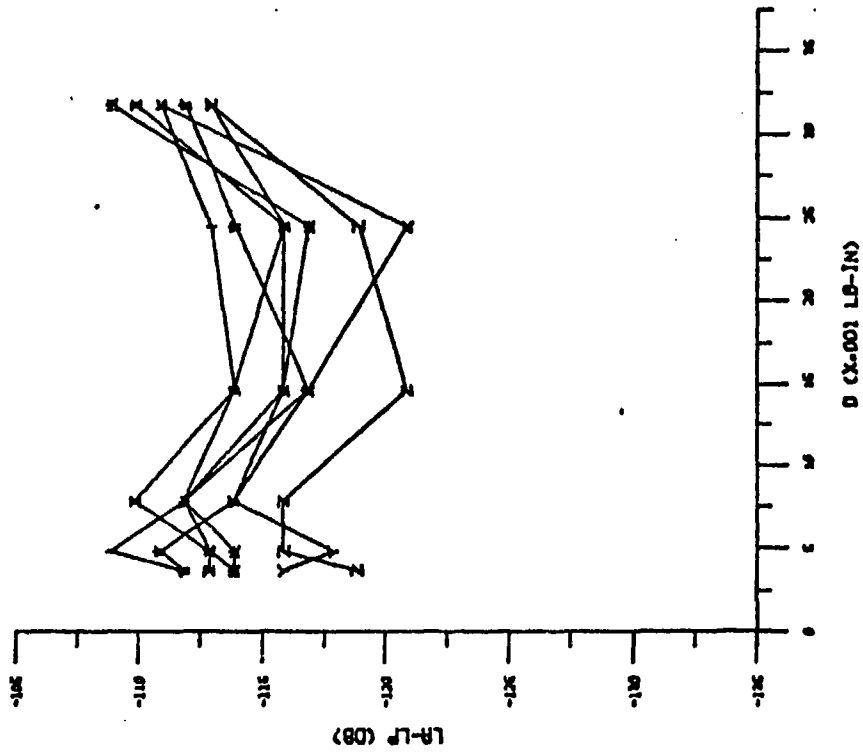


Fig. 44. Prediction Curve, Accelerometer 1, Variation in Stiffness

- Z CENTER BAND FREQ. 620 HZ, ACC. 2
- Y CENTER BAND FREQ. 800 HZ, ACC. 2
- X CENTER BAND FREQ. 1000 HZ, ACC. 2
- W CENTER BAND FREQ. 1250 HZ, ACC. 2
- V CENTER BAND FREQ. 1600 HZ, ACC. 2
- U CENTER BAND FREQ. 2000 HZ, ACC. 2
- T CENTER BAND FREQ. 2500 HZ, ACC. 2



- D CENTER BAND FREQ. 100 HZ, ACC. 2
- C CENTER BAND FREQ. 125 HZ, ACC. 2
- A CENTER BAND FREQ. 160 HZ, ACC. 2
- + CENTER BAND FREQ. 200 HZ, ACC. 2
- X CENTER BAND FREQ. 260 HZ, ACC. 2
- o CENTER BAND FREQ. 315 HZ, ACC. 2
- o CENTER BAND FREQ. 400 HZ, ACC. 2
- X CENTER BAND FREQ. 500 HZ, ACC. 2

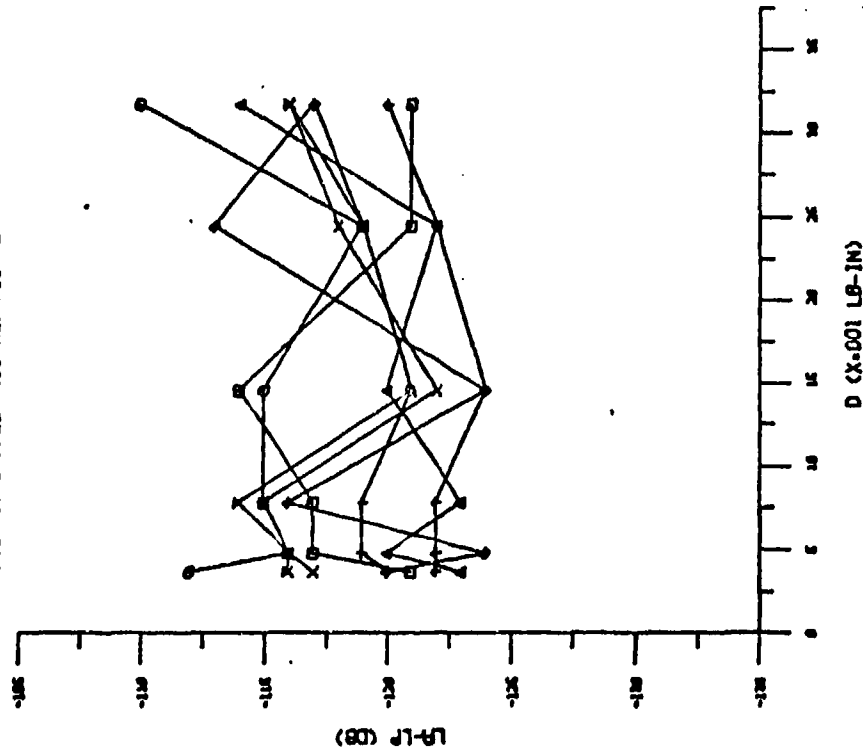
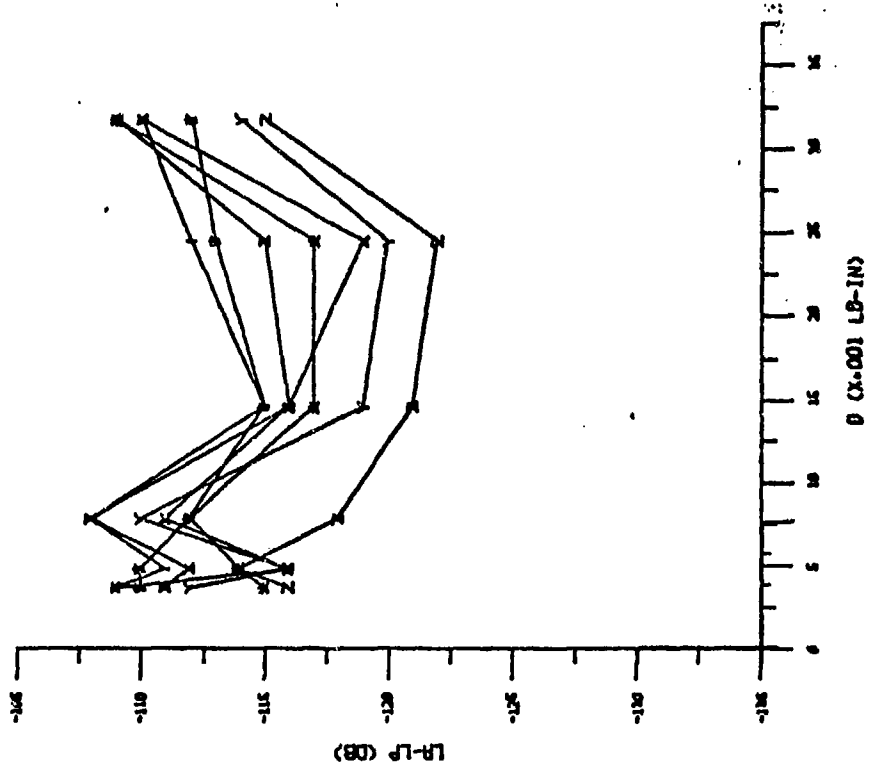


Fig. 45. Prediction Curve, Accelerometer 2, Variation in Stiffness

- Z CENTER BAND FREQ. 620 HZ, ACC. 3
- Y CENTER BAND FREQ. 800 HZ, ACC. 3
- X CENTER BAND FREQ. 1000 HZ, ACC. 3
- CENTER BAND FREQ. 1250 HZ, ACC. 3
- ▲ CENTER BAND FREQ. 1600 HZ, ACC. 3
- ∇ CENTER BAND FREQ. 2000 HZ, ACC. 3
- ▼ CENTER BAND FREQ. 2500 HZ, ACC. 3



- CENTER BAND FREQ. 100 HZ, ACC. 3
- CENTER BAND FREQ. 125 HZ, ACC. 3
- ▲ CENTER BAND FREQ. 160 HZ, ACC. 3
- △ CENTER BAND FREQ. 200 HZ, ACC. 3
- × CENTER BAND FREQ. 260 HZ, ACC. 3
- ◆ CENTER BAND FREQ. 315 HZ, ACC. 3
- ◇ CENTER BAND FREQ. 400 HZ, ACC. 3
- × CENTER BAND FREQ. 500 HZ, ACC. 3

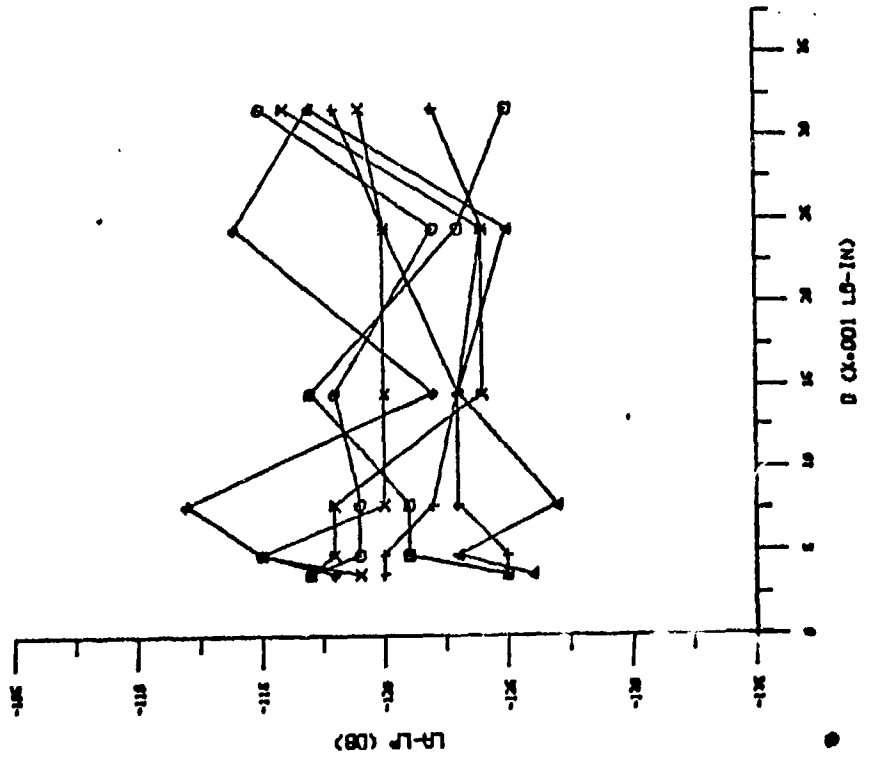
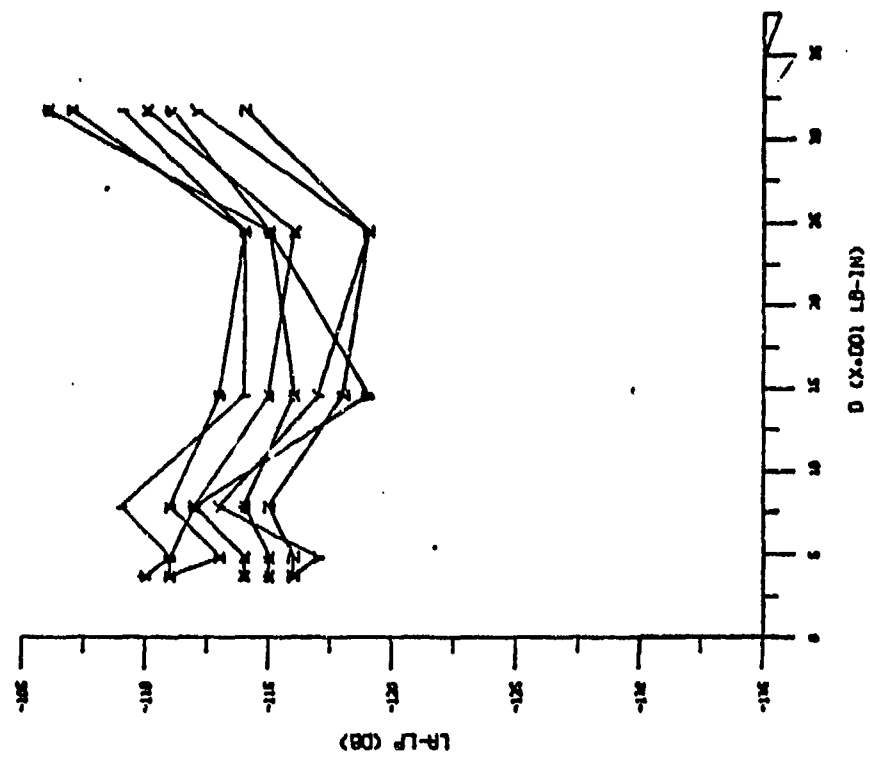


Fig. 46. Prediction Curve, Accelerometer 3, Variation in Stiffness

- Z CENTER BAND FREQ. 620 HZ, ACC. 6
- Y CENTER BAND FREQ. 600 HZ, ACC. 4
- X CENTER BAND FREQ. 1000 HZ, ACC. 4
- W CENTER BAND FREQ. 1250 HZ, ACC. 4
- V CENTER BAND FREQ. 1600 HZ, ACC. 6
- U CENTER BAND FREQ. 2000 HZ, ACC. 6
- T CENTER BAND FREQ. 2500 HZ, ACC. 6



- Q CENTER BAND FREQ. 100 HZ, ACC. 6
- P CENTER BAND FREQ. 125 HZ, ACC. 6
- O CENTER BAND FREQ. 160 HZ, ACC. 6
- N CENTER BAND FREQ. 200 HZ, ACC. 6
- M CENTER BAND FREQ. 260 HZ, ACC. 6
- L CENTER BAND FREQ. 315 HZ, ACC. 6
- K CENTER BAND FREQ. 400 HZ, ACC. 6
- J CENTER BAND FREQ. 500 HZ, ACC. 6

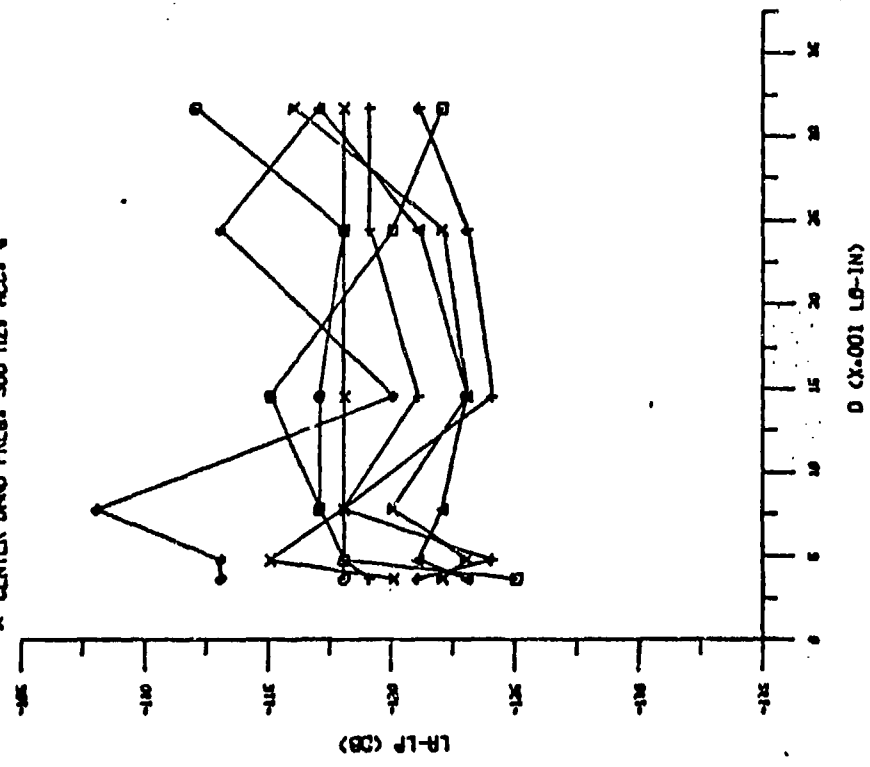
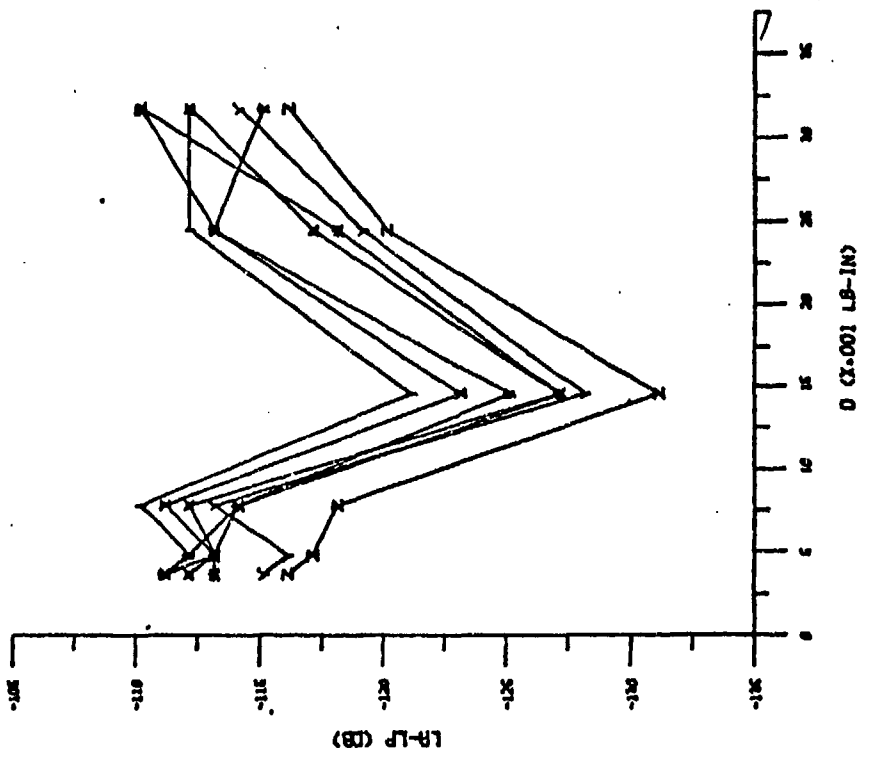


Fig. 47. Prediction Curve, Accelerometer 4, Variation in Stiffness

- Z CENTER BAND FREQ. 620 HZ, ACC. 5
- Y CENTER BAND FREQ. 600 HZ, ACC. 5
- X CENTER BAND FREQ. 1000 HZ, ACC. 5
- M CENTER BAND FREQ. 1250 HZ, ACC. 5
- N CENTER BAND FREQ. 1600 HZ, ACC. 5
- I CENTER BAND FREQ. 2000 HZ, ACC. 5
- F CENTER BAND FREQ. 2500 HZ, ACC. 5



- Q CENTER BAND FREQ. 100 HZ, ACC. 5
- R CENTER BAND FREQ. 125 HZ, ACC. 5
- A CENTER BAND FREQ. 160 HZ, ACC. 5
- T CENTER BAND FREQ. 200 HZ, ACC. 5
- X CENTER BAND FREQ. 260 HZ, ACC. 5
- C CENTER BAND FREQ. 315 HZ, ACC. 5
- D CENTER BAND FREQ. 400 HZ, ACC. 5
- Z CENTER BAND FREQ. 500 HZ, ACC. 5

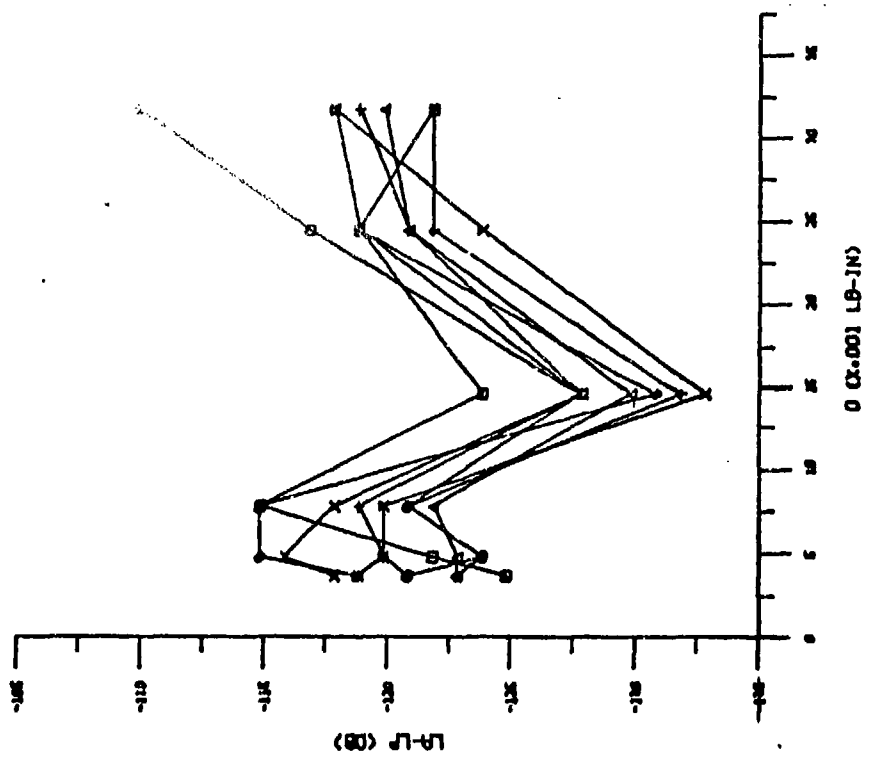
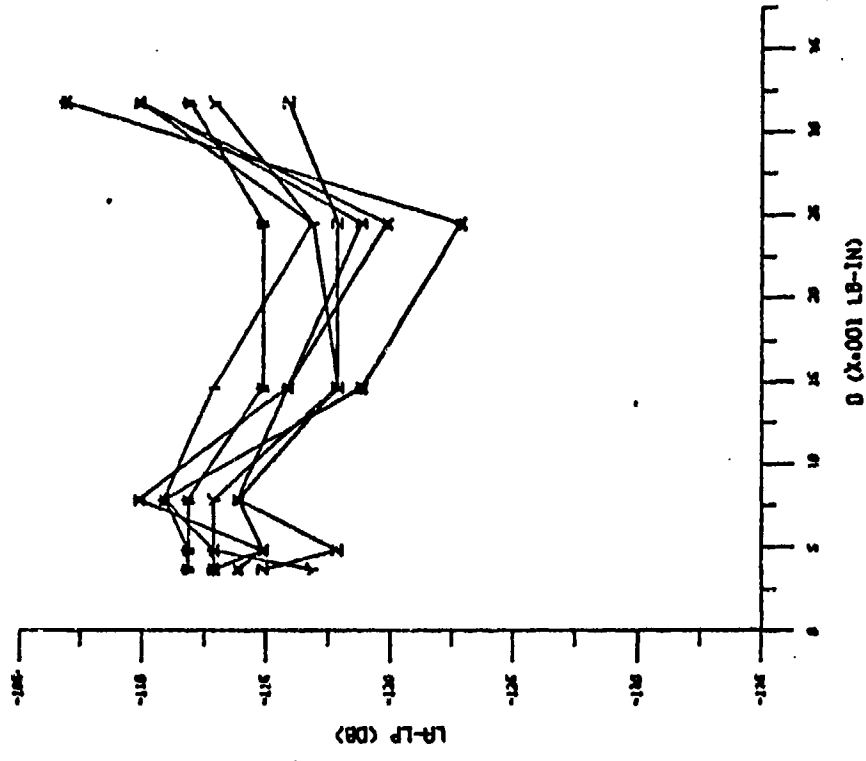


Fig. 48. Prediction Curve, Accelerometer 5, Variation in Stiffness

- Z CENTER BAND FREQ. 620 HZ, ACC. 6
- Y CENTER BAND FREQ. 600 HZ, ACC. 6
- X CENTER BAND FREQ. 1000 HZ, ACC. 6
- # CENTER BAND FREQ. 1250 HZ, ACC. 6
- CENTER BAND FREQ. 1600 HZ, ACC. 6
- ! CENTER BAND FREQ. 2000 HZ, ACC. 6
- ∇ CENTER BAND FREQ. 2500 HZ, ACC. 6



- 6 CENTER BAND FREQ. 100 HZ, ACC. 6
- CENTER BAND FREQ. 125 HZ, ACC. 6
- ▲ CENTER BAND FREQ. 160 HZ, ACC. 6
- † CENTER BAND FREQ. 200 HZ, ACC. 6
- × CENTER BAND FREQ. 260 HZ, ACC. 6
- ◆ CENTER BAND FREQ. 315 HZ, ACC. 6
- ‡ CENTER BAND FREQ. 400 HZ, ACC. 6
- ⊗ CENTER BAND FREQ. 500 HZ, ACC. 6

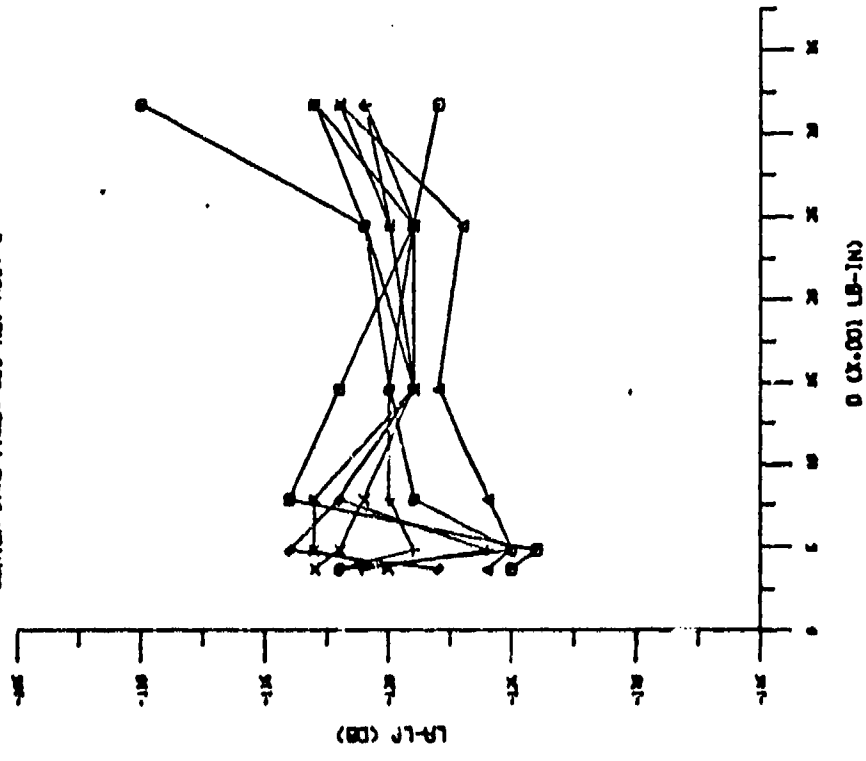
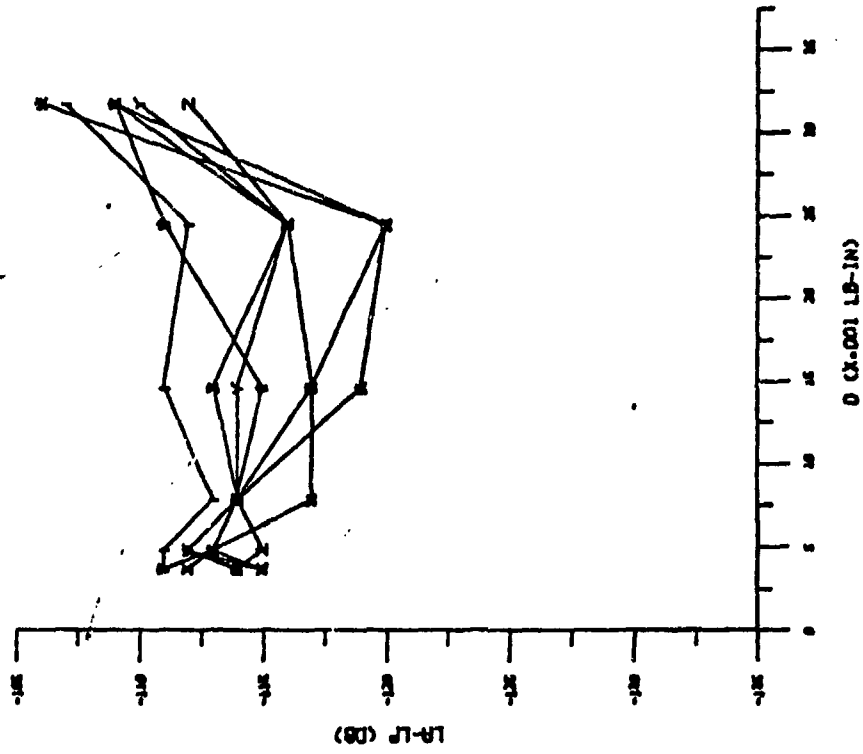


Fig. 49. Prediction Curve, Accelerometer 6, Variation in Stiffness

- Z CENTER BAND FREQ. 620 HZ, ACC. 7
- Y CENTER BAND FREQ. 800 HZ, ACC. 7
- X CENTER BAND FREQ. 1000 HZ, ACC. 7
- * CENTER BAND FREQ. 1250 HZ, ACC. 7
- z CENTER BAND FREQ. 1600 HZ, ACC. 7
- l CENTER BAND FREQ. 2000 HZ, ACC. 7
- f CENTER BAND FREQ. 2500 HZ, ACC. 7



- o CENTER BAND FREQ. 100 HZ, ACC. 7
- o CENTER BAND FREQ. 125 HZ, ACC. 7
- ▲ CENTER BAND FREQ. 160 HZ, ACC. 7
- ♦ CENTER BAND FREQ. 200 HZ, ACC. 7
- x CENTER BAND FREQ. 260 HZ, ACC. 7
- ◆ CENTER BAND FREQ. 315 HZ, ACC. 7
- ◇ CENTER BAND FREQ. 400 HZ, ACC. 7
- z CENTER BAND FREQ. 500 HZ, ACC. 7

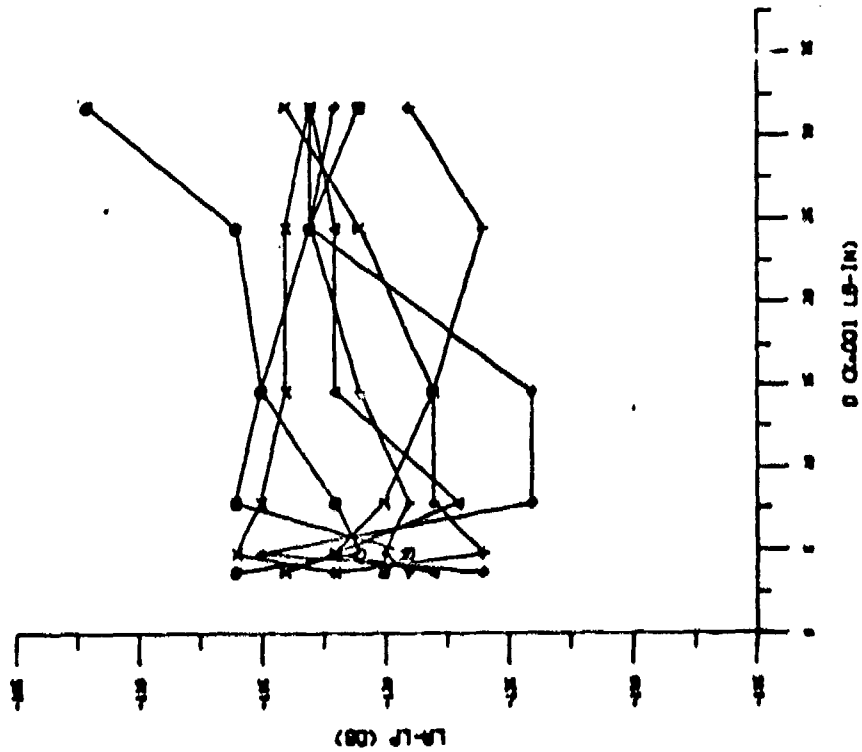
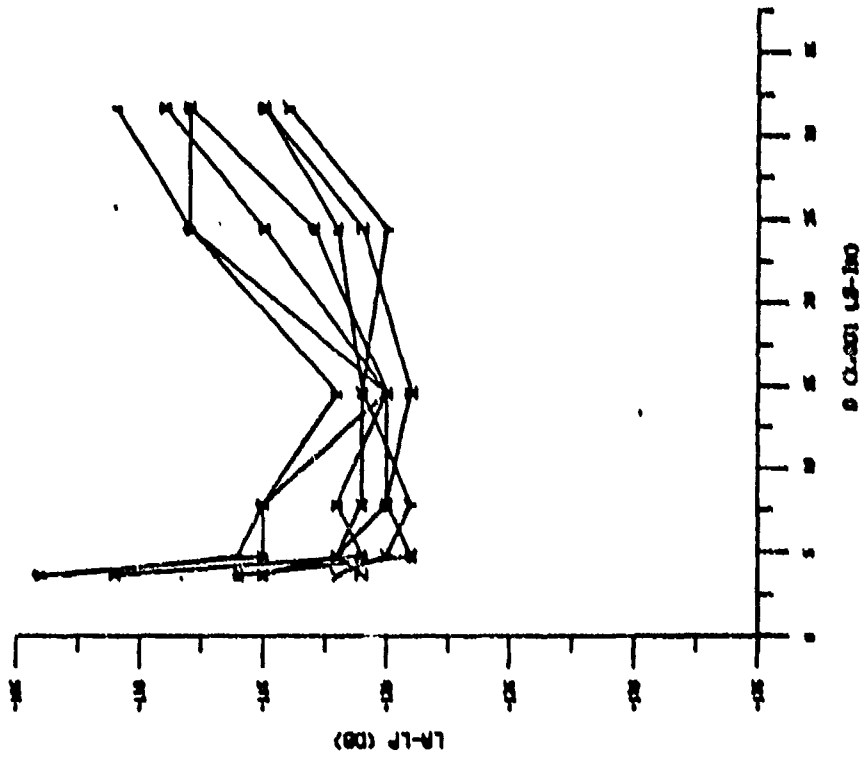


Fig. 50. Prediction Curve, Accelerometer 7, Variation in Stiffness

- Z CENTER BAND FREQ. 620 HZ, ACC. 6
- Y CENTER BAND FREQ. 600 HZ, ACC. 6
- X CENTER BAND FREQ. 1000 HZ, ACC. 6
- W CENTER BAND FREQ. 1250 HZ, ACC. 6
- V CENTER BAND FREQ. 1600 HZ, ACC. 6
- U CENTER BAND FREQ. 2000 HZ, ACC. 6
- T CENTER BAND FREQ. 2500 HZ, ACC. 6



- Q CENTER BAND FREQ. 100 HZ, ACC. 6
- P CENTER BAND FREQ. 125 HZ, ACC. 6
- O CENTER BAND FREQ. 160 HZ, ACC. 6
- N CENTER BAND FREQ. 200 HZ, ACC. 6
- M CENTER BAND FREQ. 260 HZ, ACC. 6
- L CENTER BAND FREQ. 375 HZ, ACC. 6
- K CENTER BAND FREQ. 600 HZ, ACC. 6
- J CENTER BAND FREQ. 500 HZ, ACC. 6

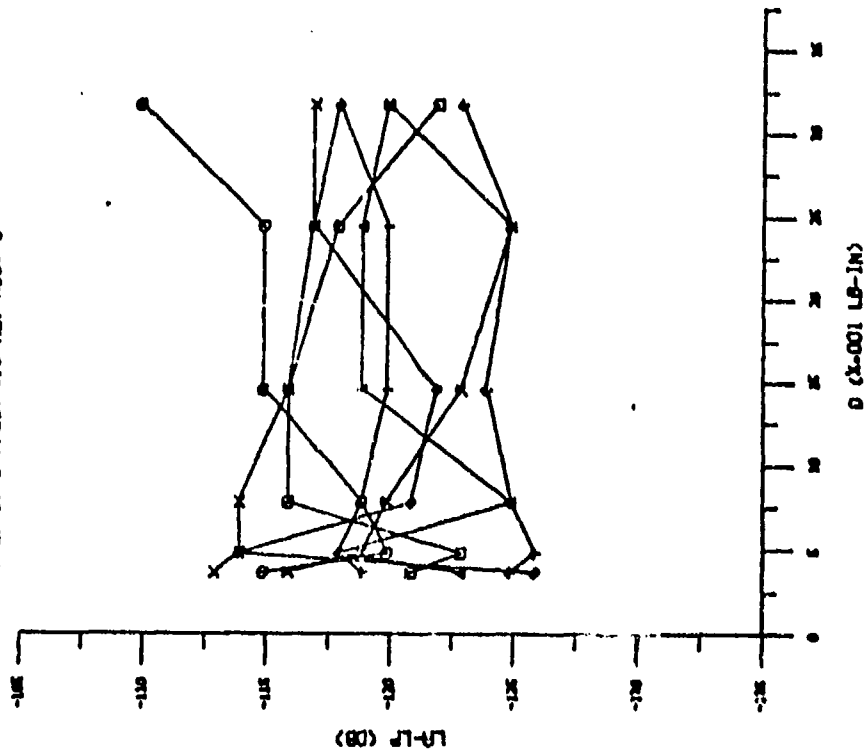
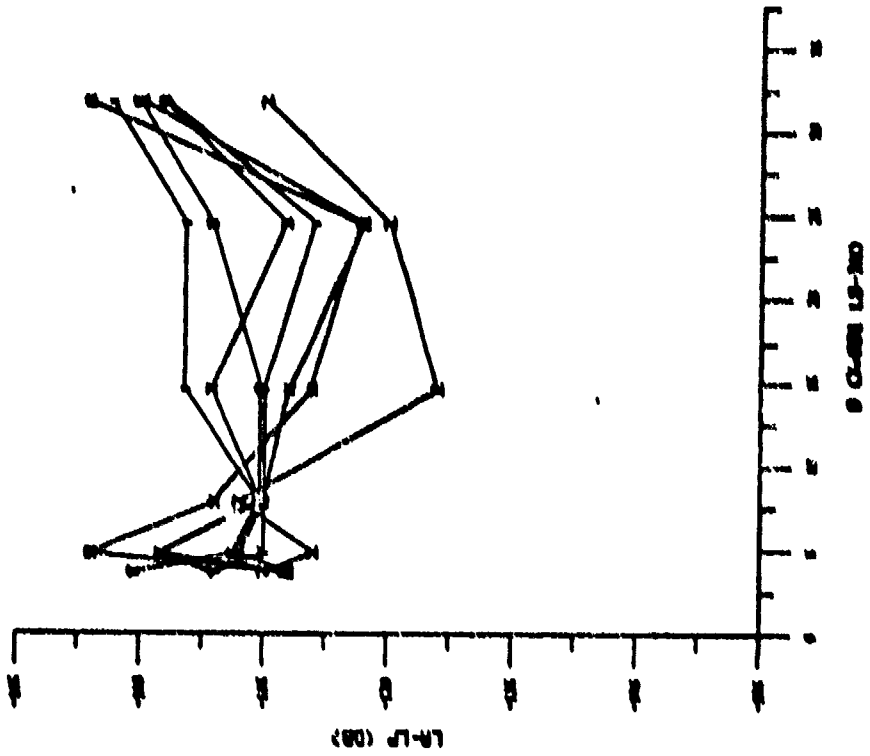


Fig. 51. Prediction Curve, Accelerometer 8, Variation in Stiffness

- 2 CENTER BAND FREQ. 620 Hz, ACC. 9
- Y CENTER BAND FREQ. 620 Hz, ACC. 9
- X CENTER BAND FREQ. 620 Hz, ACC. 9
- W CENTER BAND FREQ. 1000 Hz, ACC. 9
- V CENTER BAND FREQ. 1250 Hz, ACC. 9
- U CENTER BAND FREQ. 1000 Hz, ACC. 9
- T CENTER BAND FREQ. 2000 Hz, ACC. 9
- S CENTER BAND FREQ. 2000 Hz, ACC. 9



- 8 CENTER BAND FREQ. 100 Hz, ACC. 9
- 7 CENTER BAND FREQ. 125 Hz, ACC. 9
- 6 CENTER BAND FREQ. 150 Hz, ACC. 9
- 5 CENTER BAND FREQ. 200 Hz, ACC. 9
- 4 CENTER BAND FREQ. 250 Hz, ACC. 9
- 3 CENTER BAND FREQ. 315 Hz, ACC. 9
- 2 CENTER BAND FREQ. 400 Hz, ACC. 9
- 1 CENTER BAND FREQ. 500 Hz, ACC. 9

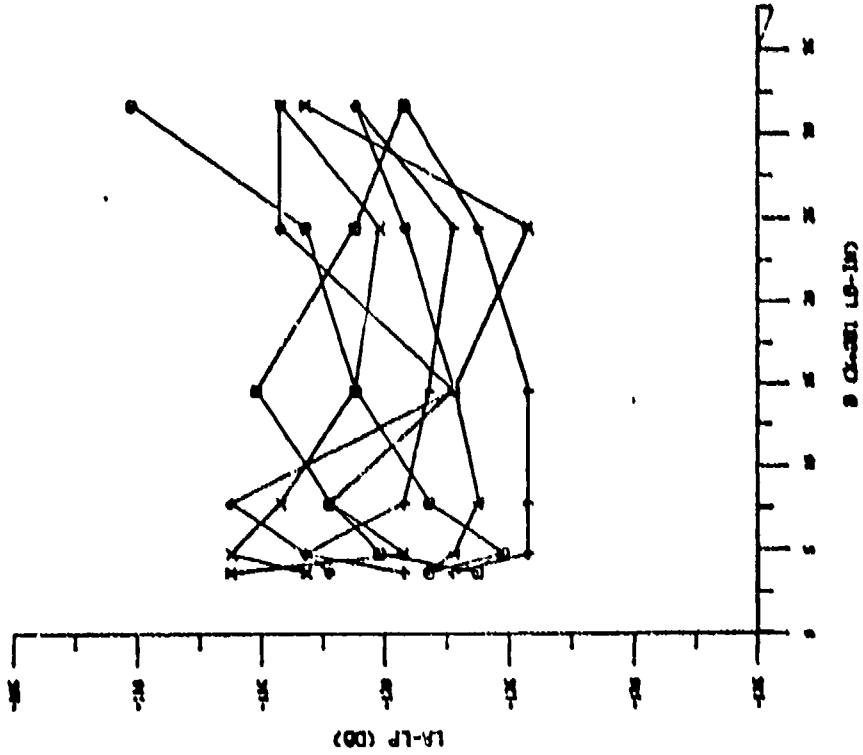


Fig. 52. Prediction Curve, Accelerometer 9, Variation in Stiffness

VITA

Clarence Mark Rose was born on 19 December 1945 in Yale, Iowa, the son of Arthur R. Rose and Margaret C. Smith. After completing high school at Minburn, Iowa, in 1964, he enrolled at Iowa State University, Ames, Iowa. The following year he received a nomination to the United States Air Force Academy, Colorado, and entered in June of 1965. He was commissioned a Second Lieutenant in the United States Air Force upon graduation in June of 1969, receiving a Bachelor of Science degree in Engineering Mechanics, with a minor degree in Materials. He served as a Technical Operations Specialist with the Foreign Technology Division, Air Force Systems Command, Wright-Patterson Air Force Base, Ohio, until his entry into the Air Force Institute of Technology in June of 1972.

Permanent address: R. R. 2
Perry, Iowa 50220

This thesis was typed by Ms. Carmma O. Troxell.